



THE HONG KONG
POLYTECHNIC UNIVERSITY

香港理工大學

Pao Yue-kong Library

包玉剛圖書館

Copyright Undertaking

This thesis is protected by copyright, with all rights reserved.

By reading and using the thesis, the reader understands and agrees to the following terms:

1. The reader will abide by the rules and legal ordinances governing copyright regarding the use of the thesis.
2. The reader will use the thesis for the purpose of research or private study only and not for distribution or further reproduction or any other purpose.
3. The reader agrees to indemnify and hold the University harmless from and against any loss, damage, cost, liability or expenses arising from copyright infringement or unauthorized usage.

IMPORTANT

If you have reasons to believe that any materials in this thesis are deemed not suitable to be distributed in this form, or a copyright owner having difficulty with the material being included in our database, please contact lbsys@polyu.edu.hk providing details. The Library will look into your claim and consider taking remedial action upon receipt of the written requests.

**DANSYL-CONJUGATED BETA-LACTAM
ANTIBIOTIC AS A FLUORESCENT DRUG-
BASED SENSOR FOR BETA-LACTAMASE
DETECTION AND *IN VITRO* DRUG SCREENING**

YIP CHUN YIN KARL

M. Phil

The Hong Kong Polytechnic University

2015

The Hong Kong Polytechnic University

Department of Applied Biology and Chemical Technology

**Dansyl-Conjugated Beta-Lactam Antibiotic as a
Fluorescent Drug-Based Sensor for Beta-Lactamase
Detection and *In Vitro* Drug Screening**

Yip Chun Yin Karl

A thesis submitted in partial fulfillment

of the requirements for the degree of

Master of Philosophy

Jun 2014

Certificate of Originality

I hereby declare that this thesis is my own research work carried out since my registration at the Hong Kong Polytechnic University for the degree of Master of Philosophy in June, 2011, and, that, to the best of my knowledge and belief, it reproduces no material previously published or neither written, nor material that has been accepted for the award of any other degree or diploma, except where due acknowledgement has been made in the text.

YIP CHUN YIN KARL

Jun 2014

Abstract

Beta-lactam antibiotics have been widely used as antibacterial agents in the clinical treatment of bacterial infections. These drugs can irreversibly bind to the active site of penicillin-binding proteins in bacteria, thus inhibiting these proteins from synthesizing cell walls and leading to cell death. The overuse of beta-lactam antibiotics has, however, led to the increasing emergence of various beta-lactamases, which are enzymes produced by bacteria to inactivate beta-lactam antibiotics. These enzymes can efficiently catalyze the hydrolysis of the beta-lactam ring, thus rendering the antibiotic clinically inactive. The TEM family is a large group of beta-lactamase which has more than 100 variants derived from the ancestor TEM-1 through one or more amino acid mutation(s). Many TEM-type beta-lactamases, including TEM-1, are clinically relevant, and therefore the detection of such enzymes and the development of new beta-lactam antibiotics/inhibitors against TEM-type beta-lactamases are important in combating antibiotic-resistant bacteria capable of producing TEM-type beta-lactamases. Nitrocefin, which is a colorimetric beta-lactam antibiotic, has been routinely used as a probe for detecting beta-lactamase activity. This colorimetric antibiotic is, however, very expensive and unstable in aqueous solution. As such, it is highly desirable to develop a convenient tool that can provide both beta-lactamase sensing and *in vitro* drug screening functions.

In this project, we have successfully developed a versatile dansyl-conjugated beta-lactam antibiotic as a 'turn-on' fluorescent sensor which can detect the activity of the TEM-1 beta-lactamase and perform *in vitro* drug screening. Mass spectrometric studies have shown that this fluorescent antibiotic can bind to the active site of TEM-

1 through the formation of covalent enzyme-substrate complex. Upon binding to TEM-1, the fluorescent antibiotic exhibits a characteristic blue shift in emission wavelength (555 to 513 nm) and stronger fluorescence, presumably due to experiencing a hydrophobic environment upon binding to the active site. Time-course fluorescence measurements indicated that this 'turn-on' fluorescent antibiotic can detect TEM-1 at sub-nanomolar level (0.1 nM). Our fluorescence studies on the fluorescent antibiotic with different proteins have shown that this sensor can specifically recognize TEM-1. The ability of the fluorescent antibiotic to perform *in vitro* drug screening was also studied by time-course fluorescence measurements. In the presence of inhibitors that can inactivate TEM-1, the binding of the fluorescent antibiotic to TEM-1 is largely suppressed, thus making the fluorescent antibiotic to fluoresce weakly at a longer wavelength. In contrast, in the presence of drug candidates that are unable to bind and hence inactivate TEM-1, the binding of the fluorescent antibiotic to TEM-1 becomes favourable and therefore makes the fluorescent antibiotic to fluoresce stronger at a shorter wavelength. These characteristic fluorescence profiles highlight the useful *in vitro* drug screening function of the fluorescent antibiotic. The characteristic fluorescence responses of the dansyl-conjugated beta-lactam antibiotic to beta-lactamase binding and other drug candidates in drug screening highlight its versatile functions in beta-lactamase detection and *in vitro* drug screening.

Acknowledgements

I am deeply indebted to my chief supervisor Dr. Pak-Ho Chan for his encouragement, supervision and discussion throughout the course for my study and his valuable comments on the draft of this thesis. My appreciation is also given to my co-supervisor Dr. Man-Kin Wong for his guidance and encouragement. His professional knowledge on chemistry inspired my interest in chemical synthesis.

I would like to thank Dr. Lan Zou for her guidance and advice in modifying the structure of 7-ACMA. I deeply appreciate Dr. Pui-Kin So for his assistance in mass spectrometric studies. My deepest gratitude should also go to Prof. Thomas Yun-Chung Leung, Mr. Wing-Lam Cheong and Mr. Leo Hok-Kiu Lui for their advice in the preparation of the TEM-1 beta-lactamase and the TEM-1 E166N mutant.

I would also like to thank my colleagues, Dr. Michael Wing-Yiu Yu, Dr. Karen Ka-Yan Kung, Dr. James Yuk-Tai Choi, Dr. Richard Wai-Wing Chan, Dr. Joe Ka-Ho Ng, Mr. Wai-Hong Leung, Mr. Franco King-Chi Leung, Mr. Paul Chun-Wo Chan, Mr. Sean Hon-Wah Lam, Mr. Oscar Fo-Ning Ng, Mr. Larry Yan-Fung Lau and Mr. Siu-Fung Lo for their advice, support and encouragement in the course of my study.

I would like to acknowledge the Research Committee of the Hong Kong Polytechnic University for supporting my MPhil study.

Furthermore, I would like to acknowledge my family, Amanda, my friends, and brothers and sisters in the Lord for supporting me and pray for me.

Last but not least, to God only wise, be glory through Jesus Christ for ever.

Amen.

Table of Contents

Certificate of Originality	i
Abstract.....	ii
Acknowledgment.....	iv
Table of Contents	vi
Chapter 1 Introduction.....	1
1.1 Modern antibiotic era.....	2
1.2 Penicillin: an amazing antibacterial drug	3
1.2.1 Discovery of penicillin	3
1.2.2 Structure of penicillins	4
1.2.3 Action of penicillins	5
1.2.4 Beta-lactam family	9
1.3 Emergence of antibiotic-resistant bacteria – a worrying clinical problem	19
1.3.1 Beta-lactamase	19
1.3.2 Serine-type beta-lactamases (Class A, C, and D).....	21
1.3.3 Class B beta-lactamases	26
1.4 Conventional methods for beta-lactamase detection	28
1.4.1 Colorimetric methods	29
1.5 Advanced methods for beta-lactamase detection	31
1.5.1 Electrochemiluminescence method	31
1.5.2 Surface plasmon resonance (SPR) method	33
1.5.3 Fluorogenic beta-lactam antibiotics	34
1.6 Aims and objectives.....	39
References.....	41
Chapter 2 Materials and Methods.....	45
2.1 Chemical and reagents.....	46
2.2 Instruments	46
2.3 Synthesis of the fluorescent dansyl-conjugated beta-lactam antibiotic.....	47
2.4 Preparation of the wild-type and mutant forms of the TEM-1 beta-lactamase	55
2.5 Fluorescence studies	55
2.6 UV-Visible absorption measurements.....	56
2.7 Electrospray ionization mass spectrometric (ESIMS) studies.....	57
References.....	58

Chapter 3 Studies of the Beta-Lactamase-Sensing Function of the Fluorescent Dansyl-Conjugated Beta-Lactam Antibiotic	59
3.1 Introduction.....	60
3.2 Results.....	61
3.2.1 Fluorescence studies.....	61
3.2.2 Specificity studies	64
3.2.3 Enzyme-substrate binding studies	69
3.2.4 Enzyme kinetic studies.....	75
3.3 Discussion.....	78
3.4 Conclusions.....	82
References.....	83
Chapter 4 <i>In Vitro</i> Drug Screening Studies	85
4.1 Introduction.....	86
4.2 Results.....	89
4.2.1 Fluorescence studies.....	89
4.2.2 Nitrocefin assays	94
4.3 Discussion.....	98
4.4 Conclusions.....	102
References.....	103
Chapter 5 General Conclusions and Further Studies.....	104

Chapter 1

Introduction

1.1 Modern antibiotics era

The discovery of antibiotics represents a substantial medical breakthrough in antibacterial therapies. These small molecules are fatal to pathogenic microbes but not to humans. Antibiotic treatments have enabled humans to effectively control the spread of infectious diseases, thus greatly reducing human mortality. Paul Ehrlich and Alexander Fleming both contributed significantly to the discovery of antibiotics. Ehrlich introduced the first commercially available antibiotic (Prontosil) and was likely the first one to conduct large-scale chemical screening; this strategy continues to be applied in the pharmaceutical industry for drug development (Figure 1-1). Fleming discovered penicillin, which was the first antibiotic that could be generated by fermentation broth. This began the golden era of novel antibiotic development. Various antibiotics with a core structure of four-membered beta-lactam ring (as similar to that of penicillin) were produced, and a large class of antimicrobial agents was formed: beta-lactam antibiotics.^{1,2} Approximately, half of antibiotic prescriptions involve beta-lactams.³

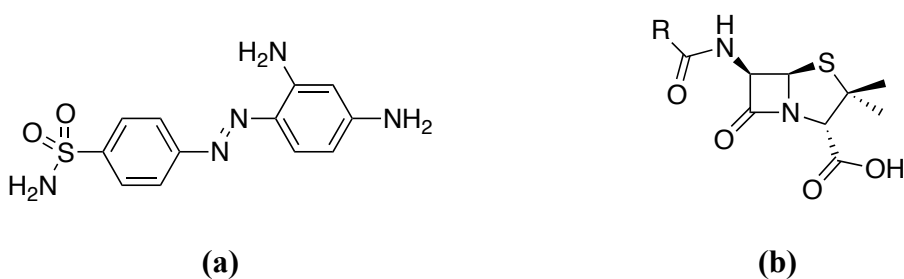


Figure 1-1 Chemical structures of (a) protosil and (b) penicillin.

1.2 Penicillin: an amazing antibacterial drug

1.2.1 Discovery of penicillin

In the late 19th century, various microbiologists, including Pasteur and Joubert, investigated the antagonism or antibiosis present in molds and bacteria. In a single culture, the presence of molds was found to inhibit bacterial growth; for example, *Staphylococcus pyrogenes* inhibits the growth of *Bacillus fluorescens*, and *Penicillium glaucum* inhibits the growth of *Escherichia coli* (*E. coli*).

In 1884, Lister treated the infected wounds of a patient using *Penicillium* as an additive, but the treatment was simply reported as an anecdote. The investigation of microbial antagonism continued, and researchers suggested a new idea: a specific substance released by an interacting organism might cause antagonism. Further investigation into this substance was conducted on a small scale because such an exploration was outside of the mainstream of microbiology, and very few scientists realized the potential of using molds as antimicrobial agents.

Researchers placed their focus on molds after a serendipitous incident in Fleming's laboratory in 1928; an agar plate containing *Staphylococcus aureus* was contaminated with *Penicillium notatum*, and the bacteria were lysed. Fleming was curious why the bacteria were lysed and subsequently discovered penicillin, a compound toxic to bacteria but not harmful to humans.^{1,2,4}

However, substantial time elapsed before penicillin became available for clinical testing, because pure penicillin was not obtained until 1938. Howard Florey and Ernest Chain of Oxford University solved the difficulty in purification, and penicillin could then be mass-produced and distributed five years later.^{1,5}

1.2.2 Structure of penicillins

The structure of penicillins was elucidated in 1945, revealing its two distinct forms: Penicillin G and Penicillin F, which were discovered in the United States and England, respectively (Figure 1-2).²

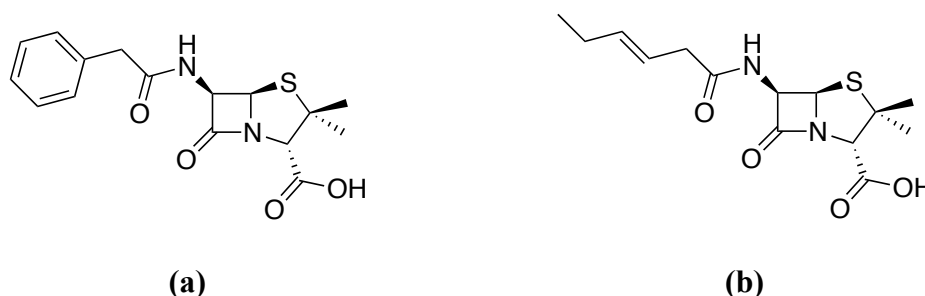


Figure 1-2 Chemical structures of (a) penicillin G and (b) penicillin F.

Both forms of penicillin share a common four-membered beta-lactam ring, but vary in the C6 acyl side chain (Figure 1-3).

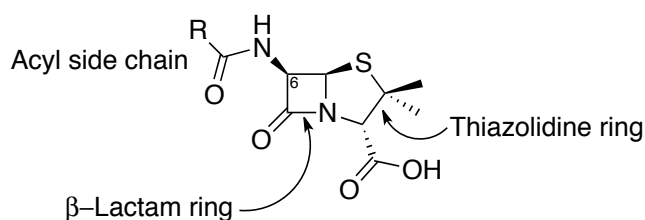


Figure 1-3 Chemical structure of penicillin antibiotics.

With its bicyclic structure, the four-membered beta-lactam ring is fused with a five-membered thiazolidine ring, and the structural conformation of penicillins resembles a half-open book (Figure 1-4). It was suggested that penicillins originated from two amino acids: cysteine and valine (Scheme 1-1). The C6 side-chain can be varied by adding acids to a fermentation medium; for example, adding phenylacetic acid to a medium yields penicillin G, whereas adding *trans*-3-hexanoic acid yields Penicillin F.

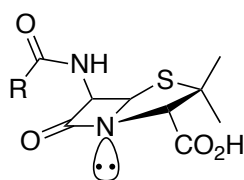
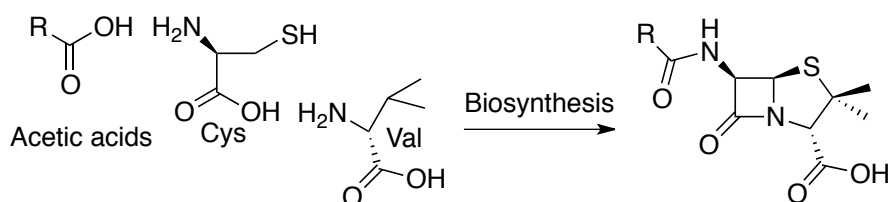


Figure 1-4 Structural conformation of penicillins.



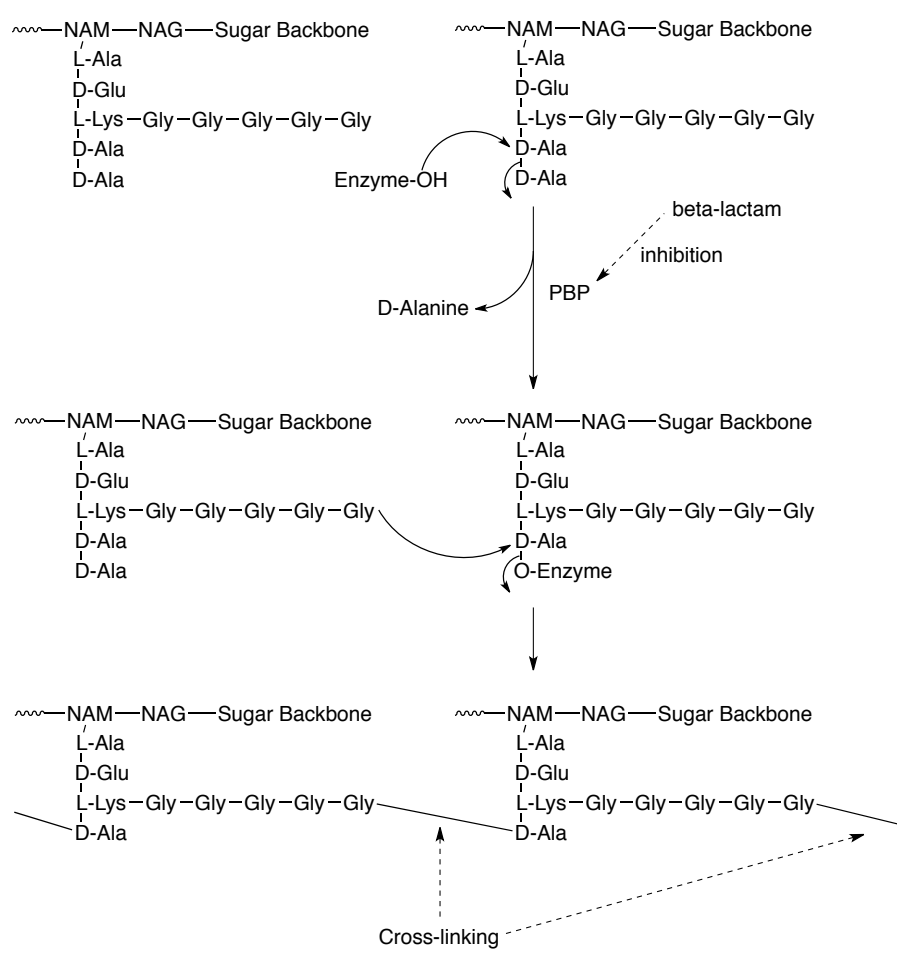
Scheme 1-1 Biosynthesis of penicillins.

The beta-lactam ring is highly strained, making beta-lactam antibiotics highly unstable. The carbonyl group in the beta-lactam ring is more susceptible to hydrolysis than other typical carbonyl groups.^{2,5}

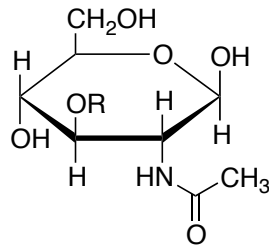
1.2.3 Action of penicillins

Penicillins can inactivate DD-transpeptidase (also called penicillin-binding proteins; PBPs), which is an enzyme responsible for catalyzing the synthesis of bacterial cell walls (Scheme 1-2).^{5,6} When this biosynthetic process is inhibited, bacteria will die as a result of cell lysis.⁵ Before understanding the biological function of PBPs, the structure of the bacterial cell wall must be understood. Two types of peptidoglycan components, N-acetylglucosamine (NAG) and N-acetylmuramic acid (NAM), form the backbone of bacterial cell walls (Figure 1-5). A peptide chain with the sequence of L-Ala-D-Glu-L-Lys-D-Ala-D-Ala is bound to a NAM monomer. During the

production of bacterial cell walls, the peptide chain in this NAM monomer cross-links with another peptide chain on NAM through the displacement of the D-Alanine with its glycine, forming rigid cell walls. PBPs, which are serine enzymes, catalyze the cross-linking process by using its serine residue in the active site to acylate the peptide chain in the first step of cell wall synthesis (Scheme 1-3).

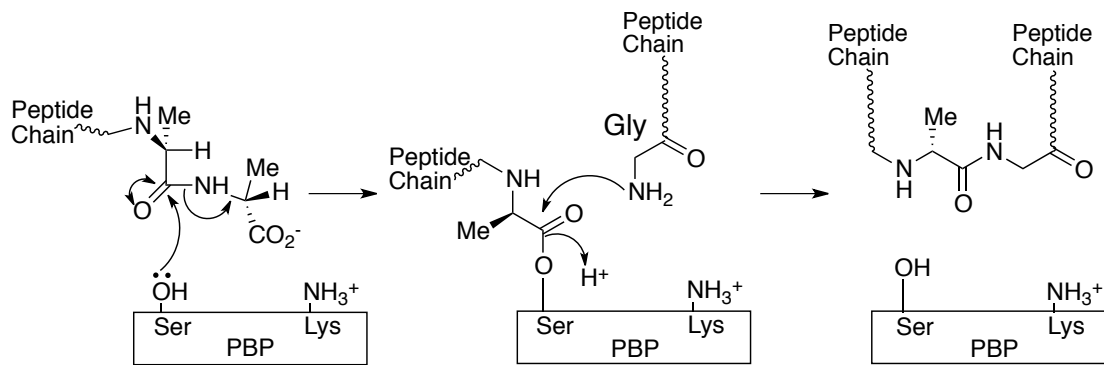


Scheme 1-2 Cross-linking process of bacterial peptidoglycan cell walls.



NAG; R = H, NAM; R = CHMeCO₂H

Figure 1-5 Chemical structures of the peptidoglycan components: NAM and NAG.



Scheme 1-3 Mechanism of the cross-linking process catalyzed by penicillin-binding proteins.

Part of the structure of penicillins is similar to that of D-Ala-D-Ala. Thus, penicillins can bind to the $-OH$ group of serine to form an acyl-enzyme complex and subsequently block the active site, thereby preventing PBPs from binding to their peptide substrate (Figure 1-6). The hydrolytic process by which the acyl-enzyme intermediate yields the free PBP enzyme is extremely slow because of the high stability of the penicillin-enzyme complex (Scheme 1-4). When PBPs are inactivated by beta-lactam antibiotics, the cross-linking process of cell-wall structures will be inhibited, giving fragile cell walls with very low resistance to osmotic pressure and consequently causing bacterial lysis.⁵

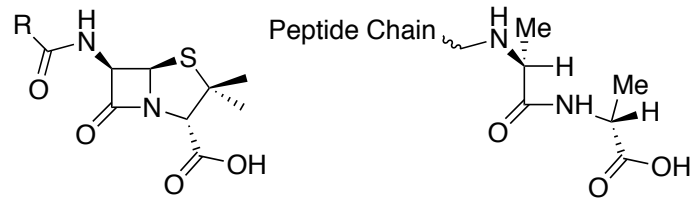
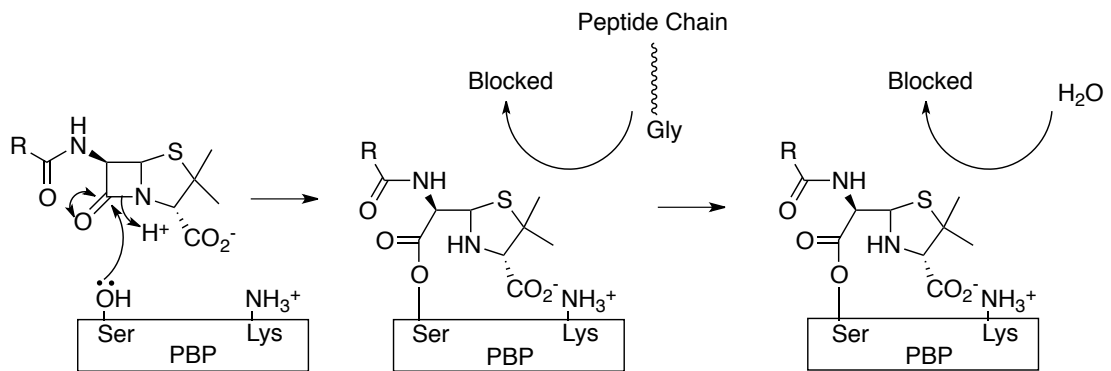


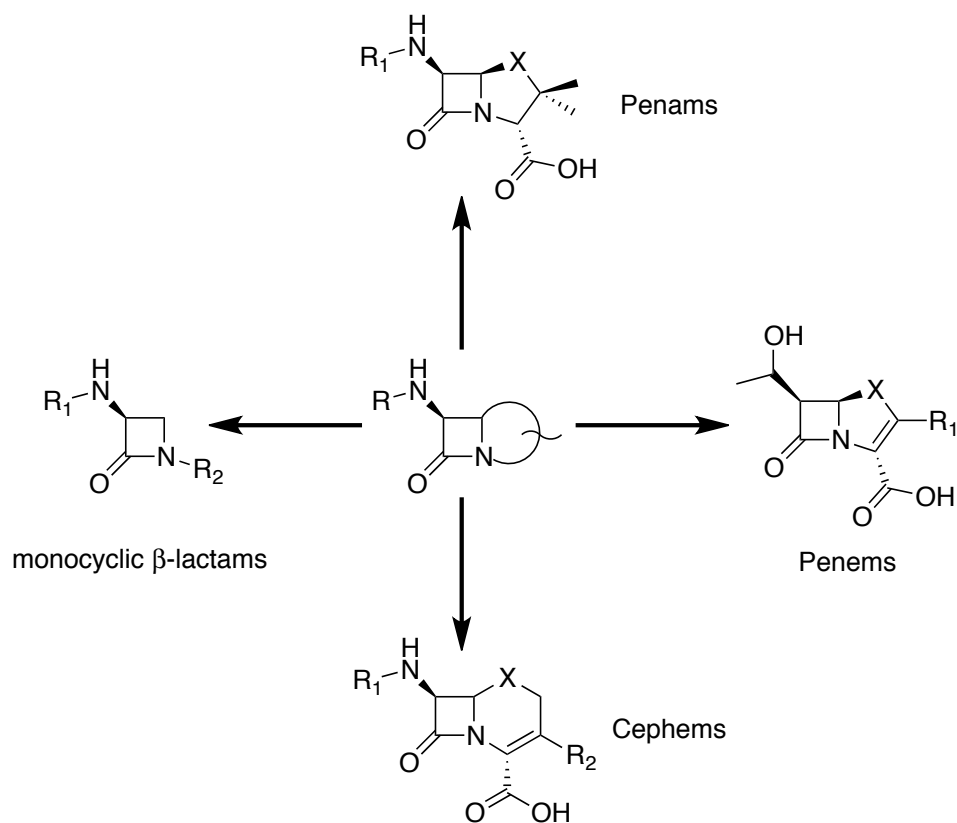
Figure 1-6 Chemical structures of penicillin (**left**) and D-Ala-D-Ala (**right**).



Scheme 1-4 General mechanism of the inactivation of penicillin-binding proteins by penicillin antibiotics.

1.2.4 Beta-lactam family

More beta-lactam antibiotics were discovered or synthesized after the discovery of penicillin, and the beta-lactam family has been substantially expanded. Beta-lactam antibiotics can be classified into penams, penems, cephems and monocyclic beta-lactams (Scheme 1-5).⁴



Scheme 1-5 Classification of beta-lactam antibiotics.

1.2.4.1 Penams

Penams are beta-lactam antibiotics in which the beta-lactam ring is fused with a saturated pentacyclic ring and a side chain is attached to the C6 position. The atom at the 1' position (X) can be sulfur, oxygen, or carbon, yielding penicillins, oxapenams, and carbapenams, respectively (Figure 1-7).⁴

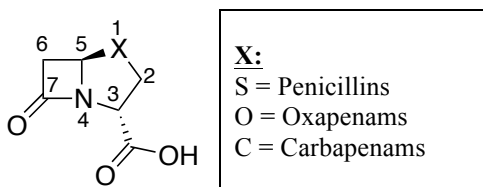


Figure 1-7 General chemical structure of penams.

Penicillins represent the major branch of penams. A series of penicillin derivatives has been developed with different C6 side chains and antibacterial activities.⁵ Penicillin V is an example of an acid-resistant penicillin antibiotic (Figure 1-8). The phoxymethyl group at the C6 side chain reduces the electron density of the carbonyl oxygen, thus reducing the reactivity of the compound toward nucleophiles. As a result of this characteristic structure, penicillin V is more resistant to stomach acid.

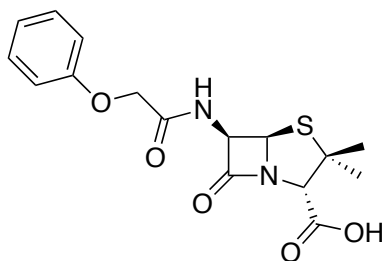


Figure 1-8 Chemical structure of penicillin V.

Many antibiotic-resistant bacteria can produce beta-lactamases, which are enzymes capable of destroying beta-lactam antibiotics through beta-lactam hydrolysis, especially for penicillin G. Thus, a series of penicillin derivatives has been developed by modifying the C6 side chain with various bulky structures. For example, a phenyl ring at the C6 side chain can prevent the antibiotic from accessing to the active site of beta-lactamases. Such derivatives include methicillin and nafcillin (Figure 1-9).

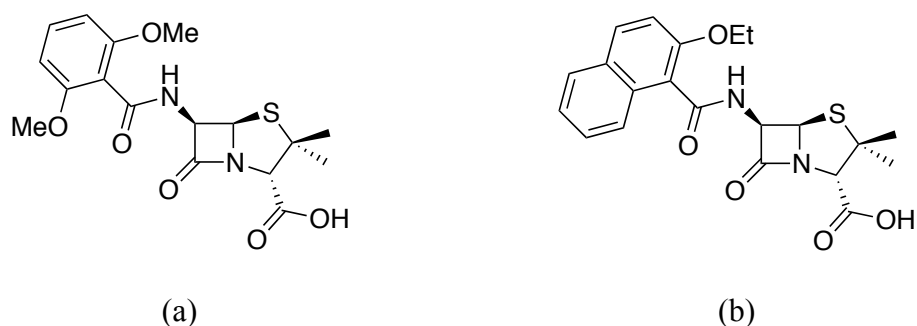
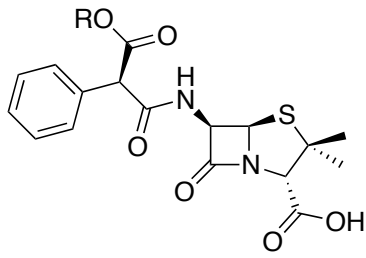
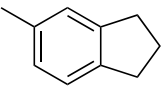


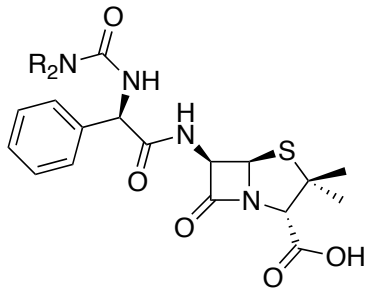
Figure 1-9 Chemical structure of **(a)** methicillin and **(b)** nafcillin.

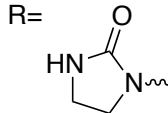
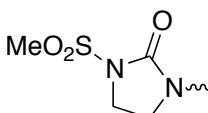
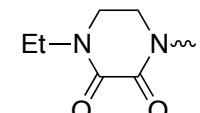
Penicillin antibiotics have different antibacterial activities, depending on the bacterial strains. Some penicillin antibiotics are active to Gram-positive bacteria but not to Gram-negative bacteria or vice versa. To increase the effectiveness of antibacterial therapies, broad-spectrum penicillin antibiotics have been developed by attaching a hydrophilic group to the C6 side chain (e.g. carbenicillin and ureidopenicillins) (Figure 1-10).⁵



R= H	Carbenicillin
Ph	Carfecillin
	Indanyl carbenicillin

(a)



R= 	Azlocillin
	Mezlocillin
	Piperacillin

(b)

Figure 1-10 Chemical structures of (a) carbenicillin and (b) ureidopenicillins.

1.2.4.2 Penems

The core structure of penems is similar to that of penams except that penems have a C=C bond at the 2'-3' position. Varying the atom at the 1' position can yield penems, oxapenems, or carbapenems (Figure 1-11). Penems are synthetic compounds introduced by Woodward in 1976.⁴ The first synthetic penem was 7-phenyl-2-methyl penem (Figure 1-12).

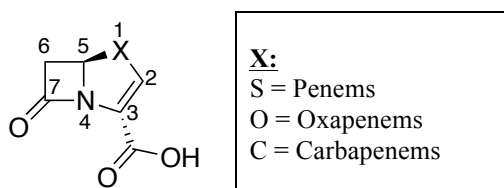


Figure 1-11 General chemical structure of penems.

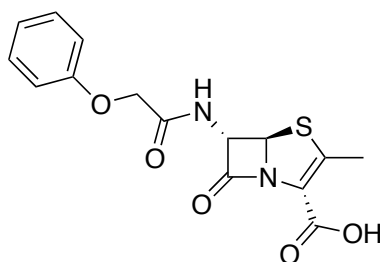


Figure 1-12 Chemical structure of 7-phenyl-2-methyl penem.

Although penems have been developed for a long time, only faropenem is commercially available in Japan (Figure 1-13).^{4,7}

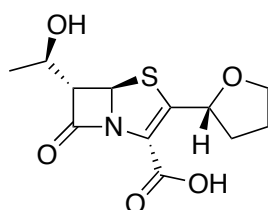


Figure 1-13 Chemical structure of faropenem.

In the late 1970s, thienamycin, a carbapenem, was discovered as a natural product from the extract of *Streptomyces cattleya*. Researchers were interested in this compound because it was a beta-lactam antibiotic with a broad spectrum of activity against many beta-lactamases. This exciting finding has shown that the carbapenem structure is a promising beta-lactamase inhibitor. For example, imipenem is a carbapenem antibiotic modified from thienamycin with higher structural stability (Figure 1-14).^{4,5,7}

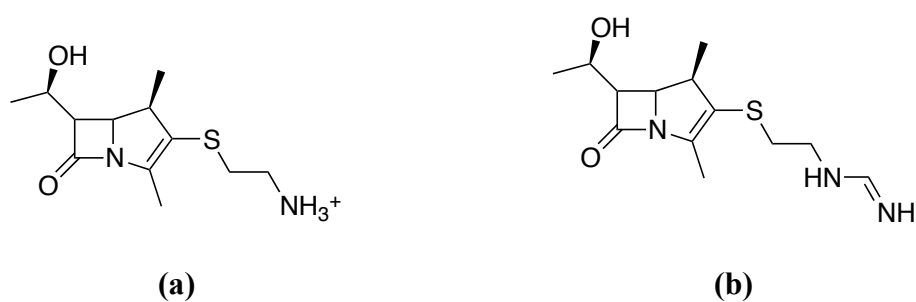


Figure 1-14 Chemical structures of (a) thienamycin and (b) imipenem.

1.2.4.3 Cephems

Since the 1970s, cephem antibiotics have been the most effective and commonly prescribed beta-lactam antibiotics. Cephem antibiotics were discovered in 1945 in the bacterial strain *Cephalosporium acremonium*, which was isolated from the sewage in the island of Sardinia.² The cephem antibiotic isolated from the bacterial culture was cephalosporin C. Abraham and Newton reported that cephalosporin C is resistant to penicillinase, a beta-lactamase capable of efficiently hydrolyzing penicillin antibiotics.¹¹ This resistance against penicillinase occurs because cephem antibiotics have a core structure slightly different from that of penam antibiotics. In cephem antibiotics, the beta-lactam ring is fused with a 3, 4 unsaturated 6-membered ring, which can relieve the ring strain in the beta-lactam ring while remaining its activity against penicillinase. Similar to the structures of penams and penems, the atom at the 1' position of cephem antibiotics can be sulfur, oxygen or carbon (Figure 1-15).

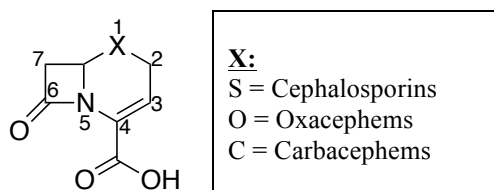


Figure 1-15 General chemical structure of cephem antibiotics.

Cephalosporin antibiotics constitute the major group of cephem antibiotics. Four generations of cephalosporin antibiotics have been developed. In general, cephalosporin antibiotics of later generations have stronger resistance to beta-lactamases. Common cephalosporin antibiotics include cephalothin (first generation), cephamycin (second generation), ceftazidime (third generation) and cefepime (fourth generation) (Figure 1-16).⁵

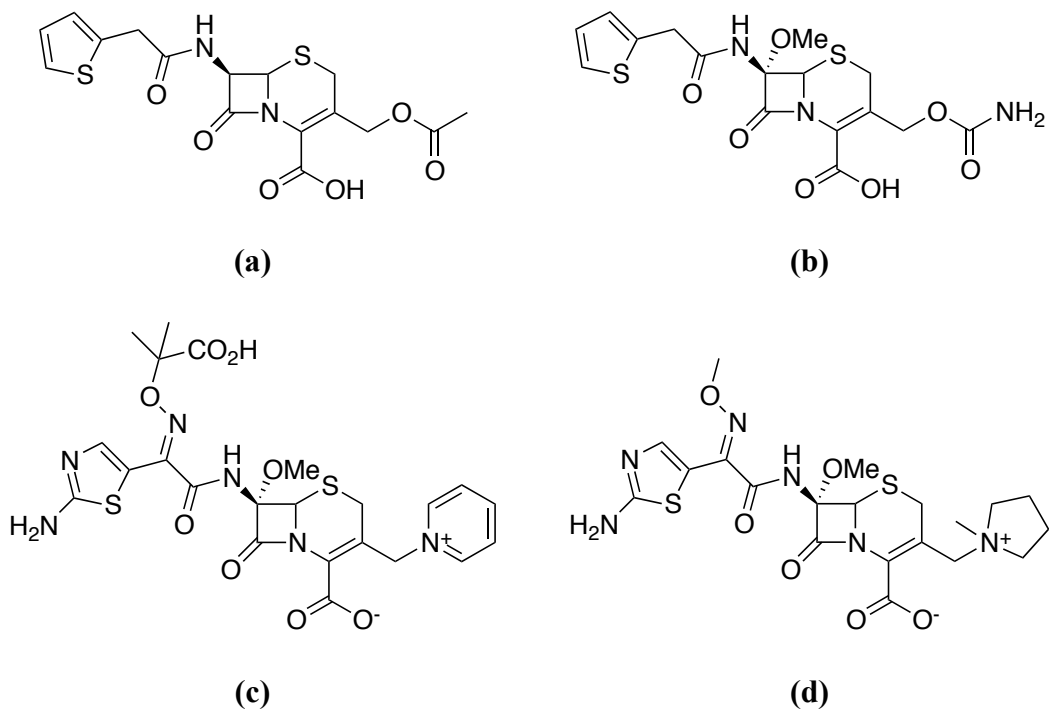


Figure 1-16 Chemical structures of (a) cephalothin, (b) cephemycin, (c) ceftazidime and (d) cefepime.

1.2.4.4 Monocyclic beta-lactams

Monocyclic beta-lactams contain a beta-lactam ring in the core structure only (Figure 1-17). These beta-lactams are active to a narrow group of Gram-negative bacteria, such as *Pseudomonas aeruginosa*, but not to Gram-positive bacteria. Examples of monocyclic beta-lactams include nocardicin A and aztreonam (Figure 1-18).^{4,5}

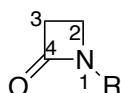


Figure 1-17 General chemical structure of monocyclic beta-lactams.

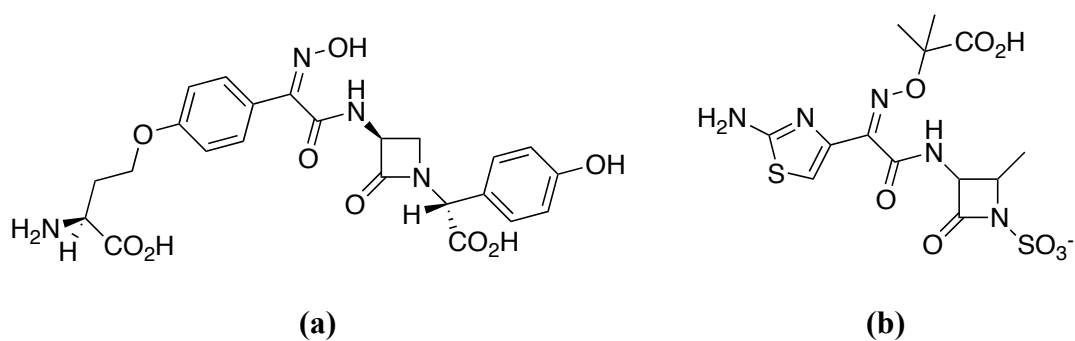


Figure 1-18 Chemical structures of (a) nocardicin and (b) aztreonam.

1.2.4.5 Beta-lactamase inhibitors

Beta-lactamase inhibitors also have a beta-lactam ring, and these inhibitors can irreversibly inhibit the hydrolytic activity of beta-lactamases. Examples include penicillanic acid sulfone (sulbactam), oxapenam (clavulanic acid) and carbapenam (MM13902, Figure 1-19). To enhance the antibacterial activity of beta-lactam antibiotics against antibiotic-resistant bacteria capable of producing beta-lactamases, a combined drug formula of beta-lactam antibiotic with beta-lactamase inhibitor is sometimes prescribed to patients with serious bacterial infections.⁷

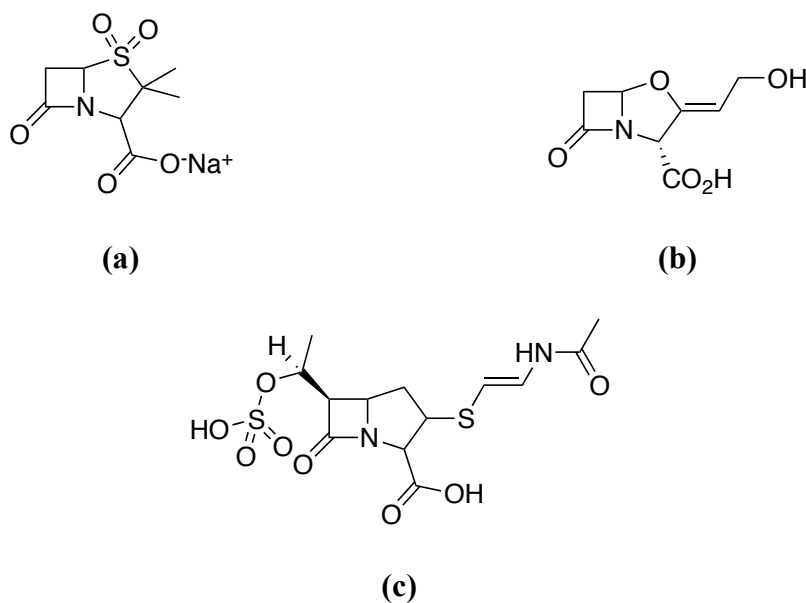


Figure 1-19 Chemical structures of (a) sulbactam, (b) clavulanic acid and (c) MM13902.

1.3 Emergence of antibiotic-resistant bacteria – a worrying clinical problem

Over the past several decades, extensive biomedical studies have shown that bacteria have developed a number of methods for fighting against beta-lactam antibiotics, including the modification of PBPs with weaker susceptibility to beta-lactams as well as and the development of active efflux systems and modified diffusion barriers. In addition to these defense mechanisms, more and more bacteria are able to counteract beta-lactam antibiotics by producing beta-lactamases, which are enzymes capable of inactivating beta-lactam antibiotics through beta-lactam hydrolysis. The ability to produce beta-lactamases has been widespread among various bacteria through the transfer of plasmids with beta-lactamase genes. In recent years, the increasing emergence of beta-lactamases with a broad substrate and activity spectrum has become a worldwide clinical problem. Such bacterial enzymes can hydrolyze a wide range of beta-lactam antibiotics, thus rendering many beta-lactams clinically useless.^{5,6,8,9}

1.3.1 Beta-lactamases

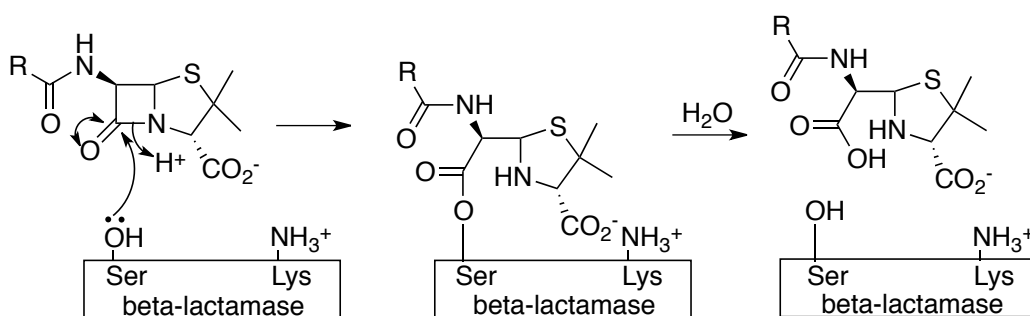
Before beta-lactam antibiotics were widely applied in clinical settings, beta-lactamase was first discovered in *E. coli* in 1940. However, the effect of beta-lactamase production in bacteria was not elucidated until a decade later.^{4,10,11} In the late 1950s, penicillin was frequently used to treat bacterial infections. Since then, more and more bacteria have become resistant to beta-lactam antibiotics. To defend against beta-lactam antibiotics, bacteria produce beta-lactamases to inactivate beta-lactam antibiotics by opening the beta-lactam ring through beta-lactam hydrolysis. To respond to the increasing emergence of beta-lactamases with different substrate and

activity profiles, researchers have been keen on the development of new-generation beta-lactam antibiotics and inhibitors to address the pressure of antibiotic resistance.⁴

Based on their amino acid sequences, beta-lactamases can be classified into four classes: class A, B, C and D. Members of class A, C and D are serine-type beta-lactamases, which make use of their active-site serine to open beta-lactams. Members in class B are metallo-beta-lactamases (MBLs), and the active site of these enzymes contain one or two Zn(II) ion(s). The metal ion in the MBLs plays a critical role in beta-lactam hydrolysis.^{4,6,8,10}

1.3.2 Serine-type beta-lactamases (Class A, C and D)

Serine-type beta-lactamases are similar to PBPs. X-ray crystallographic studies have shown that both enzymes have a serine residue in their active sites for hydrolyzing the beta-lactam ring. However, the hydrolytic process carried out by acyl-beta-lactamase complexes is much faster than that of PBPs. Thus, beta-lactamases return to their free enzyme state rapidly to inactivate other beta-lactam antibiotics for protecting PBPs (Scheme 1-6).⁶



Scheme 1-6 General mechanism of the beta-lactam hydrolysis catalyzed by serine-type beta-lactamases.

1.3.2.1 Class A beta-lactamases

Class A beta-lactamases are the most prevalent enzymes among the serine-type beta-lactamases. These enzymes are of medium size with a molecular mass of about 29 kDa (containing 260–280 amino acids) (Figure 1-20). Nine important amino acids in the active site (including Ser70, Lys73, Ser130 and Glu166) are involved in the catalytic process of beta-lactam hydrolysis. Part of the class A beta-lactamases can be inhibited by beta-lactamase inhibitors, such as clavulanic acid, sulbactam and tazobactam.

In 1963, a special beta-lactamase was identified in *E. coli* from a woman named Temorina, who got urinary tract infection that could not be treated using ampicillin. This enzyme was special because the gene encoding this enzyme was in plasmids, which could be transmitted to other bacteria. This plasmid-mediated enzyme was named TEM-1, which confers penicillin and ampicillin resistance on *Klebsiella pneumoniae*, *Haemophilus influenzae*, and *Neisseria gonorrhoeae*.^{4,6,8,12,13} Enzymes derived from the TEM-1 beta-lactamase (regarded as the ancestor in the TEM family) through one or two amino acid replacement(s) are classified as TEM variants. To date, more than 181 TEM variants have been identified, and these enzymes have broad substrate and activity profiles; for example, inhibitor resistant TEM (IRT) beta-lactamases and TEM-type extended spectrum beta-lactamases (ESBLs) are more resistant to the conventional beta-lactamase inhibitors (e.g. clavulanic acid) and early-generation cephalosporin antibiotics (respectively) compared to the TEM-1 beta-lactamase.

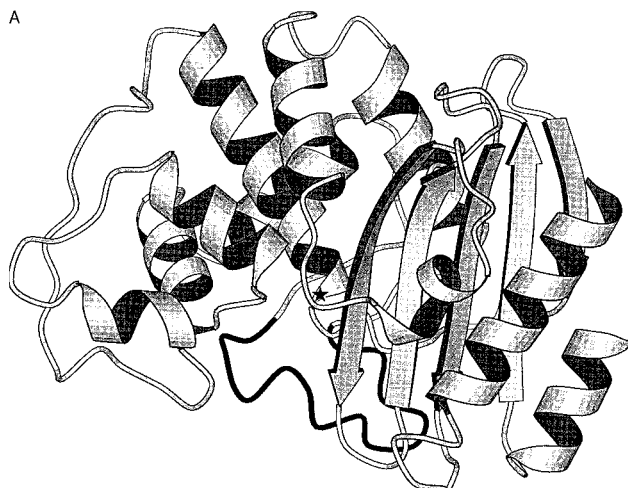


Figure 1-20 General structure of class A beta-lactamases.

SHV-type beta-lactamases are also common in bacteria. These enzymes were first discovered in *K. pneumoniae*. To date, more than 140 SHV variants have been identified. The primary sequence of SHV beta-lactamases shares 68% similarity with that of TEM-type beta-lactamases. The active site of SHV-type beta-lactamases is, in general, larger than that of TEM-type beta-lactamases.^{8,12,13}

In addition to TEM- and SHV-type beta-lactamases, CTX-M-type beta-lactamases were found in South America, Eastern Europe, and Asia after 1995. The CTX-M beta-lactamase was first isolated from *E. coli* in 1986, and its name originated from its ability to hydrolyze cefotaxime. About 40 CTX-M-type variants have been identified.^{4,14-16}

1.3.2.2 Class C beta-lactamases

Bacteria, such as *C. freundii*, *E. cloacae*, *P. aeruginosa* and *K. pneumoniae*, can produce class C beta-lactamases. Usually, the concentration of chromosomal class C beta-lactamases is low and “repressed.” This repression can be altered when specific beta-lactam antibiotics (e.g., ceftiofur) are present so that the enzyme concentration will be increased.^{4,8}

Class C beta-lactamases have a molecular mass of about 39 kDa (Figure 1-21). Members in this class can hydrolyze not only penicillin antibiotics, but also new cephalosporin antibiotics (e.g. ceftiofur, cefotetan, ceftriaxone and cefotaxime). The hydrolytic process of class C beta-lactamases is, in general, less efficient than that of class A beta-lactamases. However, conventional beta-lactamase inhibitors cannot

efficiently inhibit class C beta-lactamases. Examples of class C beta-lactamases include CMY, FOX, MIR and MOX.^{4,6,8}

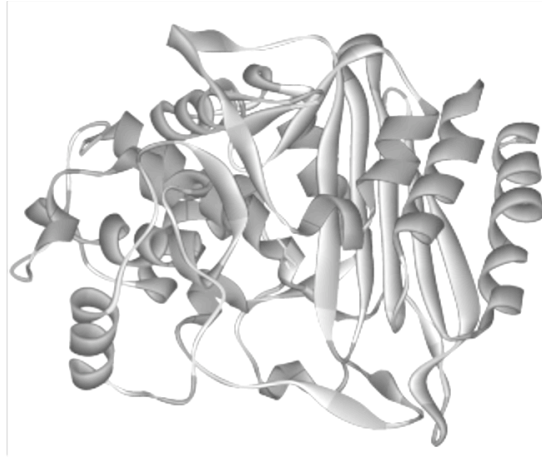


Figure 1-21 General structure of class C beta-lactamases.

1.3.2.3 Class D beta-lactamases

Members in class D are also called OXA-type beta-lactamases because these enzymes can hydrolyze oxacillin at a rate 50% higher than class A and C beta-lactamases do. In the last decade, increasing studies have reported antibiotic resistance caused by class D beta-lactamases, and these enzymes can be found in bacteria, such as *Acinetobacter baumannii* and *Pseudomonas aeruginosa*. The molecular mass of class D enzymes is about 27–31 kDa. Similar to class C beta-lactamases, members in class D are resistant to the inhibitory activity of conventional beta-lactamase inhibitors (e.g. clavulanate, sulbactam and tazobactam). Examples of class D beta-lactamases include OXA-1, OXA-23 and OXA-50.^{4,6,8,17}

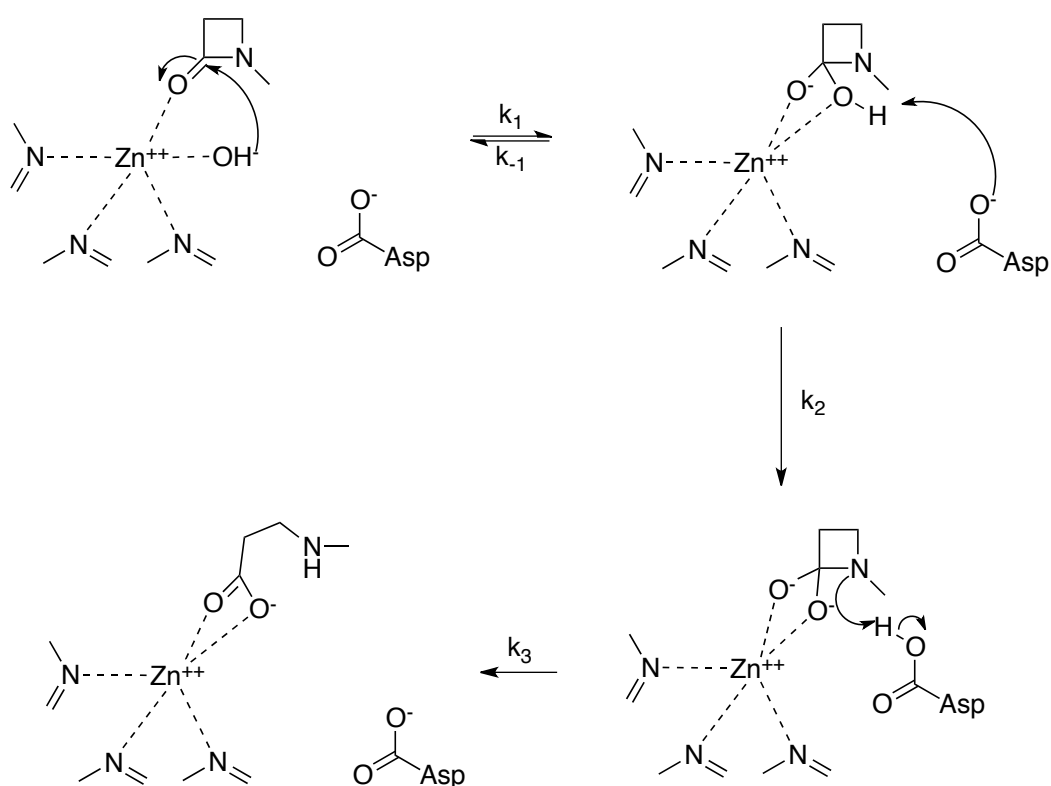
1.3.3 Class B beta-lactamases

Members in class B are regarded as metallo-beta-lactamases (MBLs), which contain one or two Zn(II) ion(s) at their active site. Conventional beta-lactamase inhibitors (e.g. clavulanic acid and sulbactam), which can inhibit many class A beta-lactamases through the irreversible covalent modification of their active-site serine residue, are not effective to MBLs. Class B beta-lactamases can hydrolyze nearly all beta-lactam antibiotics, including penicillins, cephalosporins, carbapenems and cephamycins. Because of their very broad substrate and activity profiles, class B beta-lactamases confer very strong antibiotic resistance on pathogenic bacteria. A notorious example of MBLs is NDM-1, which is able to make bacteria become “superbugs”. Other examples of class B beta-lactamases include BcII, CcrA, BlaB, IMP-1 and SPM-1.^{6,18,19}

The Zn²⁺ in the active site is thought to perform three functions. The first function involves the stabilization of the negative charge of carbonyl oxygen on the tetrahedral intermediate by coordinating the oxygen to the Zn²⁺ ion.¹⁸⁻²⁰ The second function involves acting as a Lewis acid, which attracts the electrons from the carbonyl oxygen to make the carbonyl carbon become highly electrophilic, thereby enabling the nucleophile (OH⁻) to attack the carbonyl group on the beta-lactam ring.¹⁹ Furthermore, the Zn²⁺ ion can coordinate a water molecule, and such binding can decrease the pKa of the water molecule (i.e. facilitating the deprotonation of the bound water molecule). The resulting OH⁻ ion then attacks the carbonyl carbon in the beta-lactam ring to open the ring structure.^{19,21}

It is generally believed that two catalytically important groups are involved in the proposed mechanism by which the class B beta-lactamase BcII hydrolyzes beta-

lactam antibiotics: Zn(II) and Asp. Both the Asp residue and water molecule bound to the Zn²⁺ ion are deprotonated under the physiological pH. The OH⁻ group bound to Zn²⁺ then attacks the carbonyl carbon in the beta-lactam ring, forming a tetrahedral intermediate. The negatively charged carbonyl oxygen in the ring structure is then coordinated to the Zn²⁺ ion to neutralize its charge. The side-chain -COO⁻ group of the Asp residue then abstracts the proton of the -OH group in the ring structure to form a dianionic tetrahedral intermediate, and the protonated Asp residue becomes a proton donor to facilitate the C-N bond cleavage. (Scheme 1-7).



Scheme 1-7 Proposed mechanism of the beta-lactam hydrolysis catalyzed by class B beta-lactamases.

1.4 Conventional methods for beta-lactamase detection

Because beta-lactamases are the major cause of antibiotic resistance in pathogenic bacteria, beta-lactamase detection is of great importance in clinical settings. Various methods have been developed to detect beta-lactamases. Both biological methods (e.g. antibiotic susceptibility tests) and chemical methods (e.g. colorimetric and acidimetric tests) have been applied in biochemical laboratories.

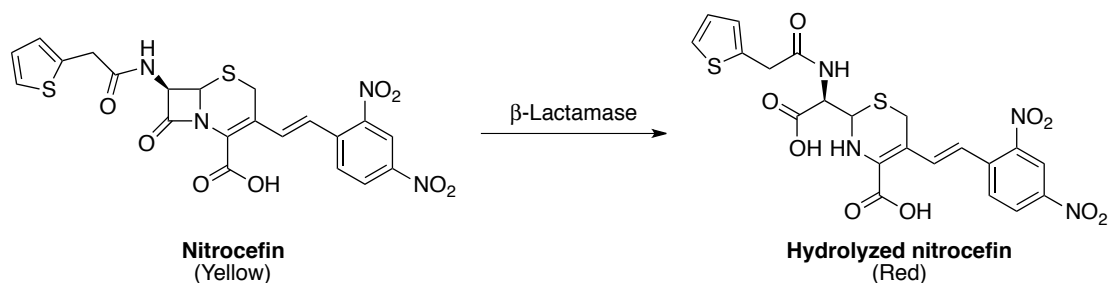
Antibiotic susceptibility tests are conducted by incubating bacteria on a culture plate in the presence of a beta-lactam antibiotic. The bacterial growth and zone of inhibition are observed, and the inhibitory activity of the beta-lactam antibiotic can be evaluated. However, a long incubation period (e.g. overnight) is usually required to obtain testing results. Moreover, although automated systems are available for this method, the operation usually requires high technical competence. Therefore, rapid methods involving the use of chromogenic beta-lactam antibiotics or the detection of color changes with an indicator have also been developed.^{4,22-24}

1.4.1 Colorimetric methods

Chromogenic cephalosporins and iodometric/acidimetric tests can provide rapid beta-lactamase detection in a visual way.

1.4.1.1 Chromogenic cephalosporins

Chromogenic cephalosporin is a beta-lactam antibiotic that gives a characteristic color change as a result of beta-lactam hydrolysis. The commonly used chromogenic cephalosporin is nitrocefin. This antibiotic is yellow before beta-lactam hydrolysis, but turns red when it is hydrolyzed by beta-lactamases (Scheme 1-8).^{25,26}



Scheme 1-8 Colorimetric response of nitrocefin in the presence of beta-lactamases.

Nitrocefin can detect beta-lactamases with high sensitivity. However, this chromogenic antibiotic is very expensive and has low stability in water. Moreover, nitrocefin cannot directly probe its binding to the active site of beta-lactamase; it detects beta-lactamase activity through the formation of a red acid product after beta-lactam hydrolysis.^{23,27-29}

1.4.1.2 Iodometric and acidimetric tests

Hydrolysis of beta-lactam antibiotics by beta-lactamases generates acid products, which can be detected by iodometric and acidimetric tests. For iodometric tests, the acidic hydrolyzed product can reduce iodine and decolorize violet iodine-starch complexes. For acidimetric tests, the acidity of culture medium is monitored in an unbuffered system with a pH indicator, such as aqueous phenol red solution. In the presence of beta-lactamases, beta-lactam antibiotics will be hydrolyzed, and therefore the color of the culture medium will change from violet to yellow. Both iodometric and acidimetric tests can be used to determine beta-lactamase activity within 5 min. These tests, however, have poor sensitivity toward the beta-lactamases produced by Gram-negative bacteria.^{23,30}

1.5 Advanced methods for beta-lactamase detection

The increasing emergence of new beta-lactamases with different substrate and activity profiles has become a serious clinical concern over the past decades due to overuse of beta-lactam antibiotics in different areas, ranging from clinical treatment to animal farming. As such, a rapid, specific and sensitive detection method is highly desired for detecting beta-lactamases and screening for potent beta-lactam antibiotics. A number of advanced beta-lactamase-sensing methods have been developed, such as electrochemiluminescence (ECL), surface plasmon resonance (SPR), fluorogenic beta-lactam antibiotics, and high-performance liquid chromatographic (HPLC).^{23,31}

1.5.1 Electrochemiluminescence method

In 1996, Liang et al. reported a new method for detecting beta-lactamase activity based on electrochemiluminescence (ECL).³² ECL is generated through the electrode-induced oxidation of the ruthenium(II) (tris)bipyridine complex $[\text{Ru}(\text{bpy})_3^{2+}]$ to $\text{Ru}(\text{bpy})_3^{3+}$. This complex then oxidizes amine-containing organic molecules to reach its excited state $[\text{Ru}(\text{bpy})_3^{2+*}]$. Light is then emitted from $\text{Ru}(\text{bpy})_3^{2+*}$ upon radiative relaxation.

Hydrolyzed beta-lactam antibiotics produced by beta-lactamases are amine-containing molecules detectable by ECL. This electrochemical method can detect beta-lactamase within 2 h. The selectivity of this instrumental technique, however, remains a technical difficulty. He et al. has reported that the amino acid tyrosine can quench the ECL reaction because it contains a hydroxyl group. Amoxicillin, a beta-lactam

antibiotic, has similar behavior, resulting in false positive drug testing results (Figure 1-22).^{24,33}

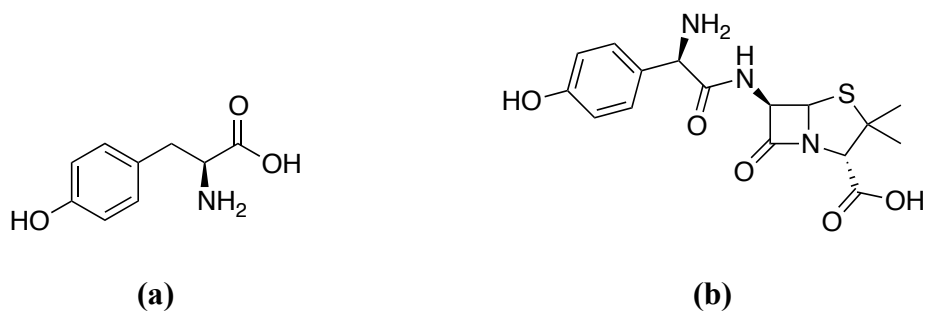
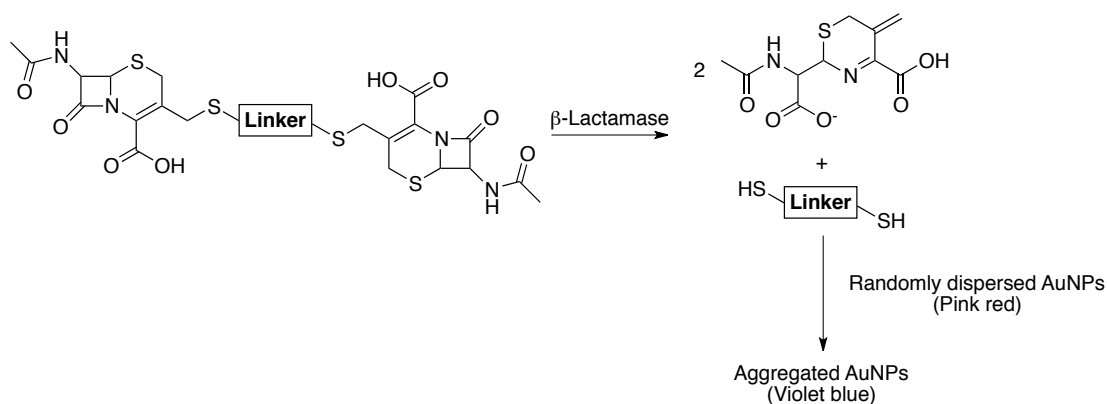


Figure 1-22 Chemical structures of (a) tyrosine and (b) amoxicillin.

1.5.2 Surface plasmon resonance (SPR) method

Gold contains d electrons that travel freely through its structure. The mean free path of Au is approximately 50 nm, and when Au nanoparticles (AuNPs) are smaller than the mean electron free path, the interaction between the surface and electrons can be observed. When AuNPs coherently interact with the visible light, surface plasmon resonance will take place, causing light absorption. The wavelength of light absorption depends on the size, shape, medium and distance between nanoparticles. Altering these factors can, therefore, change the light absorption wavelength, giving a color change.^{29,34}

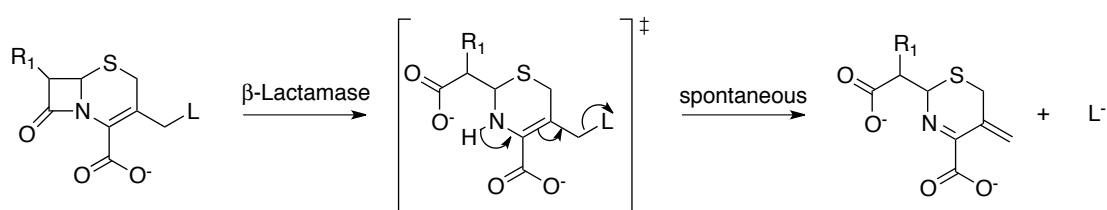
In 2007, Liu et al. reported a beta-lactamase-sensing method involving the use of AuNPs. Two cephalosporin antibiotics are interlinked with a dithiol linker. When this antibiotic complex is hydrolyzed by a beta-lactamase, the dithiol linker at the 3' position will be released. The thiol (-SH) group of the linker is then bound to the surface of AuNPs, leading to AuNP aggregation and hence a color change in the AuNP solution (from red to blue) in 20 min (Scheme 1-9).



Scheme 1-9 The working principle of beta-lactamase detection by the gold nanoparticle method.

1.5.3 Fluorogenic beta-lactam antibiotics

Hydrolysis of cephalosporin antibiotics by beta-lactamases can release the chemical group (L) at the 3' position (Scheme 1-10).^{35,36} Because of this characteristic reaction, cephalosporins can act as a useful probe for detecting beta-lactamases after conjugating with fluorogenic or bioluminogenic molecules.



Scheme 1-10 Elimination of the 3' leaving group from a cephalosporin antibiotic after beta-lactam hydrolysis by beta-lactamases.

In 1998, the Zlokarnik group reported a gene expression visualization technique involving a fluorogenic beta-lactam antibiotic. In this method, a cephalosporin antibiotic is labeled with two fluorophores at the 7' and 3' positions (**CCF2**, Figure 1-23). **CCF2** detects beta-lactamase activity based on the principle of Förster resonance energy transfer (FRET). After beta-lactam hydrolysis, the fluorophore at the 3' position will be released, thus preventing the FRET process to take place and shifting the emission wavelength from 520 to 447 nm.³⁷ This method has been successfully applied in mammal tissue culture studies. However, **CCF2** has low solubility in aqueous solution, and its large molecular weight prevents itself from accessing to thick-walled cells.

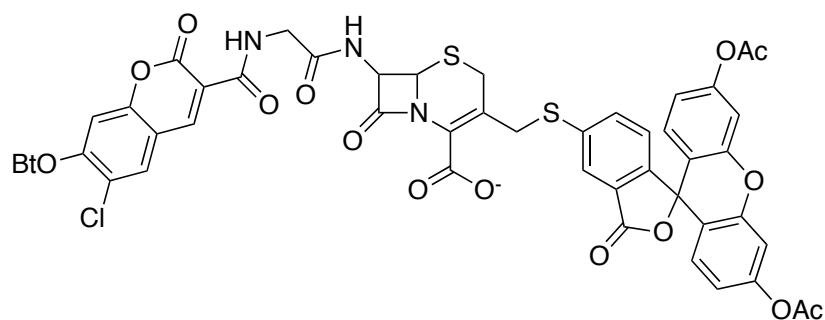


Figure 1-23 Chemical structure of **CCF2**.

In 2003, the Gao group modified the technique by labeling a cephalosporin antibiotic with the fluorophore umbelliferone through an allylic ester bond at the 3' position (**CC1**, Figure 1-24). In the absence of beta-lactamases, **CC1** does not fluoresce. Upon hydrolysis by beta-lactamases, **CC1** releases the umbelliferone molecule and gives strong fluorescence at 460 nm.³⁸ Subsequently, Xing et al. reported the near-infrared fluorogenic substrate **CNIR1** with low autofluorescence and improved sensitivity for beta-lactamase detection (Figure 1-25).³⁹

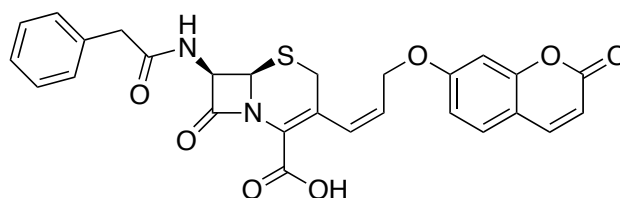
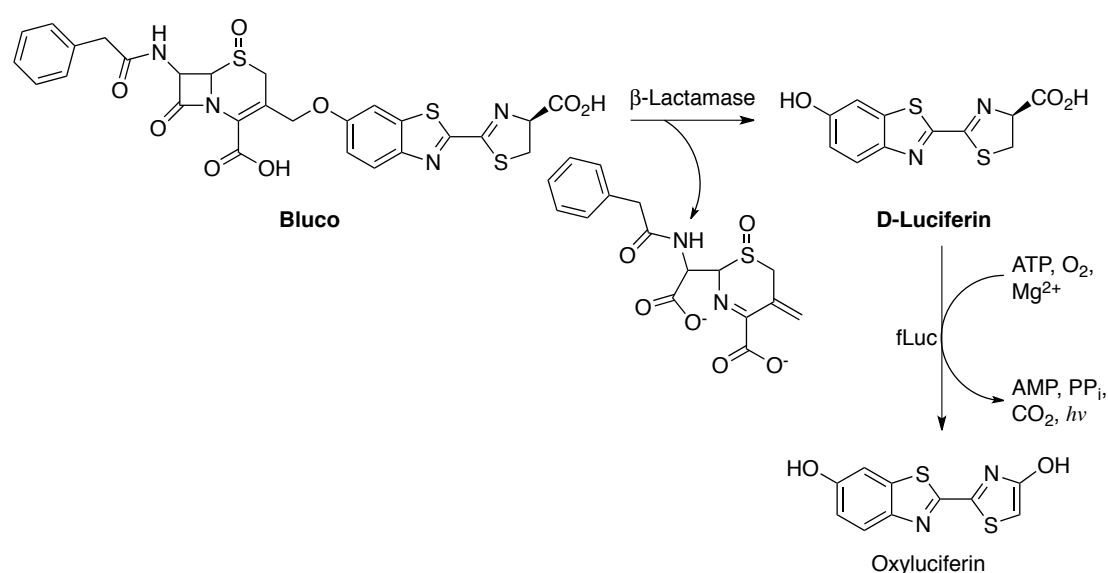


Figure 1-24 Chemical structure of **CC1**.

The Yao group has reported a bioluminogenic substrate, **Bluco**, which is a cephalosporin antibiotic carrying D-luciferin as the leaving group at the 3' position. D-Luciferin can be oxidized by firefly luciferase to form oxyluciferin. Light will be emitted during this enzymatic oxidation, thus enabling the detection of beta-lactamase (Scheme 1-11).⁴⁰ However, the bioluminescence signal appears in a short time during the oxidation process, and the signal declines quickly after reaction.



Scheme 1-11 The working principle of beta-lactamase detection by **Bluco**.

In 2010, the Chan group reported a switch-on fluorescence method involving the use of fluorogenic cephalosporin antibiotics coated on solid beads (Tantagel) and amyloid fibrils (Figure 1-26). The cephalosporin antibiotic is conjugated with the environment-sensitive fluorophore dansylaminothiophenol (DTA). When the DTA-antibiotic complex is hydrolyzed by the TEM-1 beta-lactamase, the DTA molecule will be released to solution and adsorbed onto amyloid fibrils of hen lysozyme. These

fibrils provide a hydrophobic environment for DTA, which exhibits much stronger green fluorescence at 514 nm that can be observed by naked eyes. Without the TEM-1 beta-lactamase, no beta-lactam hydrolysis will take place, and therefore the DTA molecule will remain attached to the cephalosporin antibiotic on the solid beads. As a result, no DTA will be released to solution for hen lysozyme fibrils to adsorb to give fluorescence. This approach can detect the TEM-1 beta-lactamase at sub-nanomolar level.³¹

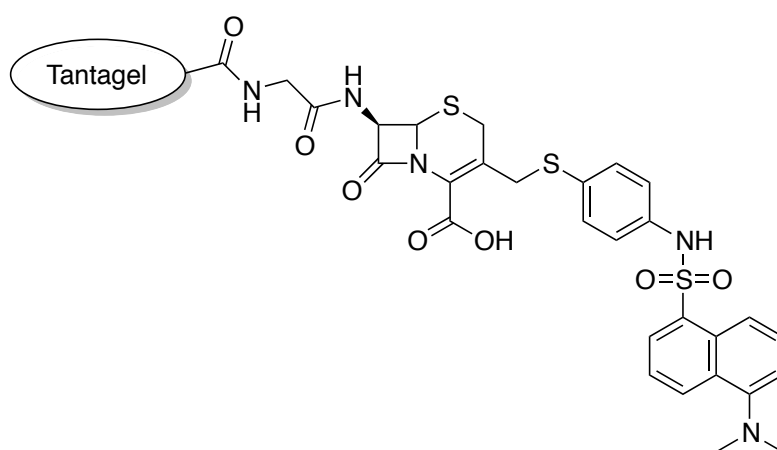


Figure 1-26 Fluorescent DTA-antibiotic complex anchored to the solid bead Tantagel.

Recent studies have also been directed to the development of fluorophore-conjugated cephalosporin antibiotics for beta-lactamase detection because the high sensitivity of fluorescence technique. Thus, the use of fluorogenic beta-lactam antibiotics is a promising approach for beta-lactamase detection.^{38,41,42}

1.6 Aims and objectives

The beta-lactamase family has been rapidly expanding over the past several decades due to overuse of beta-lactam antibiotics, making bacteria strongly resistant to a wide range of beta-lactam antibiotics. This worrying clinical problem has alerted humans in the fight against pathogenic bacteria in the future; we will soon enter the “post antibiotic” era in which very few antibiotic choices are available for antibacterial therapies. To protect the public health, beta-lactamase detection and new drugs development (e.g. new inhibitors and new-generation beta-lactam antibiotics) against clinically significant beta-lactamases are both important for the monitoring and control of spread of antibiotic-resistant bacteria, clinical diagnosis of bacterial infections, and antibacterial therapies.

In this project, we aim to develop a fluorescent drug-based sensor (Complex **4**) that can satisfy the two important needs: beta-lactamase detection and *in vitro* drug screening against beta-lactamases. To this end, a cephalosporin-type beta-lactam antibiotic is chemically modified with the small and environment-sensitive fluorophore DTA (Complex **4**). The cephalosporin antibiotic acts as a specific carrier to bring the fluorescent DTA molecule to the active site of beta-lactamases for biosensing purposes. With this rational molecular design, the DTA-antibiotic complex, which has a relatively small size, can bind to beta-lactamases with high specificity and affinity. Such active-site binding allows the environment-sensitive DTA molecule in the antibiotic complex to experience local environmental changes and hence give characteristic photophysical changes (fluorescence change and emission wavelength

shift). This biosensing approach can directly probe the binding to the active site of beta-lactamases and detect beta-lactamases with high specificity and sensitivity.

The synthesis of the fluorescent drug-based sensor and the details of various experimental studies will be described in Chapter 2. The beta-lactamase-sensing function of the fluorescent drug-based sensor and its biosensing mechanism were studied by fluorescence spectroscopy, electrospray ionization mass spectrometry (ESI-MS) and enzyme kinetic assays, using the TEM-1 beta-lactamase as the protein model because of its clinical relevance and ancestor role in the giant TEM family.^{2,4,43-46} The findings of these studies will be presented in Chapter 3. The *in vitro* drug screening function of the fluorescent drug-based sensor against TEM-1 was also investigated by fluorescence measurements. The results of this application study will be presented in Chapter 4.

References

1. Aminov, R. I. A brief history of the antibiotic era: lessons learned and challenges for the future. *Front Microbiol* [Online] **2010**, *1*, Article Archive. doi: 10.3389/fmicb.2010.00134 (accessed Dec 7, 2014)
2. Queener, S. F.; Webber, J. A.; Queener, S. W. *Beta-lactam Antibiotics for Clinical Use*; M. Dekker: 1986.
3. Mölstad, S.; Stålsby Lundborg, C.; Karlsson, A.; Cars, O. Antibiotic prescription rates vary markedly between 13 European countries. *Scand J Infect Dis* **2002**, *34*, 366-371.
4. Bryskier, A. *Antimicrobial Agents: Antibacterials and Antifungals*; ASM Press: 2005.
5. Patrick, G. L.; Spencer, J. *An Introduction to Medicinal Chemistry*; OUP Oxford: 2009.
6. Matagne, A.; Dubus, A.; Galleni, M.; Frere, J. M. The beta-lactamase cycle: a tale of selective pressure and bacterial ingenuity. *Nat Prod Rep* **1999**, *16*, 1-19.
7. Dalhoff, A.; Janjic, N.; Echols, R. Redefining penems. *Biochem Pharm* **2006**, *71*, 1085-1095.
8. Drawz, S. M.; Bonomo, R. A. Three Decades of beta-Lactamase Inhibitors. *Clin Microbiol Rev* **2010**, *23*, 160-201.
9. Frère, J. Beta-lactamases and bacterial resistance to antibiotics. *Mol Microbiol* **1995**, *16*, 385-395.
10. Bush, K. Bench-to-bedside review: The role of beta-lactamases in antibiotic-resistant Gram-negative infections. *Crit Care* [Online] **2010**, *14*, Article Archive. doi: 10.1186/cc889 (accessed Dec 7, 2014).
11. Abraham, E. P.; Chain, E. An enzyme from bacteria able to destroy penicillin. *Nature* **1940**, *146*, 837-837.
12. Ribes, J.; Rapp, R. P. Why is the Microbiology Lab Calling About an Extended-Spectrum Beta-Lactamase Bacterium From a Wound Culture? *Orthopedics* **2005**, *28*, 1322-1325.
13. Faruque, S. M. *Foodborne and Waterborne Bacterial Pathogens: Epidemiology, Evolution and Molecular Biology*; Caister Academic Press: 2012.
14. Pournaras, S.; Ikonomidis, A.; Kristo, I.; Tsakris, A.; Maniatis, A. N. CTX-M enzymes are the most common extended-spectrum beta-lactamases among *Escherichia coli* in a tertiary Greek hospital. *J Antimicrob Chemother* **2004**, *54*, 574-575.

15. Bonnet, R. Growing Group of Extended-Spectrum beta-Lactamases: the CTX-M Enzymes. *Antimicrob Agents Chemother* **2004**, *48*, 1-14.
16. Canton, R.; Gonzalez-Alba, J. M.; Galan, J. C. CTX-M Enzymes: Origin and Diffusion. *Front Microbiol* [Online] **2012**, *3*, Article Archive. doi: 10.3389/fmicb.2012.00110 (accessed Dec 7, 2014)
17. Poirel, L.; Naas, T.; Nordmann, P. Diversity, epidemiology, and genetics of class D beta-lactamases. *Antimicrob Agents Chemother* **2010**, *54*, 24-38.
18. Thomas, P. W.; Zheng, M.; Wu, S.; Guo, H.; Liu, D.; Xu, D.; Fast, W. Characterization of Purified New Delhi Metallo-beta-lactamase-1. *Biochemistry* **2011**, *50*, 10103-10113.
19. Page, M. I.; Badarau, A. The mechanisms of catalysis by metallo beta-lactamases. *Bioinorg Chem Appl* [Online] **2008**, 576297, Article Archive. doi: 10.1155/2008/576297 (accessed Dec 7, 2014)
20. Bounaga, S.; Laws, A. P.; Galleni, M.; Page, M. I. The mechanism of catalysis and the inhibition of the *Bacillus cereus* zinc-dependent beta-lactamase. *Biochem J* **1998**, *331* (Pt 3), 703-11.
21. Goto, M.; Takahashi, T.; Yamashita, F.; Koreeda, A.; Mori, H.; Ohta, M.; Arakawa, Y. Inhibition of the metallo-beta-lactamase produced from *Serratia marcescens* by thiol compounds. *Biol Pharm Bull* **1997**, *20*, 1136-40.
22. Felten, A.; Grandry, B.; Lagrange, P. H.; Casin, I. Evaluation of three techniques for detection of low-level methicillin-resistant *Staphylococcus aureus* (MRSA): a disk diffusion method with cefoxitin and moxalactam, the Vitek 2 system, and the MRSA-screen latex agglutination test. *J Clin Microbiol* **2002**, *40*, 2766-71.
23. Livermore, D. M.; Brown, D. F. Detection of beta-lactamase-mediated resistance. *J Antimicrob Chemother* **2001**, *48* Suppl 1, 59-64.
24. Priano, G.; Ruzal, S. M.; Battaglini, F. An Electrochemiluminescent Method for the Detection of beta-Lactamases in Microorganisms. *Anal Biochem* **2001**, *290*, 379-382.
25. Montgomery, K.; L. Raymundo, J.; Drew, W. L. Chromogenic cephalosporin spot test to detect beta-lactamase in clinically significant bacteria. *J Clin Microbiol.* **1979**, *9*, 205-207.
26. O'Callaghan, C. H.; Morris, A.; Kirby, S. M.; Shingler, A. H. Novel Method for Detection of β -Lactamases by Using a Chromogenic Cephalosporin Substrate. *Antimicrob Agents Chemother* **1972**, *1*, 283-288.
27. Orenge, S.; James, A. L.; Manafi, M.; Perry, J. D.; Pincus, D. H. Enzymatic substrates in microbiology. *J Microbiol Meth* **2009**, *79*, 139-155.

28. Bebrone, C.; Moali, C.; Mahy, F.; Rival, S.; Docquier, J. D.; Rossolini, G. M.; Fastrez, J.; Pratt, R. F.; Frère, J.; Galleni, M. CENTA as a Chromogenic Substrate for Studying β -Lactamases. *Antimicrob Agents Chemother* **2001**, *45*, 1868-1871.
29. Liu, R.; Liew, R.; Zhou, J.; Xing, B. A simple and specific assay for real-time colorimetric visualization of beta-lactamase activity by using gold nanoparticles. *Angew Chem* **2007**, *46*, 8799-803.
30. Howard, B. J. *Clinical and pathogenic microbiology*; Mosby: 1994.
31. Zou, L.; Cheong, W.; Chung, W.; Leung, Y.; Wong, K.; Wong, M.; Chan, P. A Switch-On Fluorescence Assay for Bacterial β -Lactamases with Amyloid Fibrils as Fluorescence Enhancer and Visual Tool. *Chem Eur J* **2010**, *16*, 13367-13371.
32. Liang, P.; Sanchez, R. I.; Martin, M. T. Electrochemiluminescence-based detection of beta-lactam antibiotics and beta-lactamases. *Anal Chem* **1996**, *68*, 2426-31.
33. He, L.; Cox, K. A.; Danielson, N. D. Chemiluminescence Detection of Amino Acids, Peptides, and Proteins Using Tris-2,2'-Bipyridine Ruthenium (III). *Anal Lett* **1990**, *23*, 195-210.
34. Eustis, S.; El-Sayed, M. A. Why gold nanoparticles are more precious than pretty gold: Noble metal surface plasmon resonance and its enhancement of the radiative and nonradiative properties of nanocrystals of different shapes. *Chem Soc Rev* **2006**, *35*, 209-217.
35. Boyd, D. B.; Lunn, W. H. W. Electronic-Structures of Cephalosporins and Penicillins .9. Departure of a Leaving Group in Cephalosporins. *J Med Chem* **1979**, *22*, 778-784.
36. Faraci, W. S.; Pratt, R. F. Mechanism of inhibition of the PC1 β -lactamase of *Staphylococcus aureus* by cephalosporins: importance of the 3'-leaving group. *Biochemistry* **1985**, *24*, 903-910.
37. Zlokarnik, G.; Negulescu, P. A.; Knapp, T. E.; Mere, L.; Burren, N.; Feng, L.; Whitney, M.; Roemer, K.; Tsien, R. Y. Quantitation of Transcription and Clonal Selection of Single Living Cells with β -Lactamase as Reporter. *Science* **1998**, *279*, 84-88.
38. Gao, W.; Xing, B.; Tsien, R. Y.; Rao, J. Novel Fluorogenic Substrates for Imaging β -Lactamase Gene Expression. *J Am Chem Soc* **2003**, *125*, 11146-11147.
39. Xing, B.; Khanamiryan, A.; Rao, J. Cell-Permeable Near-Infrared Fluorogenic Substrates for Imaging β -Lactamase Activity. *J Am Chem Soc* **2005**, *127*, 4158-4159.
40. Yao, H.; So, M.; Rao, J. A Bioluminogenic Substrate for In Vivo Imaging of β -Lactamase Activity. *Angew Chem Int Ed Engl* **2007**, *46*, 7031-7034.

41. Rukavishnikov, A.; Gee, K. R.; Johnson, I.; Corry, S. Fluorogenic cephalosporin substrates for β -lactamase TEM-1. *Anal Biochem* **2011**, *419*, 9-16.
42. Xie, H.; Mire, J.; Kong, Y.; Chang, M.; Hassounah, H. A.; Thornton, C. N.; Sacchettini, J. C.; Cirillo, J. D.; Rao, J. Rapid point-of-care detection of the tuberculosis pathogen using a BlaC-specific fluorogenic probe. *Nat Chem* **2012**, *4*, 802-809.
43. Mroczkowska, J. E.; Barlow, M. Fitness Trade-Offs in blaTEM Evolution. *Antimicrob Agents Chemother* **2008**, *52*, 2340-2345.
44. Salverda, M. L. M.; De Visser, J. A. G. M.; Barlow, M. Natural evolution of TEM-1 β -lactamase: experimental reconstruction and clinical relevance. *FEMS Microbiol Rev* **2010**, *34*, 1015-1036.
45. Brown, N. G.; Shanker, S.; Prasad, B. V. V.; Palzkill, T. Structural and Biochemical Evidence That a TEM-1 beta-Lactamase N170G Active Site Mutant Acts via Substrate-assisted Catalysis. *J Bio Chem* **2009**, *284*, 33703-33712.
46. Ness, S.; Martin, R.; Kindler, A. M.; Paetzel, M.; Gold, M.; Jensen, S. E.; Jones, J. B.; Strynadka, N. C. J. Structure-Based Design Guides the Improved Efficacy of Deacylation Transition State Analogue Inhibitors of TEM-1 beta-Lactamase. *Biochemistry* **2000**, *39*, 5312-5321.

Chapter 2

Materials and Methods

2.1 Chemicals and reagents

7-Amino-3-chloromethyl 3-cephem-4-carboxylic acid diphenylmethyl ester hydrochloride (7-ACMA) was purchased from Yick-Vic Chemicals & Pharmaceuticals (Hong Kong) Ltd. 2,6-Lutidine, 4-aminothiophenol, sodium iodide (NaI), N-methylmorphine (NMM), dansyl chloride, pyridine, trifluoroacetic acid (TFA), anisole, penicillin G, ampicillin, tazobactam, ceftazidime, methicillin, oxallin, aspirin, cephalothin, guanidine hydrochloride, bovine κ -casein, hen egg white lysozyme, and ammonium acetate were purchased from Sigma-Aldrich (St. Louis, MO). Sodium phosphate salts (dibasic and monobasic) and nitrocefin were purchased from Carolina and Becton Dickinson, respectively.

2.2 Instruments

NMR experiments were performed using a Bruker DPX 400 MHz spectrometer. A Perkin Elmer LS-55 spectrofluorometer was used in fluorescence and enzyme kinetic studies. Electrospray ionization mass spectrometric (ESI-MS) experiments were performed using a Micromass Q-ToF-2TM mass spectrometer. UV-Visible absorption measurements were done using a Cary 4000 UV/Vis spectrophotometer.

2.3 Synthesis of the fluorescent dansyl-conjugated beta-lactam antibiotic

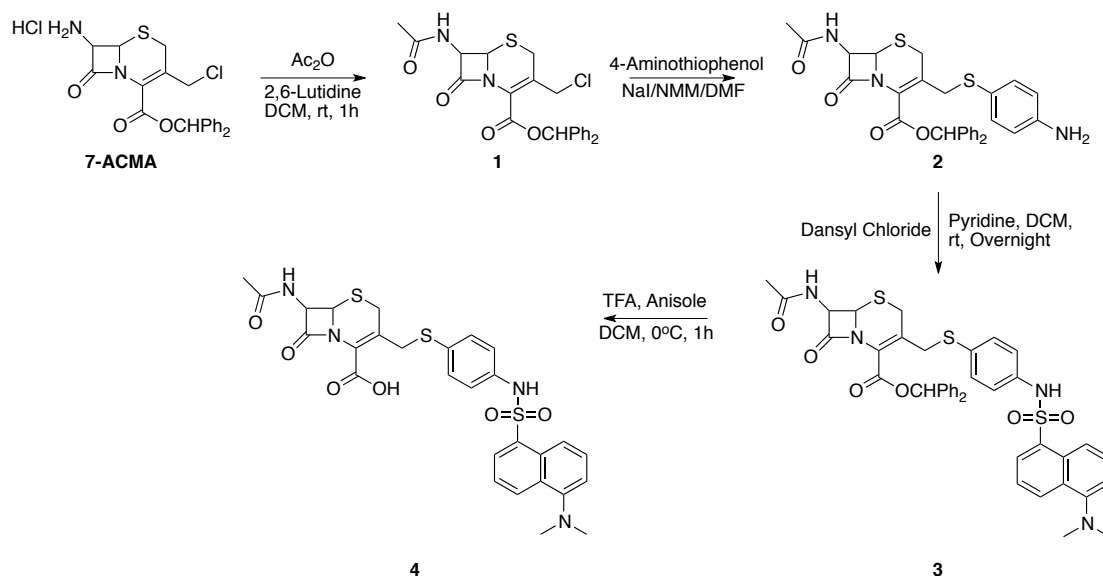


Figure 2-1 Synthetic scheme of the fluorescent dansyl-conjugated beta-lactam antibiotic (Complex 4).

Preparation of 1:

7-ACMA (0.902 g, 2 mmol) was suspended in 60 mL of dichloromethane (DCM), and 2,6-lutidine (464 μ L, 4 mmol) was added to the suspension followed by Ac₂O (378 μ L, 4 mmol). The mixture was stirred for 1 h at room temperature.¹ After removing the solvent with a rotary evaporator, the residue was purified by flash chromatography with silica gel (eluent: hexanes/ethyl acetate = 1:1 v/v), yielding 0.72 g (75%) of the product.¹ ¹H NMR (400 Mhz, CDCl₃) δ 7.44–7.26 (m, 10H), 6.97 (s, 1H), 6.48–6.46 (d, J = 8 Hz, 1H), 5.90–5.86 (dd, J = 4.8 Hz and 8.8 Hz, 1H), 4.99–4.98 (d, J = 5.2 Hz, 1H), 4.39 (s, 2H), 3.63–3.45 (m, 2H), 2.04 (s, 3H).¹³C NMR (100 Mhz, CDCl₃) δ 170.4, 165.2, 160.5, 139.0, 138.9, 128.6, 128.3, 128.2, 127.7, 127.0, 126.9, 125.7, 79.9, 59.2, 57.7, 43.1, 27.2, 22.7. ESIMS m/z : 456.99 [M + H]⁺; HRESIMS m/z : 421.1213 calcd for C₂₃H₂₁N₂O₄S.

Preparation of 2:

1 (0.46 g, 1 mmol) was first suspended in DMF (6 mL) and then added with 4-aminothiophenol (0.17 g, 1.3 mmol) and NMM (80 μ L). A catalytic amount of NaI (0.02 g) was dissolved in DMF (2 mL) and then added to the reaction mixture. The reaction mixture was stirred at room temperature for 5 h and then diluted with ethyl acetate, followed by washing with brine and water.² The crude mixture was first separated by flash chromatography with silica gel with 100 mL of DCM/ethyl acetate eluent (10:1 v/v) and then hexane/ethyl acetate (8:2 v/v) to produce the product (0.137 g, 50%).¹ H NMR (400 Mhz, CDCl₃) δ 7.42-7.26 (m, 10H), 7.10–7.08 (d, J = 8.4 Hz, 2H), 6.76 (s, 1H), 6.44–6.42 (d, J = 8 Hz, 3H), 5.80–5.76 (dd, J = 4.8 Hz and 8.8 Hz, 1H), 5.29 (s, 1H), 4.88–4.87 (d, J = 4.8 Hz, 1H), 4.17-4.13 (d, J = 13.2 Hz, 1H), 3.61–3.51 (m, 3H), 3.34–3.29 (d, J = 18 Hz, 1H), 2.94–2.88 (d, J = 27.2 Hz, 2H), 2.05 (s, 3H).¹³C NMR (100 Mhz, CDCl₃) δ . 170.12, 164.98, 160.58, 146.99, 139.60, 139.36, 135.59, 132.83, 128.48, 128.37, 128.05, 127.89, 127.64, 126.96, 124.08, 120.71, 115.43, 79.11, 60.33, 59.01, 57.80, 38.89, 28.68, 22.81, 20.98, 14.15. ESIMS m/z : 546.2 [M+H]⁺; HRESIMS m/z : 546.1533 calcd for C₂₉H₂₈N₃O₄S₂.

Preparation of 3:

2 (0.22 g, 0.4 mmol) was suspended in DCM (10 mL) and then added with pyridine (2 mL, 25 mmol). Dansyl chloride (0.11 g, 0.4 mmol) was then added to the mixture and stirred overnight. The mixture was treated with NaOH until reaching pH 7 and washed with water and brine. The crude product was then purified by flash chromatography with silica gel (eluent: hexane/ethyl acetate = 1:1), yielding 0.173 g of **3** obtained (55%).¹ H NMR (400 Mhz, d-acetone) δ 8.58–8.56 (d, J = 8 Hz, 1H),

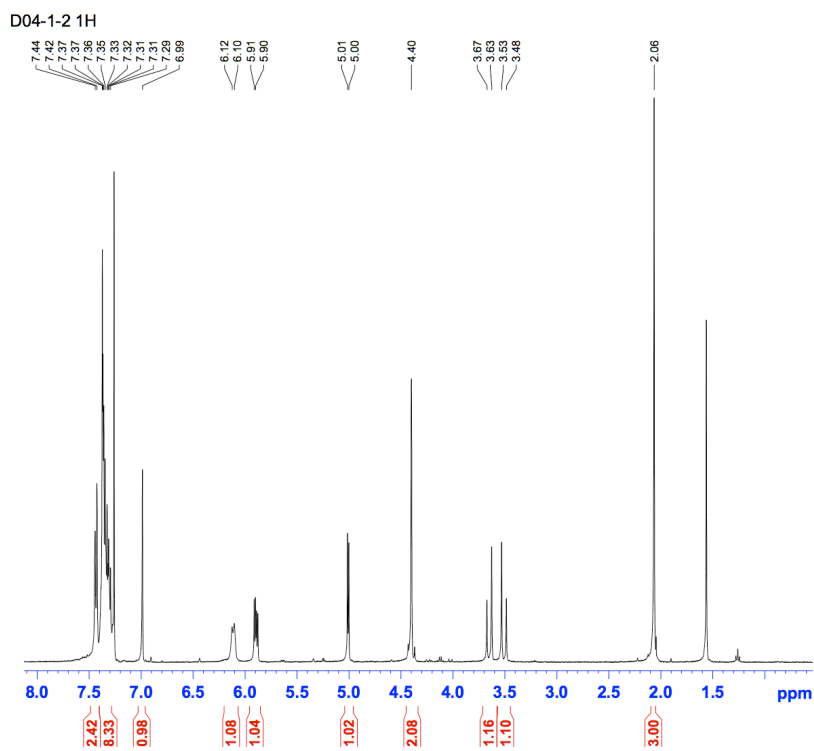
8.50–8.47 (d, $J = 12$ Hz, 1H) 8.29–8.27 (dd, $J = 1.2$ Hz and 7.2 Hz, 1H), 7.92–7.90 (d, $J = 4.4$ Hz, 1H), 7.66–7.50 (m, 2H), 7.29–7.30 (m, 15H), 7.11–7.10 (d, $J = 3.6$ Hz, 4H), 6.87 (s, 1H), 5.87–5.83 (dd, $J = 4.8$ Hz and 8.8 Hz, 1H), 5.66 (s, 1H). ^{13}C NMR (100 Mhz, d-acetone) δ 169.65, 165.21, 160.68, 152.02, 140.03, 139.89, 137.25, 135.07, 132.91, 132.42, 130.60, 130.45, 130.01, 129.81, 129.11, 129.59, 128.57, 128.51, 128.39, 128.29, 128.14, 127.98, 127.83, 127.79, 127.32, 126.87, 126.59, 126.54, 124.56, 123.17, 120.52, 120.33, 118.97, 115.28, 78.82, 59.33, 59.24, 58.08, 44.65, 37.11, 31.69, 27.80, 22.37, 21.46, 13.39. ESIMS m/z : 779.2 $[\text{M}+\text{H}]^+$; HRESIMS m/z : 779.2049 $[\text{M}+\text{H}]^+$ calcd for $\text{C}_{41}\text{H}_{39}\text{N}_4\text{O}_6\text{S}_3$.

Preparation of 4:

3 (0.17 g, 0.2 mmol) was suspended in DCM (10 mL), followed by the addition of TFA (4.5 mL) and anisole (500 μL). The reaction was stirred in an ice bath for 1 h. The DCM and TFA were removed using a rotatory evaporator and then stored under strong vacuum to remove the remaining TFA. The product was then precipitated with cool hexane and filtered using a Buchner funnel to collect the solid. The solid was then re-dissolved in a minimal amount of acetone, and the undissolved solid was removed by filtration. The product was then re-precipitated with a minimal amount of cool hexane, yielding 0.10 g of **4** (31%). ^1H NMR (400 Mhz, CD_3OD) δ 8.51-8.49 (d, $J = 8$ Hz, 1H), 8.45-8.43 (d, $J = 8$ Hz, 1H), 8.20-8.17 (dd, $J = 4$ Hz and 6.4 Hz, 1H), 7.63-7.59 (d, $J = 0.8$ Hz and 8 Hz, 1H), 7.54-7.50 (dd, $J = 1.2$ and 8 Hz, 1H), 7.33-7.31 (d, $J = 8$ Hz, 1H), 7.31-7.18 (d, $J = 8$ Hz, 2H), 6.95-6.93 (d, $J = 8$ Hz, 2H), 5.59-5.58 (d, $J = 4$ Hz, 1H), 4.78-4.77 (d, $J = 4$ Hz, 1H), 4.23-4.20 (d, $J = 12$ Hz, 1H), 3.75-3.71 (d, $J = 16$ Hz, 1H), 3.53-3.48 (d, $J = 20$ Hz, 1H), 3.36 (s, 1H) , 2.90 (s, 6H),

2.02 (s, 3H). ^{13}C NMR (100 Mhz, CD_3OD) δ 172.30, 164.80, 163.13, 150.54, 137.32, 134.75, 133.36, 131.37, 130.00, 129.67, 129.45, 129.27, 129.09, 127.81, 124.78, 123.13, 120.29, 119.60, 115.44, 59.16, 57.90, 44.55, 36.90, 27.69, 20.66, 12.96. ESIMS m/z : 613.1 $[\text{M}+\text{H}]^+$; HRESIMS m/z : 613.1237 calcd for $\text{C}_{28}\text{H}_{29}\text{N}_4\text{O}_6\text{S}_3$.

Figure 2-2 ¹H NMR of 1

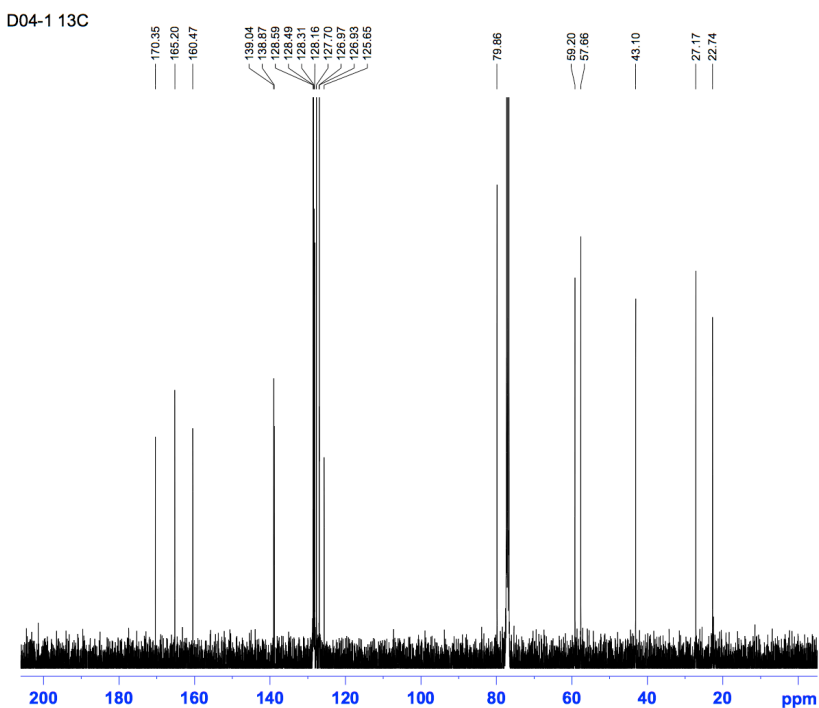


```

NAME      D04-1-2
EXPNO    1
PROCNO   1
Date_    20140323
Time     22.14
INSTRUM  spect
PROBHD   5 mm PABBO BB-
PULPROG  zg30
TD       32768
SOLVENT  CDCl3
NS       16
DS       2
SWH      6009.615 Hz
FIDRES   0.163399 Hz
AQ       2.7263477 sec
RG       322
DW       83.200 usec
DE       6.50 usec
TE       298.0 K
D1       1.00000000 sec
D10      1

===== CHANNEL f1 =====
NUC1     1H
P1       14.70 usec
PL1      0.00 dB
PL1W     11.88122272 W
SFO1     400.1328009 MHz
SI       32768
SF       400.1300100 MHz
WDW      EM
SSB      0
LB       0.30 Hz
GB       0
PC       1.00
    
```

Figure 2-3 ¹³C NMR of 1



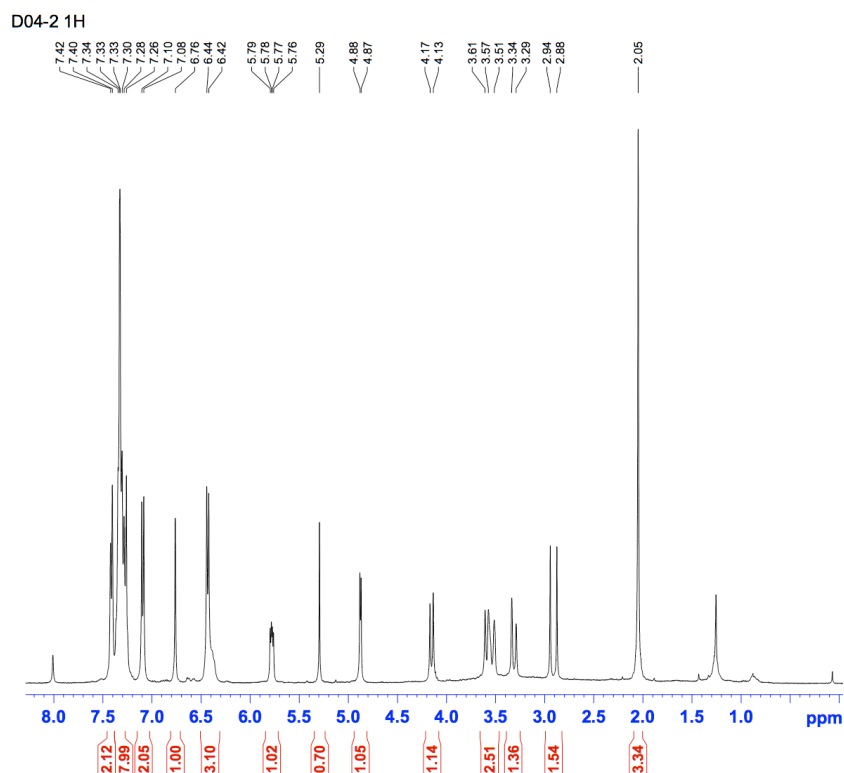
```

NAME      D04-1-13C
EXPNO    1
PROCNO   1
Date_    20130608
Time     14.11
INSTRUM  spect
PROBHD   5 mm PABBO BB-
PULPROG  zgpg30
TD       65536
SOLVENT  CDCl3
NS       514
DS       2
SWH      24038.461 Hz
FIDRES   0.366798 Hz
AQ       1.3631988 sec
RG       203
DW       20.800 usec
DE       6.50 usec
TE       300.2 K
D1       2.00000000 sec
D11      0.03000000 sec
D10      1

===== CHANNEL f1 =====
NUC1     13C
P1       9.50 usec
PL1      -2.00 dB
PL1W     58.52175522 W
SFO1     100.6228298 MHz

===== CHANNEL f2 =====
CPDPRG2  waltz16
NUC2     1H
PCPD2    80.00 usec
PL2      0.00 dB
PL12     15.00 dB
PL13     15.00 dB
PL2W     11.88122272 W
PL12W    0.37571725 W
PL13W    0.37571725 W
SFO2     400.1316005 MHz
SI       32768
SF       100.6127726 MHz
WDW      EM
SSB      0
LB       1.00 Hz
GB       0
PC       1.40
    
```

Figure 2-4 ¹H NMR of 2

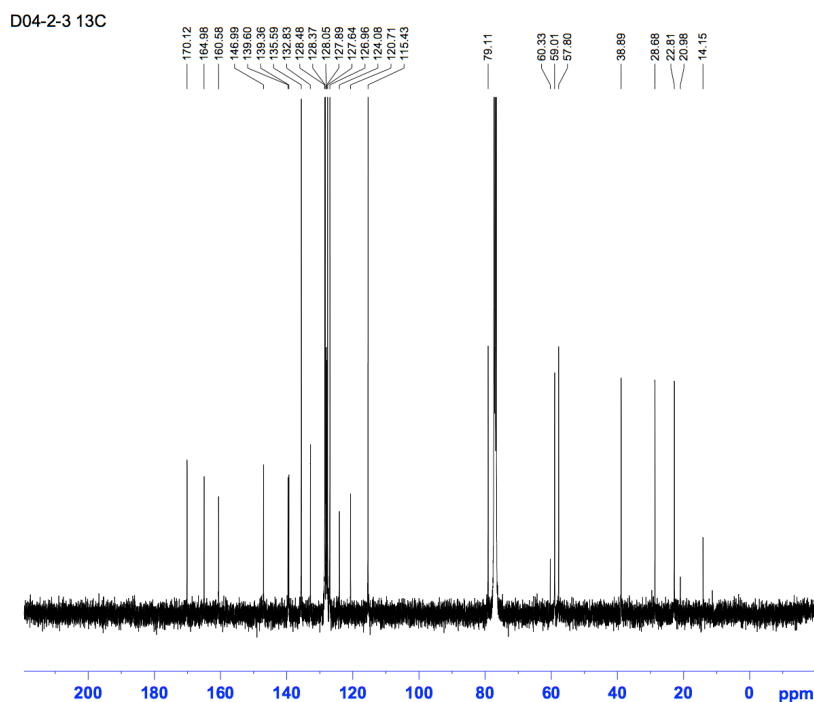


```

NAME      D04-2
EXPNO    1
PROCNO   1
Date_    20130613
Time     17.32
INSTRUM  spect
PROBHD   5 mm PABBO BB-
PULPROG  zg30
TD        32768
SOLVENT  CDCl3
NS        16
DS        2
SWH       6009.615 Hz
FIDRES    0.183399 Hz
AQ        2.7263477 sec
RG        144
DW        83.200 usec
DE        6.50 usec
TE        298.5 K
D1        1.00000000 sec
TD0       1

===== CHANNEL f1 =====
NUC1      1H
P1        14.70 usec
PL1       0.00 dB
PL1W      11.88122272 W
SFO1      400.1328009 MHz
SI        32768
SF        400.1300100 MHz
WDW       EM
SSB       0
LB        0.30 Hz
GB        0
PC        1.00
    
```

Figure 2-5 ¹³C NMR of 2



```

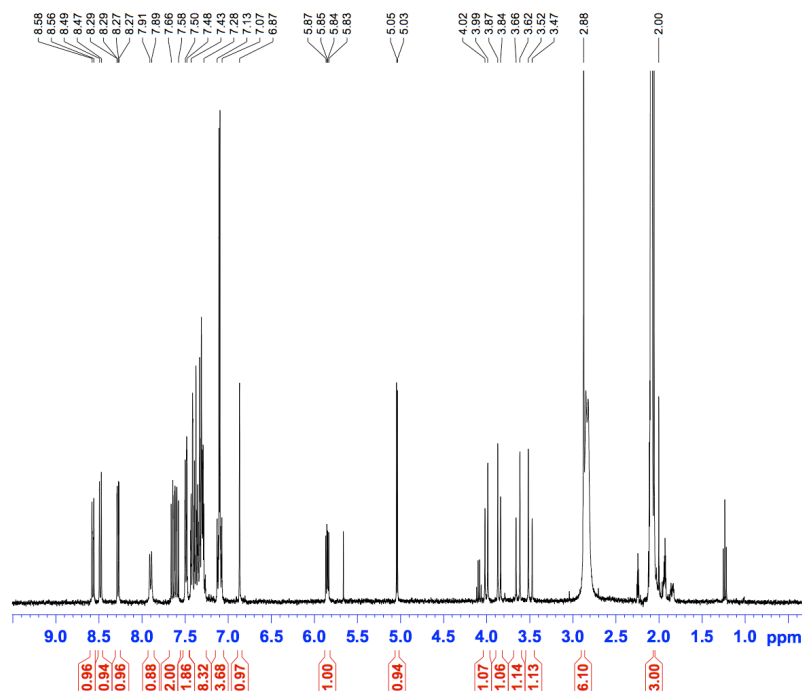
NAME      D04-2-3 13C
EXPNO    1
PROCNO   1
Date_    20140318
Time     23.57
INSTRUM  spect
PROBHD   5 mm PABBO BB-
PULPROG  zgpg30
TD        65536
SOLVENT  CDCl3
NS        5000
DS        2
SWH       24038.461 Hz
FIDRES    0.366798 Hz
AQ        1.3631988 sec
RG        181
DW        20.800 usec
DE        6.50 usec
TE        299.0 K
D1        2.00000000 sec
D11      0.03000000 sec
TD0       1

===== CHANNEL f1 =====
NUC1      13C
P1        9.50 usec
PL1       -2.00 dB
PL1W      58.52175522 W
SFO1      100.6228298 MHz

===== CHANNEL f2 =====
CPDPRG2  waltz16
NUC2      1H
PCPD2     80.00 usec
PL2       0.00 dB
PL12      15.00 dB
PL13      15.00 dB
PL2W      11.88122272 W
PL12W     0.37571725 W
PL13W     0.37571725 W
SFO2      400.1316005 MHz
SI        32768
SF        100.6127726 MHz
WDW       EM
SSB       0
LB        1.00 Hz
GB        0
PC        1.40
    
```

Figure 2-6 ¹H NMR of 3

D04-3-5 1H

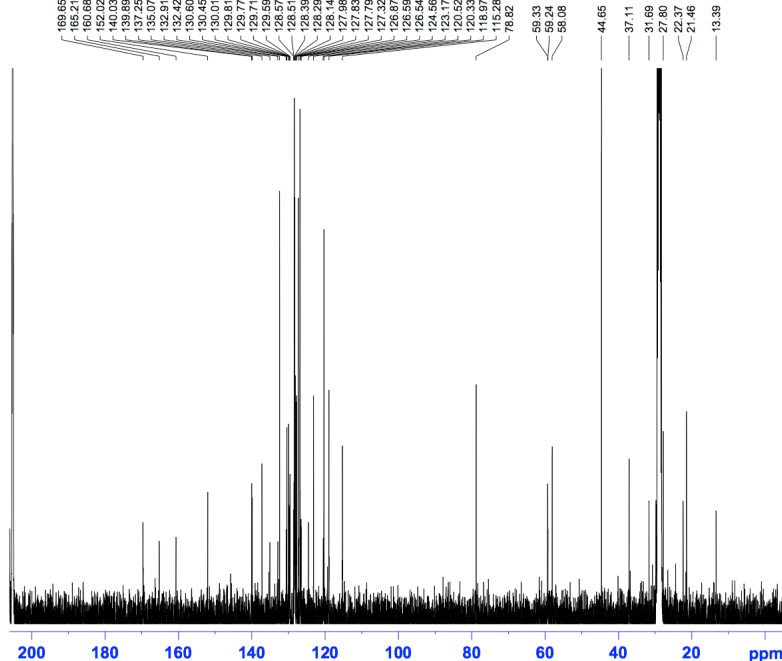


```

NAME      D04-3-5
EXPNO     1
PROCNO    1
Date_     20140326
Time      19.53
INSTRUM   spect
PROBHD    5 mm PABBO BB-
PULPROG   zg30
TD         32768
SOLVENT   Acetone
NS         16
DS         2
SWH        6009.615 Hz
FIDRES     0.183399 Hz
AQ         2.7263477 sec
RG         362
DW         83.200 usec
DE         6.50 usec
TE         298.2 K
D1         1.00000000 sec
D10       1
===== CHANNEL f1 =====
NUC1      1H
P1         14.70 usec
PL1        0.00 dB
PL1W      11.88122272 W
SFO1      400.1328009 MHz
SI         32768
SF         400.1299907 MHz
WDW        EM
SSB        0
LB         0.30 Hz
GB         0
PC         1.00
    
```

Figure 2-7 ¹³C NMR of 3

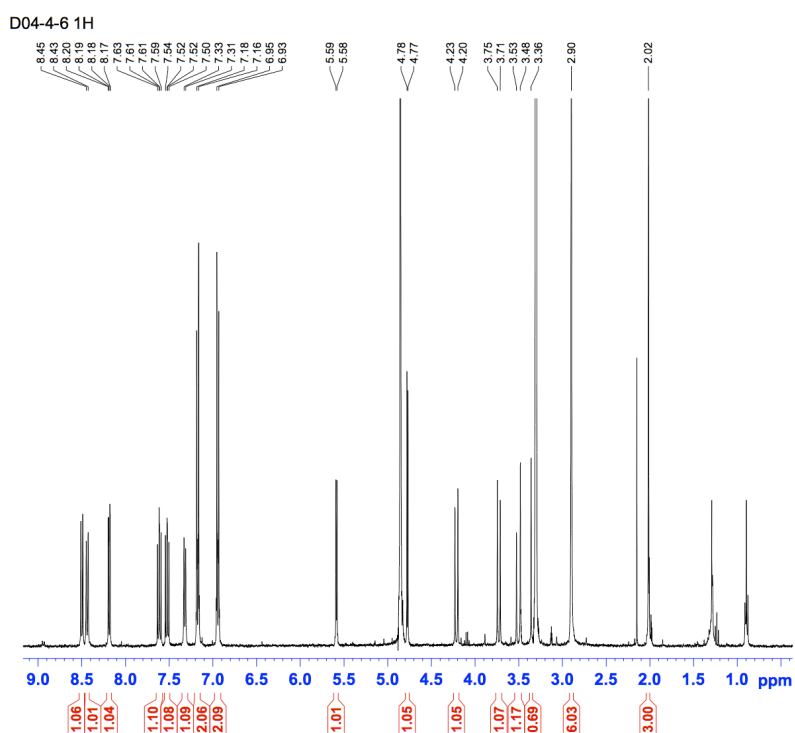
D04-3-4 13C



```

NAME      D04-3-4 13C
EXPNO     1
PROCNO    1
Date_     20140405
Time      18.44
INSTRUM   spect
PROBHD    5 mm PABBO BB-
PULPROG   zgpg30
TD         65536
SOLVENT   Acetone
NS         1983
DS         2
SWH        24038.461 Hz
FIDRES     0.366798 Hz
AQ         1.3631988 sec
RG         114
DW         20.800 usec
DE         6.50 usec
TE         298.8 K
D1         2.00000000 sec
D11       0.03000000 sec
D10       1
===== CHANNEL f1 =====
NUC1      13C
P1         9.50 usec
PL1        -2.00 dB
PL1W      58.52175522 W
SFO1      100.6228298 MHz
===== CHANNEL f2 =====
CPDPRG2   waltz16
NUC2      1H
PCPD2     80.00 usec
PL2        0.00 dB
PL12      15.00 dB
PL13      15.00 dB
PL2W      11.88122272 W
PL12W     0.37571725 W
PL13W     0.37571725 W
SFO2      400.1316005 MHz
SI         32768
SF         100.6127726 MHz
WDW        EM
SSB        0
LB         1.00 Hz
GB         0
PC         1.40
    
```

Figure 2-8 ¹H NMR of 4

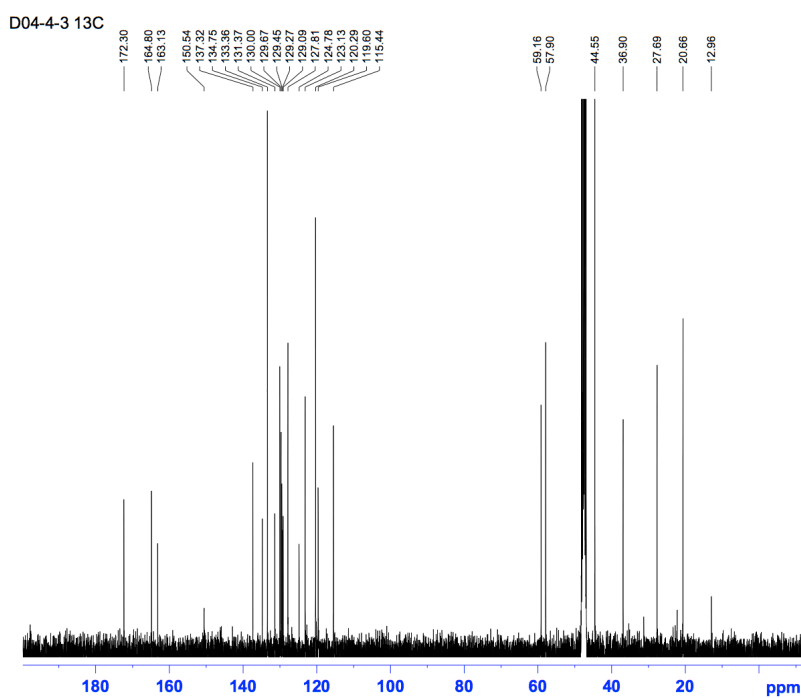


```

NAME      D04-4-6
EXPNO    1
PROCNO   1
Date_    20140327
Time     13.57
INSTRUM  spect
PROBH    5 mm PABBO BB-
PULPROG  zg30
TD        32768
SOLVENT  MeOD
NS        16
DS        2
SWH      6009.615 Hz
FIDRES   0.183399 Hz
AQ        2.7263477 sec
RG        228
DW        83.200 usec
DE        6.50 usec
TE        297.9 K
D1        1.00000000 sec
TD0       1

===== CHANNEL f1 =====
NUC1      1H
P1        14.70 usec
PL1       0.00 dB
PL1W     11.88122272 W
SFO1     400.1328009 MHz
SI        32768
SF        400.1300100 MHz
WDW       EM
SSB       0
LB        0.30 Hz
GB        0
PC        1.00
    
```

Figure 2-9 ¹³C NMR of 4



```

NAME      D04-4-3 13C
EXPNO    1
PROCNO   1
Date_    20140329
Time     22.37
INSTRUM  spect
PROBH    5 mm PABBO BB-
PULPROG  zgpg30
TD        65536
SOLVENT  MeOD
NS        1500
DS        2
SWH      24038.461 Hz
FIDRES   0.366798 Hz
AQ        1.3631988 sec
RG        322
DW        20.800 usec
DE        6.50 usec
TE        300.1 K
D1        2.00000000 sec
D11      0.03000000 sec
TD0       1

===== CHANNEL f1 =====
NUC1      13C
P1        9.50 usec
PL1       -2.00 dB
PL1W     58.52175322 W
SFO1     100.6228298 MHz

===== CHANNEL f2 =====
CPDPRG2  waltz16
NUC2      1H
PCPD2    80.00 usec
PL2       0.00 dB
PL12     15.00 dB
PL13     15.00 dB
PL2W     11.88122272 W
PL12W    0.37571725 W
PL13W    0.37571725 W
SFO2     400.1316005 MHz
SI        32768
SF        100.6127726 MHz
WDW       EM
SSB       0
LB        1.00 Hz
GB        0
PC        1.40
    
```

2.4 Preparation of the wild-type and mutant forms of the TEM-1 beta-lactamase

Both the wild-type and mutant (E166N) form of the TEM-1 beta-lactamase were produced using *E. coli* BL21 DE-3. The C-terminus of these enzymes was tagged with six histidine (His)₆. 2xTY medium was prepared by dissolving sodium chloride (5 g), yeast extract (10 g), and tryotone (16 g) in ultrapure water (1 L), and the resulting medium was sterilized by an autoclave. *E. coli* cells were incubated with kanamycin (50 µg/mL) in sterile 2xTY medium (5 mL) and then shaken at room temperature overnight. The bacterial culture was further incubated and shaken at 280 rpm at 37 °C. When OD₆₀₀ = 0.8, isopropyl beta-D-1thiogalactopyranoside (200 mg/mL) was added to the bacterial culture to induce protein expression. The culture was further incubated for 6 h and then centrifuged to yield the cell pellet. Sonication was performed to break down the bacterial cells. Finally, the TEM-1 enzyme was purified by Ni(II) affinity chromatography with a linear gradient elution of imidazole (0–0.5 M) in potassium phosphate buffer (pH 7.0). The enzyme was then dialyzed against deionized water at 4 °C, freeze-dried and stored at -20 °C.³

2.5 Fluorescence studies

The fluorescence changes of Complex 4 (10 µM) in the absence and presence of the TEM-1 beta-lactamase were monitored as a function of time using a Perkin Elmer LS-55 fluorescence spectrofluorometer. The sample solution was prepared by dissolving 0.6 mg of Complex 4 in 1.0 mL of DMSO to produce 1.0 mM stock solution. A 5.0 µL portion of this stock antibiotic solution was mixed with 50 mM sodium phosphate

(NaPi) buffer (pH 7.0) and TEM-1 (0, 0.1, 1.0 and 10 nM) to yield 500 μ L of sample solution. Fluorescence measurements were performed using a quartz cuvette with 1-cm light absorption path length, and the scan rate was 100 nm/min. Excitation and emission slits were 5 nm. Time-course fluorescence scans were performed from $\lambda = 420$ to 670 nm to obtain fluorescence spectra for 2 h at $\lambda_{\text{ex}} = 350$ nm.

In vitro drug screening

Various beta-lactam antibiotics, inhibitors and drug (penicillin G, ampicillin, tazobactam, ceftazidime, methicillin, oxacillin, aspirin and cephalothin) were used as the drug candidates in drug screening studies. The sample solution was prepared by incubating each of the drug candidates (100 μ M) with TEM-1 (1.0 nM) in 50 mM sodium phosphate buffer (pH 7.0) for 30 min. The sample solution was then mixed with Complex 4 to produce 500 μ L of sample solution, and time-course fluorescence measurements were performed using a quartz cuvette (with a 1-cm light absorption path length) at a scan rate of 100 nm/min. Excitation and emission slits were 5 nm. Time-course fluorescence scans from $\lambda = 420$ to 670 nm were performed for 2 h at $\lambda_{\text{ex}} = 350$ nm.

2.6 UV-Visible absorption measurements

The effects of penicillin G and tazobactam on the light absorption properties of nitrocefin (10 μ M) in the presence of TEM-1 were examined using a Cary 4000 UV/Vis spectrophotometer. Penicillin G (100 μ M) and tazobactam (100 μ M) were incubated with TEM-1 (1.0 nM) in 50 mM sodium phosphate buffer (pH 7.0) for 30

min. The sample solution was then mixed with nitrocefin to yield 500 μL of sample solution. UV-Visible absorption measurements were performed using a quartz cuvette of 1-cm light absorption path length. Time-course absorbance measurements were performed from $\lambda = 350$ to 600 nm for 2 h at a scan rate of 100 nm/min.

2.7 Electrospray ionization mass spectrometric (ESI-MS) studies

Detection of enzyme-substrate complexes

The formation of enzyme-substrate complexes during the enzymatic hydrolysis of Complex **4** was monitored by ESI-MS. The E166N mutant was desalted using Amicon® Ultra-15 (NMWL = 10000) centrifugal filter devices for three cycles, yielding a final volume of 150 μL before ESI-MS experiments. Complex **4** (30 μM) was incubated with the E166N mutant of TEM-1 (30 μM) in 20 mM ammonium acetate buffer (pH 7.0) for 2 h. Parts of the reaction mixture were quenched by addition of CH_3CN , which was then injected into electrospray sources at different time intervals using a Micromass Q-ToF-2TM mass spectrometer. The sample was introduced using a syringe pump (Harvard Apparatus, Model 22) at a flow rate of 5 $\mu\text{L}/\text{min}$.

The mass range was scanned from 100 to 1600 m/z to obtain the mass spectra of the complexes, and the MassLynx 4.1 Transform Program was employed to deconvolute the spectra. The spectrometer was operated using a cone and capillary voltage of 30 and 3 kV, respectively. Nitrogen was used as nebulizing gas in a fully opened setting. Nitrogen was also used as a desolvation and cone gas at a flow rate of 400 and 50 L/h, respectively.

References

1. Liu, R.; Liew, R.; Zhou, J.; Xing, B. A simple and specific assay for real-time colorimetric visualization of beta-lactamase activity by using gold nanoparticles. *Angew Chem* **2007**, *46*, 8799-803.
2. Xing, B.; Khanamiryan, A.; Rao, J. Cell-Permeable Near-Infrared Fluorogenic Substrates for Imaging β -Lactamase Activity. *J Am Chem Soc* **2005**, *127*, 4158-4159.
3. Zou, L.; Cheong, W.; Chung, W.; Leung, Y.; Wong, K.; Wong, M.; Chan, P. A Switch-On Fluorescence Assay for Bacterial β -Lactamases with Amyloid Fibrils as Fluorescence Enhancer and Visual Tool. *Chem Eur J* **2010**, *16*, 13367-13371.
4. Xie, H.; Mire, J.; Kong, Y.; Chang, M.; Hassounah, H. A.; Thornton, C. N.; Sacchetti, J. C.; Cirillo, J. D.; Rao, J. Rapid point-of-care detection of the tuberculosis pathogen using a BlaC-specific fluorogenic probe. *Nat Chem* **2012**, *4*, 802-809.

Chapter 3

Studies of the Beta-Lactamase-Sensing Function of the Fluorescent Dansyl-Conjugated Beta-Lactam Antibiotic

3.1 Introduction

Beta-lactamase detection is of particular importance in the clinical diagnosis of antibiotic-resistant bacteria and the development of new drugs against clinically significant beta-lactamases (e.g. *in vitro* drug screening of new inhibitors and new-generation beta-lactam antibiotics). In this regard, it is highly desirable to develop a specific and sensitive probe that can achieve both purposes. A good strategy is to chemically modify a beta-lactam antibiotic with an environment-sensitive fluorescent molecule because the former can serve as a specific substrate to bring the associated fluorescent molecule to the active site of beta-lactamases for specific and sensitive biosensing purposes.

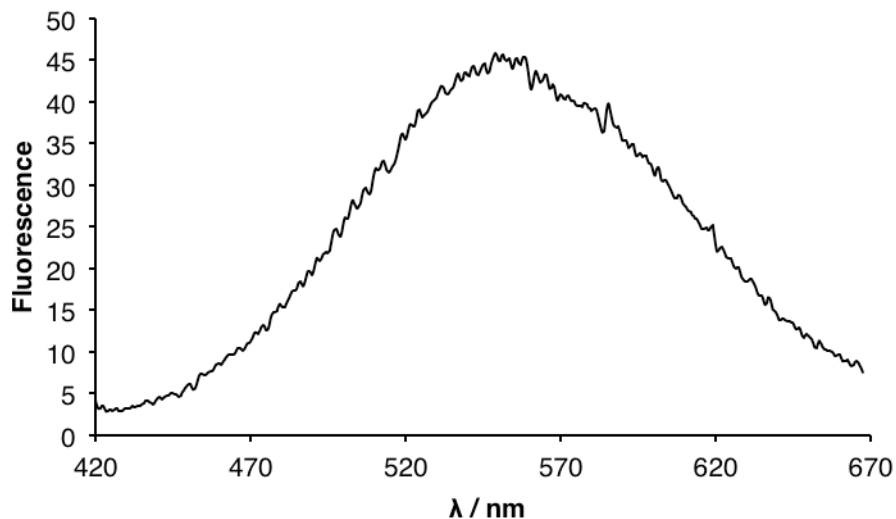
This chapter reports the fluorescence results of the fluorescent drug-based sensor (Complex **4**) constructed from a cephalosporin-type beta-lactam antibiotic (7-ACMA) which is covalently linked to the fluorescent dansyl molecule (DTA) at its 3' position¹ in response to the interaction with the TEM-1 beta-lactamase. TEM-1 was chosen because it is clinically relevant and represents the ancestor in the TEM family from which a wide variety of clinically relevant TEM variants [e.g. ESBL TEM-type beta-lactamases and inhibitor-resistant TEM (IRT) beta-lactamases] have been derived through one or two amino acid replacements.²⁻⁴ The fluorescent biosensing mechanism of Complex **4** with TEM-1 will also be discussed based on the findings from an enzyme kinetic assay and electrospray ionization mass spectrometric (ESI-MS) measurements.

3.2 Results

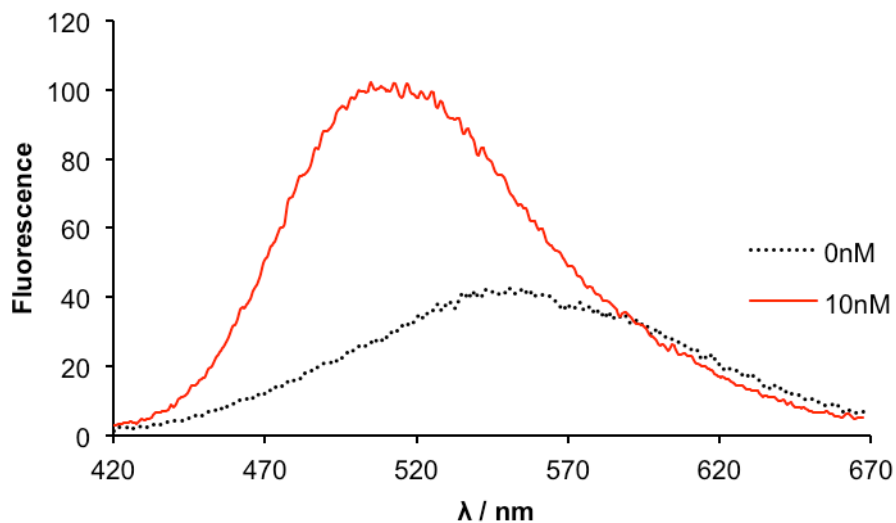
3.2.1 Fluorescence studies

The ability of Complex **4** to detect the TEM-1 beta-lactamase was examined by fluorescence spectroscopy. We first recorded a fluorescence spectrum of Complex **4** in the absence of TEM-1 with excitation at 350 nm. As shown in Figure 3-1(a), a fluorescence peak centered at 555 nm appears. In the presence of TEM-1 (10 nM), Complex **4** shows much stronger fluorescence and shifts its emission wavelength from 555 to 513 nm after incubation with TEM-1 for 2 h [Figure 3-1(b)].

The fluorescence response of Complex **4** to different concentrations of TEM-1 (0.1, 1.0 and 10 nM) was then studied. Without TEM-1, Complex **4** does not show a significant wavelength change over the time course [Figure 3-2(a)]. In the presence of 1.0 and 10 nM TEM-1, Complex **4** shows a blue shift in emission wavelength from 555 to 513 nm during the time course, and the emission wavelength decreases faster with higher [TEM-1] [Figure 3-2(a)]. We then recorded the fluorescence signals of Complex **4** at 513 nm in the absence and presence of TEM-1 as a function of time. As shown in Figure 3-2(b), Complex **4** gives no significant fluorescence changes over the time course. In the presence of TEM-1, Complex **4** gives increasing fluorescence profiles with the fluorescence signal increasing more rapidly with [TEM-1] [Figure 3-2(b)].

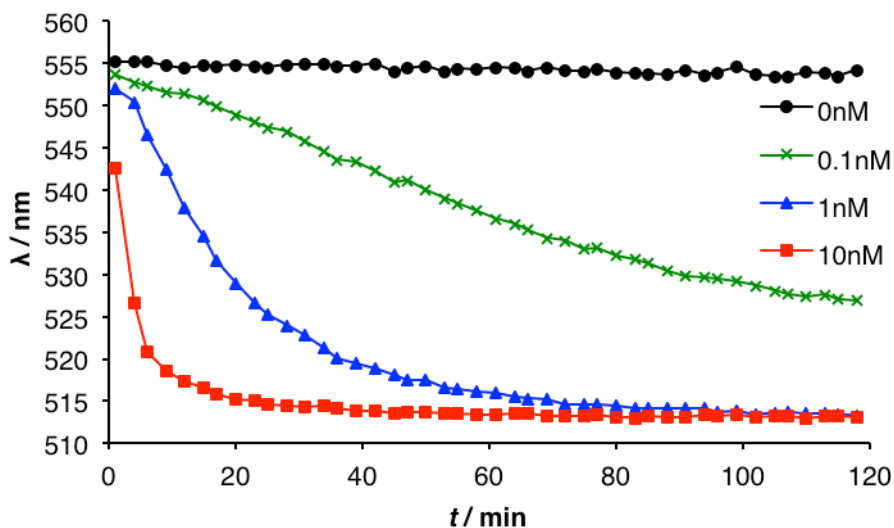


(a)

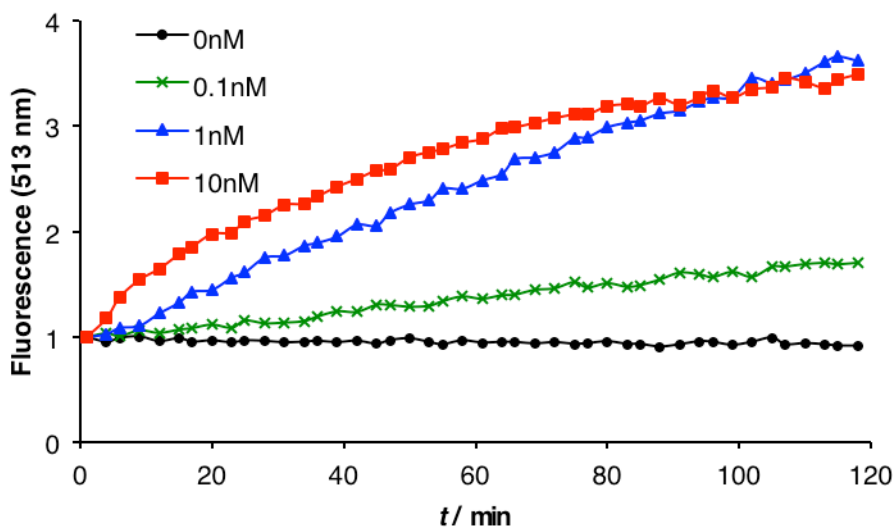


(b)

Figure 3-1 Fluorescence response of Complex **4** in the absence and presence of the TEM-1 beta-lactamase. **(a)** Fluorescence spectrum of Complex **4** alone (10 μM) and **(b)** fluorescence spectra of Complex **4** (10 μM) before incubation with TEM-1 (black line) and after incubation with TEM-1 (10 nM) for 2 h. Buffer: 50 mM sodium phosphate (pH 7.0). Fluorescence measurements on Complex **4** were done in 50 mM sodium phosphate buffer (pH 7.0) with excitation at 350 nm.



(a)



(b)

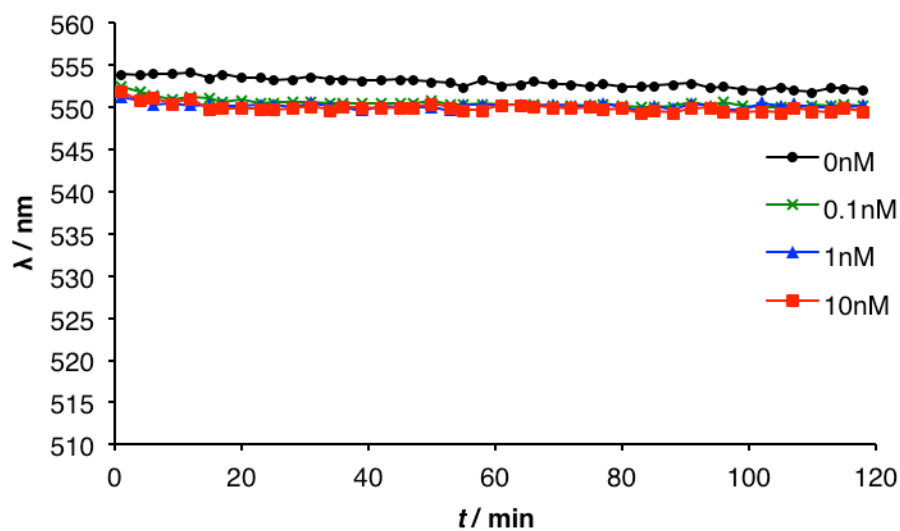
Figure 3-2 Time-course fluorescence measurements on Complex 4 in the absence and presence of TEM-1. **(a)** Plot of the emission wavelength of Complex 4 (10 μ M) with and without TEM-1; [TEM-1] = 0 nM (black), 0.1 nM (green), 1.0 nM (blue) and 10 nM (red). **(b)** Fluorescence signals (513 nm) of Complex 4 (10 μ M) incubated with 0 nM (black), 0.1 nM (green), 1.0 nM (blue) and 10 nM (red) TEM-1. Fluorescence measurements on Complex 4 were done in 50 mM sodium phosphate buffer (pH 7.0) with excitation at 350 nm.

3.2.2 Specificity studies

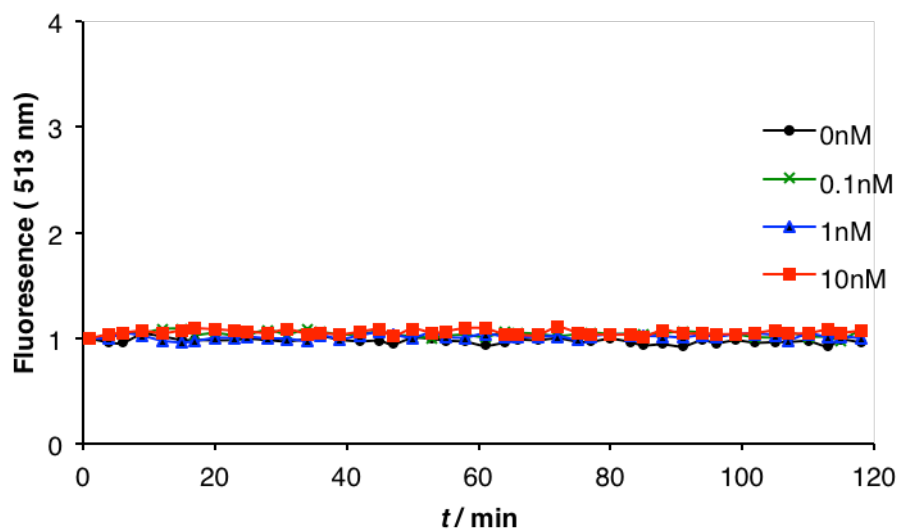
To investigate whether the characteristic fluorescence response of Complex **4** arises from its specific interaction with the TEM-1 beta-lactamase, we performed fluorescence studies of Complex **4** with other proteins, such as bovine κ -casein (0.1, 1.0 and 10 nM) and hen egg white lysozyme (0.1, 1.0 and 10 nM). For bovine κ -casein, Complex **4** does not show significant wavelength changes over the time course [Figure 3-3(a)]. Moreover, Complex **4** does not give significant fluorescence changes with bovine κ -casein over the time course (with respect to the case of Complex **4** alone) [Figure 3-3(b)]. Similar observations were also obtained with hen egg white lysozyme [Figure 3-4(a) and (b)].

To further investigate whether the emission wavelength shift and fluorescence enhancement of Complex **4** result from the binding interaction with the active site of the TEM-1 beta-lactamase, we conducted fluorescence measurements on Complex **4** under different solution conditions in which TEM-1 is in the folded and unfolded state. Without guanidine hydrochloride (a chemical denaturant that can cause proteins to unfold), Complex **4** shows a decrease in emission wavelength from 555 to 513 nm with TEM-1 (with respect to the case of Complex **4** alone) [Figure 3-5(a)]. Moreover, Complex **4** gives increasing fluorescence signals as a function of time [Figure 3-5(b)]. In the presence of 3 M guanidine hydrochloride (a solution condition under which TEM-1 becomes unfolded), Complex **4** shows no significant wavelength changes with TEM-1 (with respect to the case of Complex **4** alone) [Figure 3-5(a)]. Interestingly, Complex **4** does not show a significant fluorescence enhancement with TEM-1 in the

presence of 3 M guanidine hydrochloride (relative to the case of Complex **4** alone)
[Figure 3-5(b)].

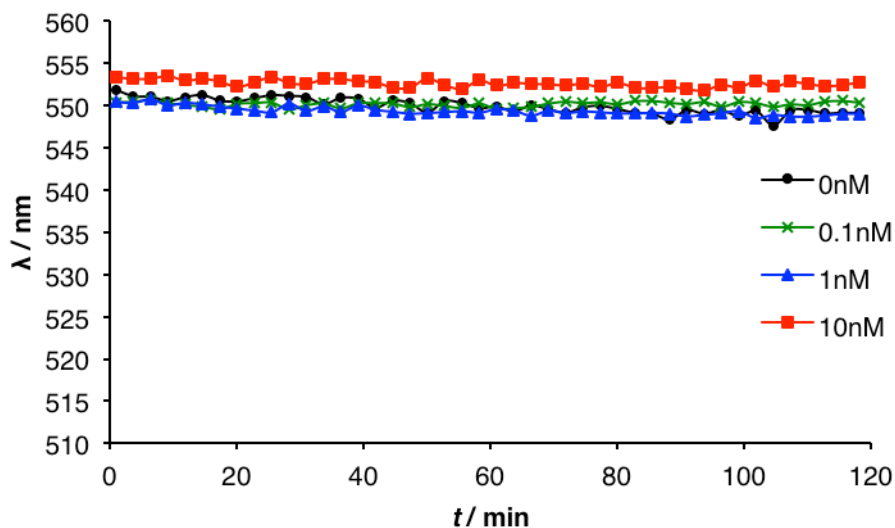


(a)

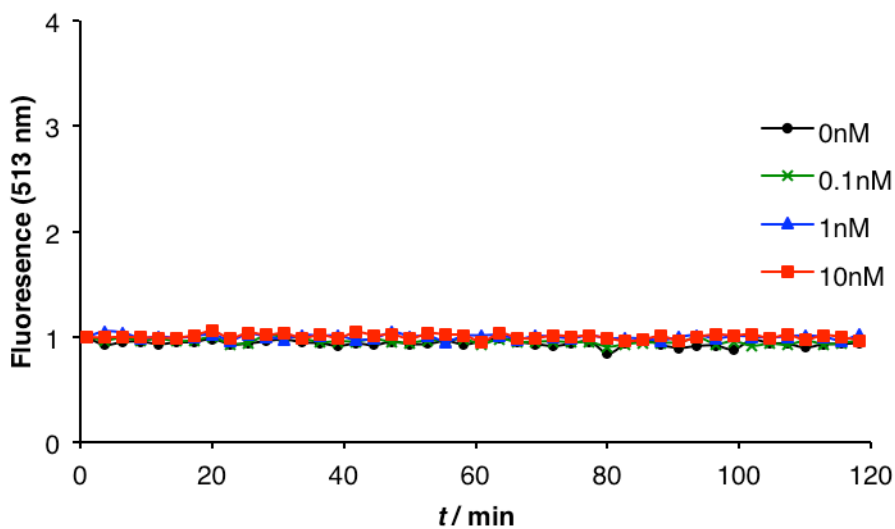


(b)

Figure 3-3 Time course fluorescence measurements of Complex 4 with bovine κ -casein. **(a)** Plot of the emission wavelength of Complex 4 (10 μ M) with different concentrations of bovine κ -casein. [Bovine κ -casein]: 0 nM (black), 0.1 nM (green), 1.0 nM (blue) and 10 nM (red). **(b)** Fluorescence signals (513 nm) of Complex 4 with 0 nM (black), 0.1 nM (green), 1.0 nM (blue) and 10 nM (red) bovine κ -casein at different time intervals. Fluorescence measurements on Complex 4 were done in 50 mM sodium phosphate buffer (pH 7.0) with excitation at 350 nm.

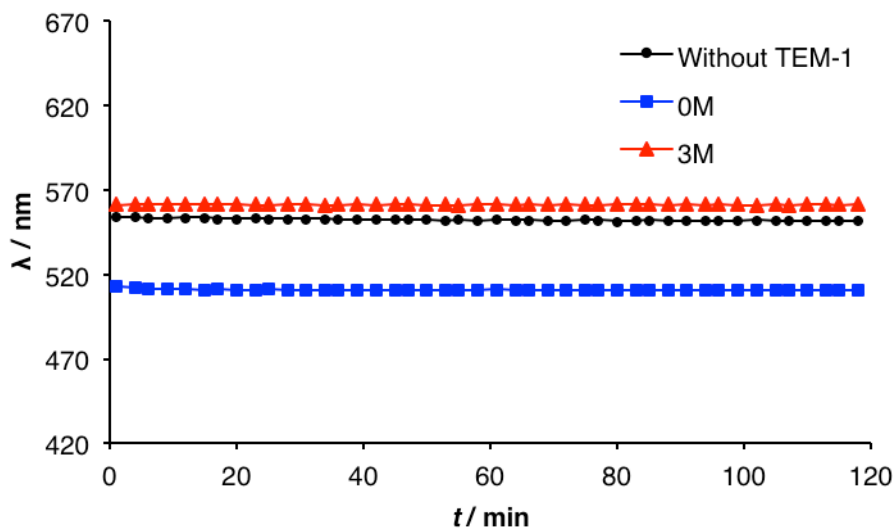


(a)

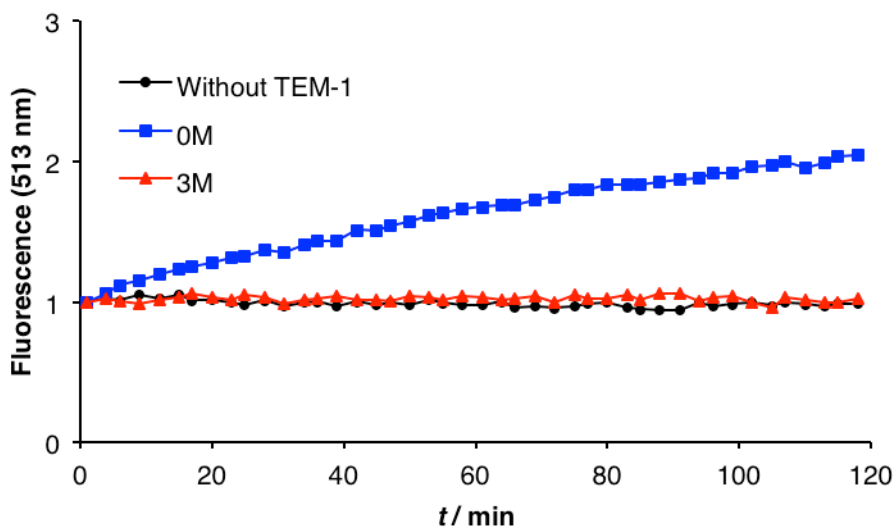


(b)

Figure 3-4 Time course fluorescence measurements of Complex **4** with hen egg white lysozyme. **(a)** Plot of the emission wavelength of Complex **4** (10 μ M) with different concentrations of hen egg white lysozyme. [Lysozyme]: 0 nM (black), 0.1 nM (green), 1.0 nM (blue) and 10 nM (red). **(b)** Fluorescence signals (513 nm) of Complex **4** with 0 nM (black), 0.1 nM (green), 1.0 nM (blue) and 10 nM (red) hen egg white lysozyme at different time intervals. Fluorescence measurements on Complex **4** were done in 50 mM sodium phosphate buffer (pH 7.0) with excitation at 350 nm.



(a)

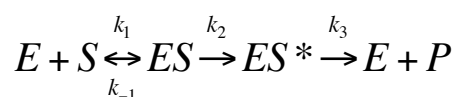


(b)

Figure 3-5 Time-course fluorescence measurements of Complex 4 with and without TEM-1 under different solution conditions (a) Plot of the emission wavelength of Complex 4 under different conditions: Complex 4 alone without TEM-1 (black), Complex 4 with TEM-1 in the absence of guanidine hydrochloride (blue), and Complex 4 with TEM-1 in the presence of 3 M guanidine hydrochloride (red). (b) Fluorescence signals (513 nm) of Complex 4 at different time intervals under different conditions: without TEM-1 (black), with TEM-1 in the absence of guanidine hydrochloride (blue), and with TEM-1 in the presence of 3 M guanidine hydrochloride (red). [Complex 4] = 10 μ M; [TEM-1] = 30 mg/mL.

3.2.3 Enzyme-substrate binding studies

Electrospray ionization mass spectrometry (ESI-MS) is a powerful tool for studying enzyme-substrate interactions because it can distinguish free enzymes from enzyme-substrate complexes based on their different mass values.⁶ In this study, ESI-MS was applied to probe the interaction between TEM-1 and Complex 4. During the enzymatic reaction, Complex 4 binds to the active site of the TEM-1 beta-lactamase (E) to form a non-covalent enzyme-substrate complex (ES) and subsequently a covalent enzyme-substrate complex (ES*) through the acylation of the -OH group of Ser70 with the beta-lactam carbonyl group. The ES* complex then undergoes deacylation to regenerate the free enzyme (E) and release the antibiotic substrate as the acid product (P) (Scheme 3-1).

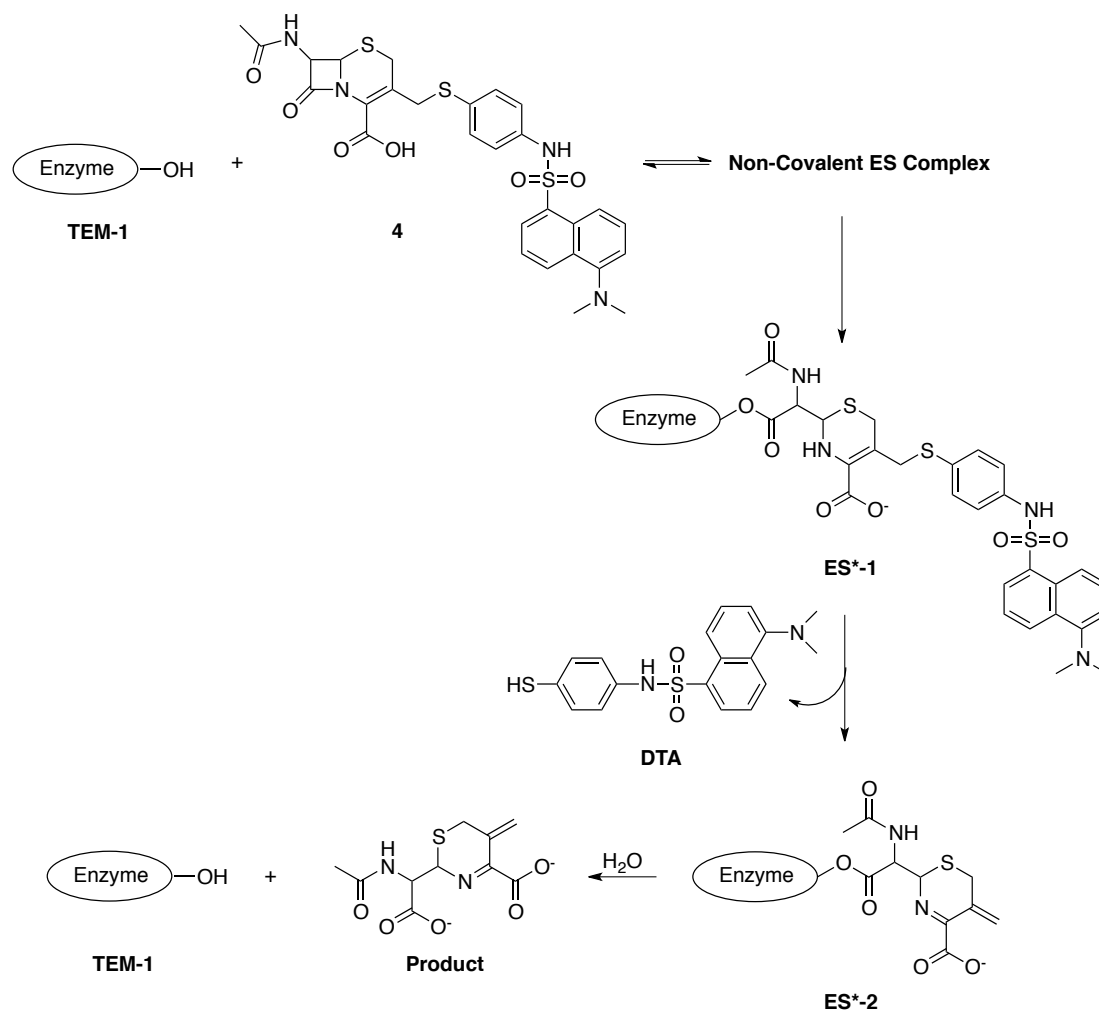


Scheme 3-1 Catalytic hydrolysis of beta-lactam antibiotics by beta-lactamases.

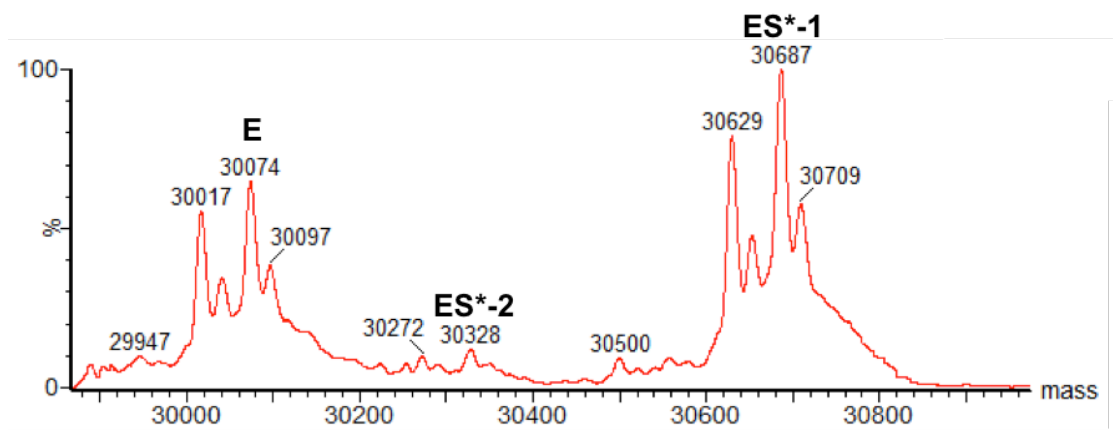
Monitoring of the relative intensities of mass peaks for E and ES* as a function of time can provide an insight into the effect of enzyme-substrate complex formation on the time-dependent fluorescence response of Complex 4. To this end, we performed a time-course ESI-MS study on the TEM-1 mutant E166N with Complex 4 (concentration ratio = 1: 1, dissolved in 20 mM ammonium acetate buffer, pH 7.0). During the enzymatic reaction, a portion of the reaction mixture was collected and quenched by CH₃CN (through protein unfolding) at different time intervals. The quenched mixtures were then analyzed by ESI-MS. The E166N mutant was chosen for the enzyme-substrate binding study because the rate of deacylation (k_3) of ES* of

the wild-type TEM-1 enzyme is extremely high, making the detection of ES* difficult; by replacing catalytically important Glu166 with another amino acid, the resulting mutant will have much slower catalytic activity, thus allowing the ES* complex to be detected. Guillaume et al. have reported that replacing Glu166 with Asn166 in wild-type TEM-1 can significantly reduce the deacylation rate (k_3) of ES* with cephalosporin C compared to the wild type TEM-1 enzyme. Thus, the E166N mutant of TEM-1 represents a good protein model in our ESI-MS study.⁷

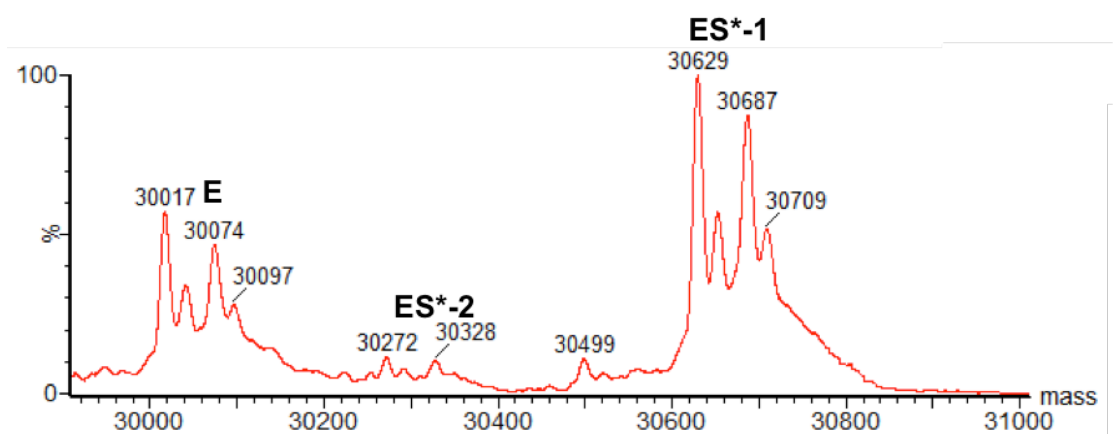
Figure 3-6 shows the ESI mass spectra of E ($M_w = 30074$ Da), ES*-1 ($M_w = E + 613$ Da), and ES*-2 ($M_w = E + 254$ Da) at different intervals (40 s, 1 min, 10 min and 30 min). The enzymatic reaction of TEM-1 with Complex 4 is described in Scheme 3-2. The MS results indicate that most E166N bind to Complex 4, yielding ES*-1 within 10 min (Figure 3-6). Furthermore, the relative population of ES*-1 increases in the first 30 min and then remains virtually steady in the remaining period (Figure 3-7). Because Complex 4 releases the fluorescent DTA molecule from its 3' position after enzymatic hydrolysis (Scheme 3-2), the mass value of ES*-2 has a reduced mass value of 359 Da (relative to that of ES*-1), which is consistent with the molecular mass of the DTA molecule.



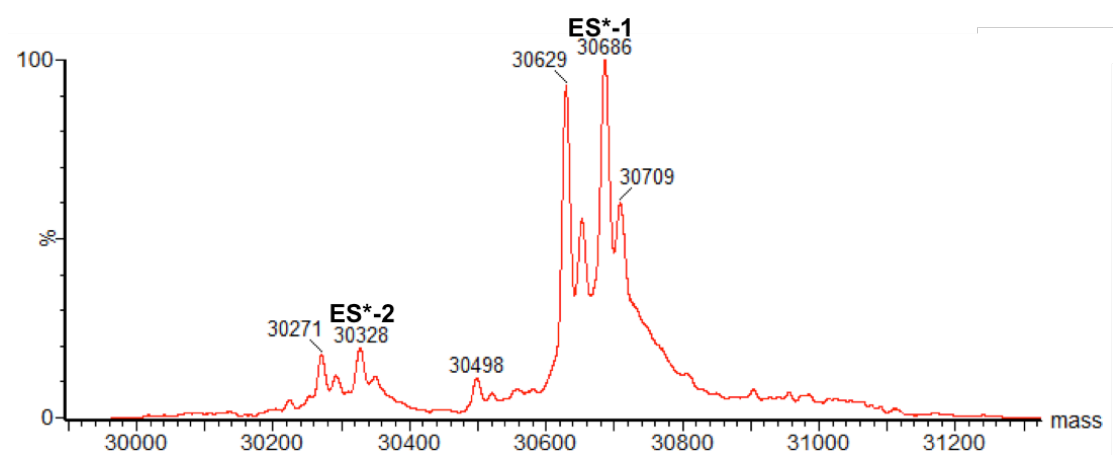
Scheme 3-2 Catalytic reaction of TEM-1 with Complex 4.



(a)



(b)



(c)

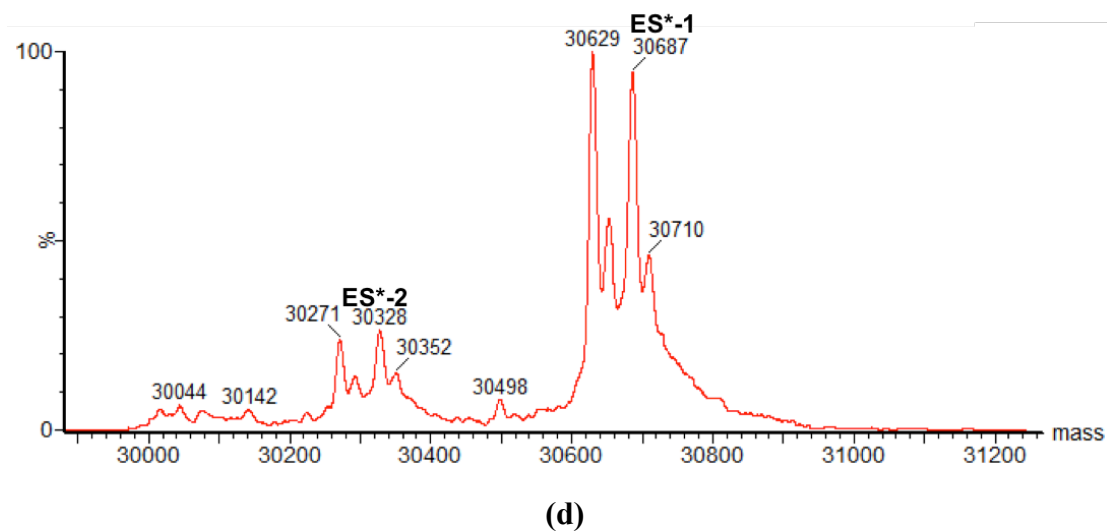


Figure 3-6 ESI mass spectra of the E166N mutant of TEM-1 incubated with Complex 4 at different time intervals. [E166N]: [Complex 4] = 1: 1. A portion of the reaction mixture was extracted at (a) 40 s, (b) 1 min, (c) 10 min, and (d) 30 min. The enzymatic reaction took place at 20°C in 20 mM ammonium acetate buffer (pH 7.0). ES*-1: the covalent complex of the TEM-1 E166N mutant with Complex 4 (with DTA); ES*-2: the covalent complex of the TEM-1 E166N mutant with Complex 4 (without DTA).

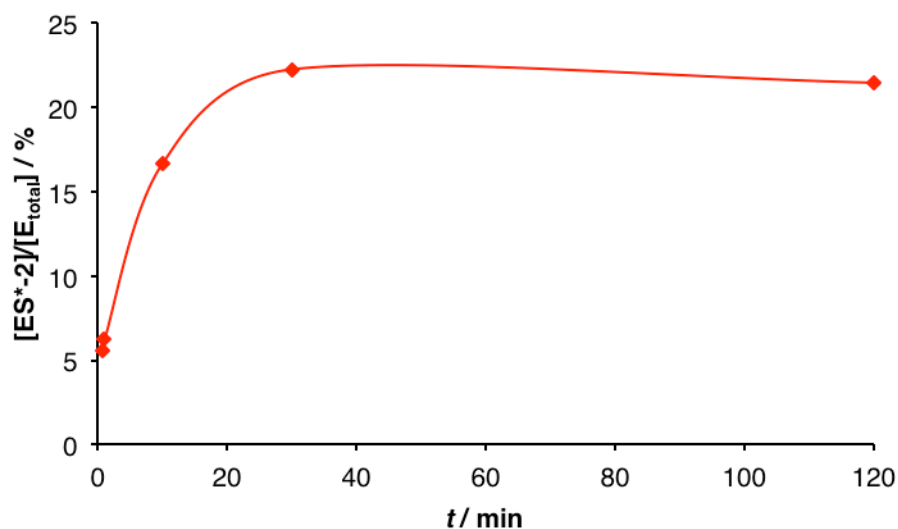


Figure 3-7 Time-course ESI-MS measurements of the binding of the TEM-1 E166N mutant to Complex 4. The red squares represent the $[ES^*-2]/[E_{total}]$ values probed by ESI-MS. $[E166N]: [Complex\ 4] = 1: 1$. The reaction of the E166N mutant with Complex 4 took place in 20 mM ammonium acetate (pH 7.0) at 20°C. ES*-2 represents the covalent complex of the TEM-1 E166N mutant with Complex 4 (without DTA). Note that the relative population of ES*-1 (with DTA) remains high relative to those of E and ES*-2 over the time-course MS experiment (Figure 3-6).

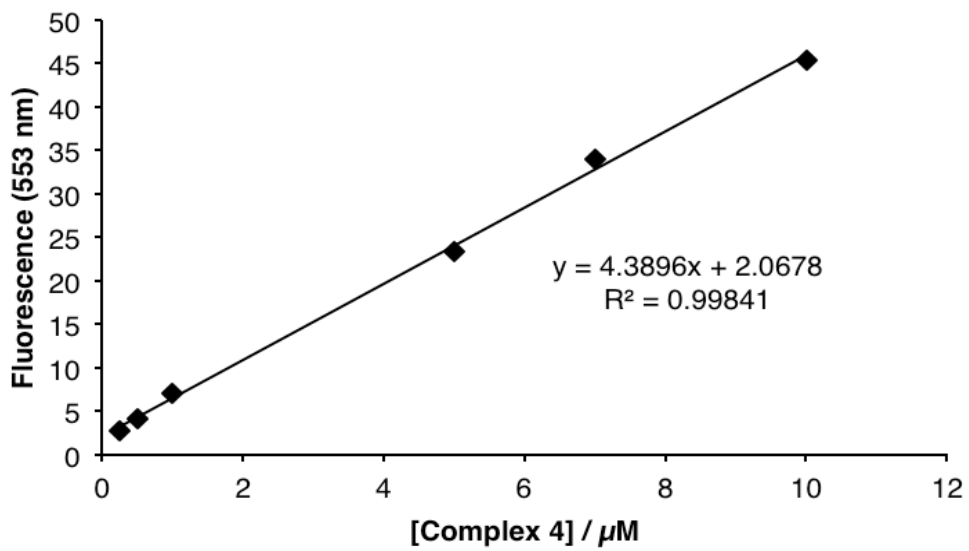
3.2.4 Enzyme kinetic studies

The kinetic parameters (k_{cat} and K_m) of TEM-1 with Complex **4** were determined by the fluorescence method.⁴ Briefly, a standard curve was first prepared by measuring the fluorescence intensity of Complex **4** at different concentrations (0.25, 0.5, 1.0, 5.0, 7.0 and 10 μ M). The fluorescence signals (553 nm) of Complex **4** at different concentrations (1.0, 2.0, 5.0, 7.0 and 10 μ M) with TEM-1 (10 nM) in 50 mM sodium phosphate buffer (pH 7.0) at 20 °C were recorded. At each substrate concentration, the decrease in fluorescence intensity in the first 150 s was determined in triplicate, and the intensity was used to determine the concentration of Complex **4** based on the standard curve. The initial rate of hydrolysis of Complex **4** was determined at each substrate concentration. The initial rates were then fitted to the Lineweaver-Burk equation using Graphpad Prism 6.0 to determine the k_{cat} and K_m values.

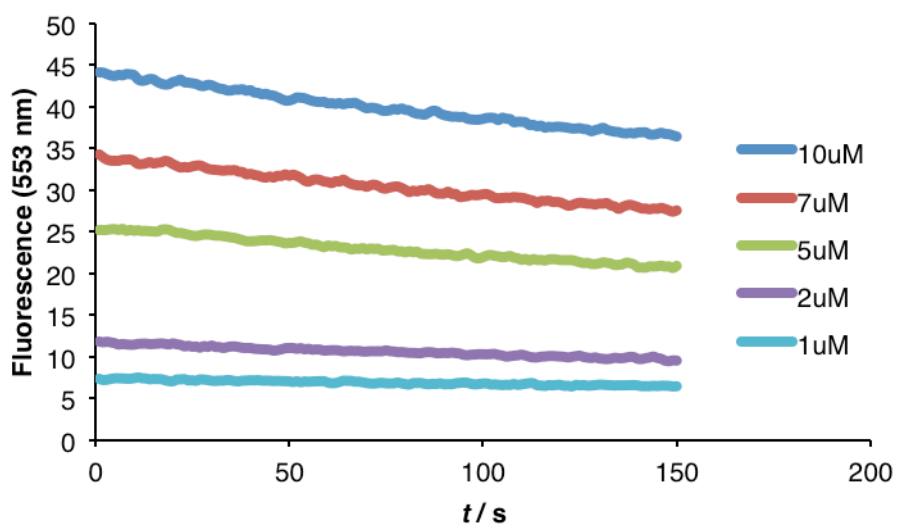
$$\frac{1}{v} = \frac{K_m}{V_{max}} \frac{1}{[S]} + \frac{1}{V_{max}}$$

where v is the initial rate of reaction, V_{max} is the maximum rate of reaction, $[S]$ is the substrate concentration, and K_m is the Michaelis constant.

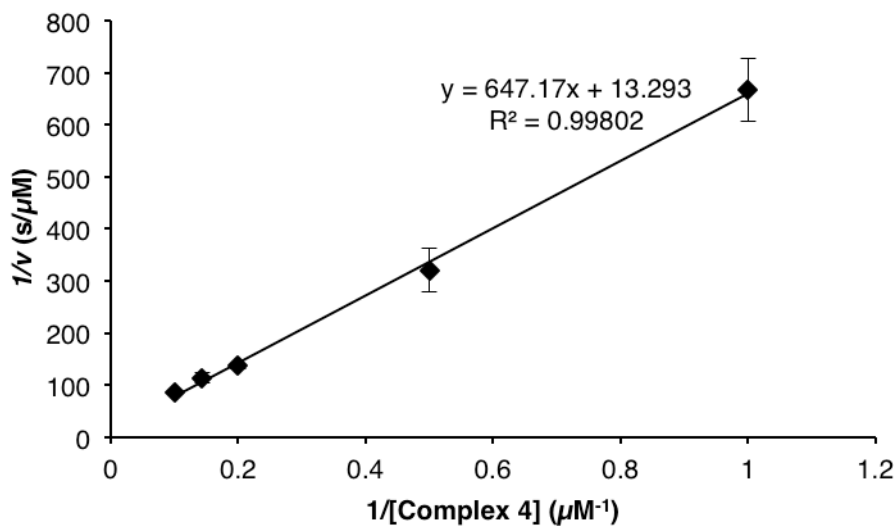
Table 3-1 shows the k_{cat} , K_m and k_{cat}/K_m values of TEM-1 with Complex **4**.



(a)



(b)



(c)

Figure 3-8 (a) Standard curve of the fluorescence signals of Complex 4 versus [Complex 4]. (b) Fluorescence measurements of Complex 4 at different concentrations (1.0, 2.0, 5.0, 7.0 and 10 μM) upon hydrolysis by TEM-1 (10 nM). (c) Lineweaver-Burk plot of the enzymatic hydrolysis of Complex 4 by TEM-1.

Table 3-1 Enzyme kinetic parameters of TEM-1 with Complex 4 as the substrate.

TEM-1	$k_{\text{cat}} (\text{s}^{-1})$	$K_{\text{m}} (\mu\text{M})$	$k_{\text{cat}}/K_{\text{m}} (\text{s}^{-1} \text{M}^{-1})$
	4 ± 1	20 ± 5	$(1.8 \pm 0.5) \times 10^5$

3.3 Discussion

The increasing emergence of bacterial beta-lactamases has led to a worldwide clinical problem. In particular, humans will soon enter the “post-antibiotic era” in which very few potent antibiotics will only be available for the treatment of bacterial infections. Thus, beta-lactamase detection and drug development against these bacterial enzymes are particularly important in combating antibiotic-resistant pathogenic bacteria. As such, there is an urgent need to develop a specific and sensitive sensing tool capable of performing both beta-lactamase detection and *in vitro* drug screening against beta-lactamases. This tool will not only facilitate clinical diagnosis of antibiotic-resistant bacteria, but also advance the development of new inhibitors and new-generation beta-lactam antibiotics against clinically significant beta-lactamases.

In our study, we have successfully developed a fluorescent drug-based sensor (Complex **4**) by coupling a cephalosporin-type beta-lactam antibiotic to environment-sensitive fluorescent dansyl probe (DTA). The beta-lactam antibiotic can specifically bind to the active site of beta-lactamases, thus allowing itself to act as an excellent carrier for the fluorescent DTA probe for specific and sensitive beta-lactamase detection. The fluorescent DTA molecule is linked to the beta-lactam antibiotic (7-ACMA) at the 3' position.⁹ DTA was chosen because the dansyl group is relatively small in size and therefore causes less steric hindrance to the binding to beta-lactamases. Moreover, the fluorescent DTA molecule is highly sensitive to local polarity changes around itself.¹⁰⁻¹⁵ With this special photophysical property, the DTA molecule in Complex **4** will exhibit characteristic fluorescence changes (e.g. emission

wavelength and fluorescence changes) upon entering the less polar active site from the highly polar external aqueous environment.

The time-course fluorescence measurements have shown that Complex **4** can fluorescently respond to the TEM-1 beta-lactamase. Without TEM-1, Complex **4** just shows weak fluorescence at 555 nm over the time course, but exhibits much stronger fluorescence at a shorter wavelength (513 nm) in the presence of TEM-1 (Figure 3-1 and Figure 3-2). These observations indicate that Complex **4** can respond to TEM-1 by exhibiting characteristic photophysical changes (i.e. a fluorescence enhancement and a blue shift in emission wavelength). Interestingly, Complex **4** can act as a “switch-on” fluorescent probe to detect TEM-1 at trace levels (down to 0.1 nM), highlighting its high sensitivity in beta-lactamase detection (Figure 3-2).

The characteristic fluorescence response of Complex **4** is very specific to the interaction with the TEM-1 beta-lactamase. This advantageous sensing property is evidenced by the facts that Complex **4** gives much stronger fluorescence accompanied by a blue shift in emission wavelength with TEM-1 (Figure 3-2), but shows no significant changes in fluorescence intensity and emission wavelength with other proteins (bovine κ -casein and hen egg white lysozyme) (Figure 3-3 and Figure 3-4). The fact that the characteristic fluorescence response of Complex **4** arises from the specific interaction with TEM-1 is further supported by the fluorescence data from the protein unfolding experiment (Figure 3-5). In the presence of 3 M guanidine hydrochloride (a solution condition under which TEM-1 becomes unfolded), Complex **4** does not show its characteristic fluorescence enhancement and blue shift

in emission wavelength, as similar to the case of Complex **4** alone (without TEM-1) (Figure 3-5). Only in the absence of guanidine hydrochloride (a solution condition under which TEM-1 becomes properly folded), Complex **4** exhibits its characteristic fluorescence changes (Figure 3-5). Furthermore, the enzyme kinetic study has also verified the specific interaction of Complex **4** with TEM-1, as indicated by the kinetic parameters (k_{cat} and K_m) resulting from the hydrolysis of the beta-lactam ring in Complex **4** by TEM-1 (Table 3-1). Taking these observations together, the characteristic fluorescence changes (i.e. fluorescence enhancement and blue shift in wavelength) of Complex **4** is very likely to arise from its specific interaction with the active site of the TEM-1 beta-lactamase. Unlike nitrocefin (a conventional colorimetric beta-lactam antibiotic) which detects beta-lactamase activity through the formation of a red acid product after beta-lactam hydrolysis, the characteristic fluorescence responses of Complex **4** in response to the active-site binding with TEM-1 highlight the ability of Complex **4** to sense beta-lactamases in a direct and specific way.

The time-course ESI-MS profile indicates that the relative population of covalent substrate-bound state (ES*-1 and ES*-2) of the TEM-1 E166N mutant with Complex **4** increases as a function of time (relative to the free-enzyme state E), implying that the substrate-bound state (ES*-1 and ES*-2) accumulates in solution during the course of enzymatic reaction (Figure 3-6 and Figure 3-7). It is interesting to note that the increasing substrate-bound state in the MS profile is similar to the time-course fluorescence profile of Complex **4** with TEM-1 (Figure 3-2); both cases give an increasing signal profile. These observations indicate that the formation of substrate-bound states (non-covalent ES and covalent ES*-1) in solution is likely to induce

Complex 4 to give stronger fluorescence at a shorter wavelength. Upon binding to the active site of TEM-1, Complex 4 is oriented in such a way that the fluorescent DTA molecule points inside the active site. With this binding conformation, the DTA molecule experiences a “hydrophobic” environment within the active site and hence gives much stronger fluorescence at a shorter wavelength due to reduced fluorescence quenching by polar water molecules in the external aqueous environment.

3.5 Conclusions

We have successfully constructed a fluorescence drug sensor from a cephalosporin-type beta-lactam antibiotic (7-ACMA) through the conjugation of the fluorescent dansyl molecule DTA (Complex **4**) and applied it as a fluorescent probe to detect the TEM-1 beta-lactamase. Complex **4** gives very weak fluorescence at 555 nm in the absence of TEM-1, but exhibits much stronger fluorescence accompanied by a significant blue shift in emission wavelength ($\lambda_{em} = 550 \text{ nm} \rightarrow 513 \text{ nm}$). These concomitant photophysical changes represent a specific response to the binding interaction with TEM-1 and can serve as reliable indicators in the biosensing of bacterial beta-lactamases. Complex **4** can directly respond to the local binding to the active site of TEM-1 by exhibiting its characteristic fluorescence enhancement and emission wavelength shift. This advantageous property allows Complex **4** to detect bacterial beta-lactamases with high specificity and sensitivity and to act as a fluorescent drug competitor in the *in vitro* drug screening of drug candidates/lead compounds in drug/chemical libraries against various beta-lactamases. The *in vitro* drug screening function of Complex **4** will be further discussed in Chapter 4.

References

1. Shiozaki, M.; Ishida, N.; Iino, K.; Hiraoka, T. Cleavage of the aminoadipoly side chain of cephamycin C to the (6R, 7S)-7-amino-7-methoxy derivative. *Chem Commun* **1978**, *12*, 517-518.
2. Mroczkowska, J. E.; Barlow, M. Fitness Trade-Offs in blaTEM Evolution. *Antimicrob Agents Chemother* **2008**, *52*, 2340-2345.
3. Salverda, M. L. M.; De Visser, J. A. G. M.; Barlow, M. Natural evolution of TEM-1 β -lactamase: experimental reconstruction and clinical relevance. *FEMS Microbiol Rev* **2010**, *34*, 1015-1036.
4. Queener, S. F.; Webber, J. A.; Queener, S. W. *Beta-lactam Antibiotics for Clinical Use*; M. Dekker: 1986.
5. Frau, J.; Coll, M.; Donoso, J.; Muñoz, F.; Vilanova, B.; García-Blanco, F. Alkaline and acidic hydrolysis of the β -lactam ring. *Electron J Theor Ch* **1997**, *2*, 56-65.
6. Mann, M.; Wilm, M. Electrospray mass spectrometry for protein characterization. *Trends Biochem Sci* **1995**, *20*, 219-224.
7. Guillaume, G.; Vanhove, M.; Lamotte-Brasseur, J.; Ledent, P.; Jamin, M.; Joris, B.; Frère, J. Site-directed Mutagenesis of Glutamate 166 in Two β -Lactamases: KINETIC AND MOLECULAR MODELING STUDIES. *J Biol Chem* **1997**, *272*, 5438-5444.
8. Lapko, V. N.; Smith, D. L.; Smith, J. B. Identification of an artifact in the mass spectrometry of proteins derivatized with iodoacetamide. *J Mass Spectrom* **2000**, *35*, 572-575.
9. Zou, L.; Cheong, W.; Chung, W.; Leung, Y.; Wong, K.; Wong, M.; Chan, P. A Switch-On Fluorescence Assay for Bacterial β -Lactamases with Amyloid Fibrils as Fluorescence Enhancer and Visual Tool. *Chem Euro J* **2010**, *16*, 13367-13371.
10. Kaur, K.; Kumar, S. Dansyl-anthracene dyads for ratiometric fluorescence recognition of Cu²⁺. *Dalton Trans* **2011**, *40*, 2451-2458.
11. Tharmaraj, V.; Pitchumani, K. An acyclic, dansyl based colorimetric and fluorescent chemosensor for Hg(II) via twisted intramolecular charge transfer (TICT). *Anal Chim Acta* **2012**, *751*, 171-175.
12. Srivastava, P.; Shahid, M.; Misra, A. Protein assisted fluorescence enhancement of a dansyl containing fluorescent reagent: Detection of Hg⁺ ion in aqueous medium. *Org Biomol Chem* **2011**, *9*, 5051-5055.
13. Shea, K. J.; Okahata, Y.; Dougherty, T. K. Fluorescence Probes in Polymer Chemistry. Application of 5-(Dimethylamino)-1-naphthalenesulfonamides to the Study of Solvation of Styrene-Divinylbenzene Copolymers. *Macromolecules* **1984**, *17*, 296-300.

14. Holmes-Farley, S. R.; Whitesides, G. M. Fluorescence Properties of Dansyl Groups Covalently Bonded to the Surface of Oxidatively Functionalized Low-Density Polyethylene Film. *Langmuir* **1986**, *2*, 266-281.
15. Buruiana, E. C.; Zamfir, M.; Buruiana, T. Dansylated acrylic copolymer with potential for sensor applications: Synthesis and properties. *J Polym Sci Pol Chem* **2008**, *46*, 3774-3782.
16. Ruitter, C. d.; Bohle, J. F.; Jong, G. J. d.; Brinkman, U. A. T.; Frei, R. W. Enhanced Fluorescence Detection of Dansyl Derivatives of Phenolic Compounds Using a Postcolumn Photochemical Reactor and Application to Chlorophenols in River Water. *Anal Chem* **1988**, *60*, 666-670.
17. Badarau, A.; Llinas, A.; Laws, A. P.; Damblon, C.; Page, M. I. Inhibitors of metallo-beta-lactamase generated from beta-lactam antibiotics. *Biochemistry* **2005**, *44*, 8578-89.
18. Kurosaki, H.; Yamaguchi, Y.; Higashi, T.; Soga, K.; Matsueda, S.; Yumoto, H.; Misumi, S.; Yamagata, Y.; Arakawa, Y.; Goto, M. Irreversible inhibition of metallo-beta-lactamase (IMP-1) by 3-(3-mercaptopropionylsulfanyl)propionic acid pentafluorophenyl ester. *Angew Chem Int Ed Engl* **2005**, *44*, 3861-4.
19. Mollard, C.; Moali, C.; Papamicael, C.; Damblon, C.; Vessilier, S.; Amicosante, G.; Schofield, C. J.; Galleni, M.; Frere, J. M.; Roberts, G. C. Thiomandelic acid, a broad spectrum inhibitor of zinc beta-lactamases: kinetic and spectroscopic studies. *J Biol Chem* **2001**, *276*, 45015-23.
20. Buruiana, E. C.; Zamfir, M.; Buruiana, T. Evidence for a fluorescence enhancement of some dansyl and stilbene derivatives used as optical chemosensors. *Revue Roumaine de Chimie* **2009**, *54*, 993-999.
21. Frei, R. W.; Thomas, M.; Frei, I. A Study of Adrenaline-Dansyl Derivatives for Separation by Liquid Chromatography. Application to Blood Plasma Analysis. *J Liq Chrom* **1978**, *1*, 443-455.

Chapter 4

***In Vitro* Drug Screening Studies**

4.1 Introduction

The increasing emergence of bacterial beta-lactamases with different substrate and activity profiles has been a major health concern. In particular, humans will soon enter the “post-antibiotic” era in which very few drug choices are available for antibacterial therapies. A recent notorious example is NDM-1, which is a metallo-beta-lactamase capable of inactivating a wide range of beta-lactam antibiotics and hence conferring very strong antibiotic resistance on pathogenic bacteria. To combat antibiotic-resistant bacteria, there is an urgent need of developing new drugs (e.g. new inhibitors and new-generation beta-lactam antibiotics) to inactivate beta-lactamases. Because bacterial beta-lactamases exist in an aqueous medium, the inhibitory activities of new drug candidates/lead compounds in drug/chemical libraries against the beta-lactamase targets must be tested *in vitro* in order to successfully identify effective drug candidates/lead compounds. To satisfy this important need, it is necessary to develop a specific and sensitive sensing tool that can perform *in vitro* drug screening in a simple and rapid way.

The agar plate method usually requires a long time of bacterial incubation and is difficult to provide high-throughput drug screening functions. Nitrocefin, a colorimetric beta-lactam antibiotic, has also been used to detect beta-lactamase activity. This colorimetric antibiotic forms a red acid product after beta-lactam hydrolysis by beta-lactamases. However, nitrocefin has low stability in solution¹ and is very expensive. Moreover, nitrocefin detects beta-lactamase activity only through the formation of a red acid product after the enzymatic hydrolysis of its beta-lactam ring, rather than directly probing its binding to the active site of beta-lactamases.

We have reported in Chapter 3 that Complex **4**, consisting of a beta-lactam carrier conjugated with the environment-sensitive fluorescent DTA molecule, can as a specific and sensitive fluorescent drug-based sensor for detecting the TEM-1 beta-lactamase. Unlike nitrocefin, Complex **4** can directly probe its binding to the active site of TEM-1 by giving stronger fluorescence accompanied by a characteristic blue shift in emission wavelength. With this special beta-lactamase-sensing function, we reasoned that Complex **4** can play a useful role in *in vitro* drug screening through the principle of competitive binding; in the presence of an effective inhibitor, the active site of the beta-lactamase target will be blocked and hence the binding of Complex **4** (as the competitive binder) to the beta-lactamase target will be inhibited, resulting in the disappearance of its characteristic photophysical changes (fluorescence enhancement and emission wavelength shift), and vice versa.

In this chapter, we report our fluorescence studies on the drug-screening function of Complex **4** with various resistant and non-resistant beta-lactam antibiotics/inhibitors (e.g. penicillin G, ampicillin, tazobactam, ceftazidime, methicillin, oxacillin and cephalothin), using TEM-1 as the molecular drug target. Our fluorescence data show that Complex **4** can accurately distinguish potent antibiotics from ineffective antibiotics.

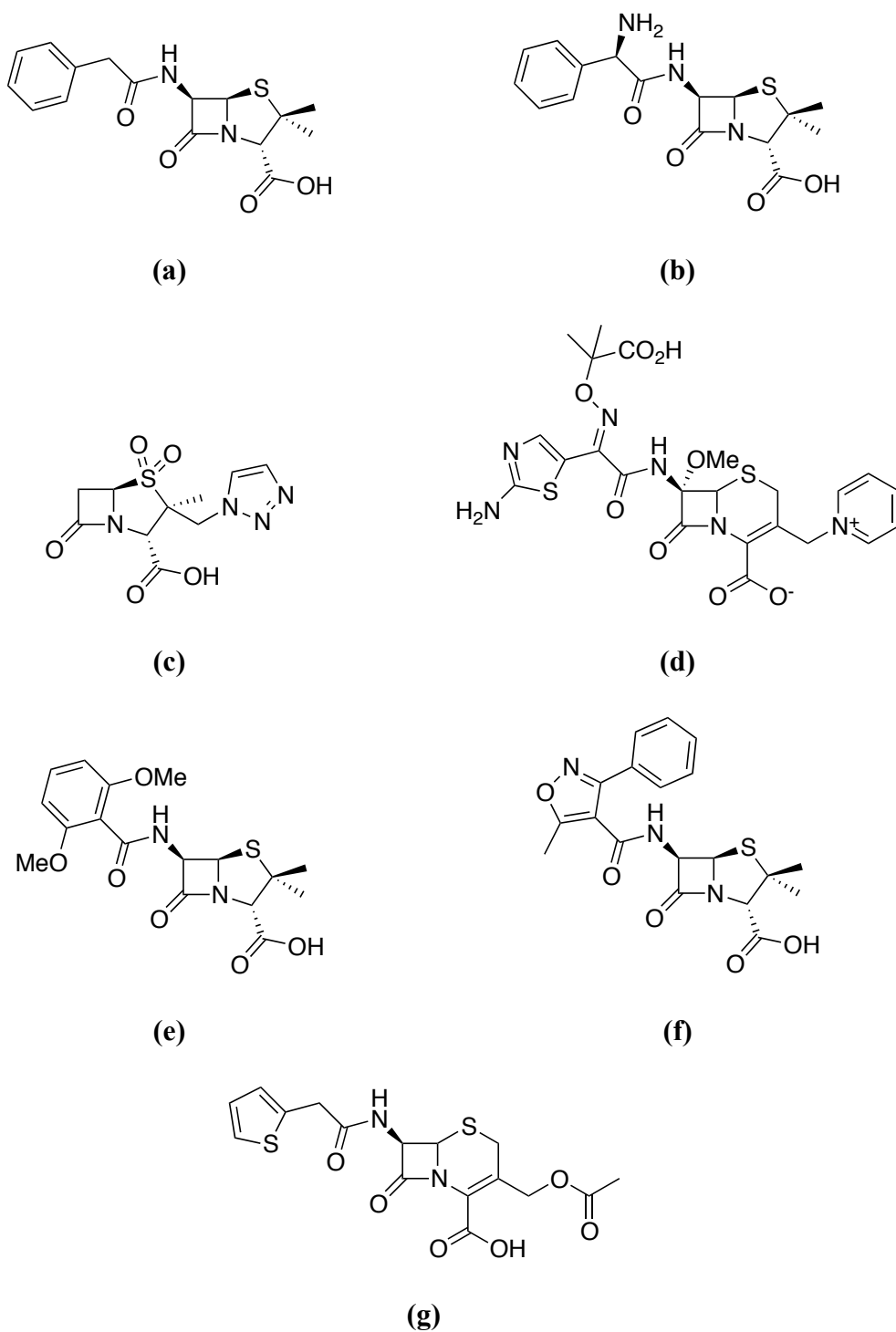


Figure 4-1 Chemical structures of the beta-lactam antibiotics and inhibitors used in the *in vitro* drug screening studies: (a) penicillin G, (b) ampicillin, (c) tazobactam, (d) ceftazidime, (e) methicillin, (f) oxacillin and (g) cephalothin.

4.2 Results

4.2.1 Fluorescence studies

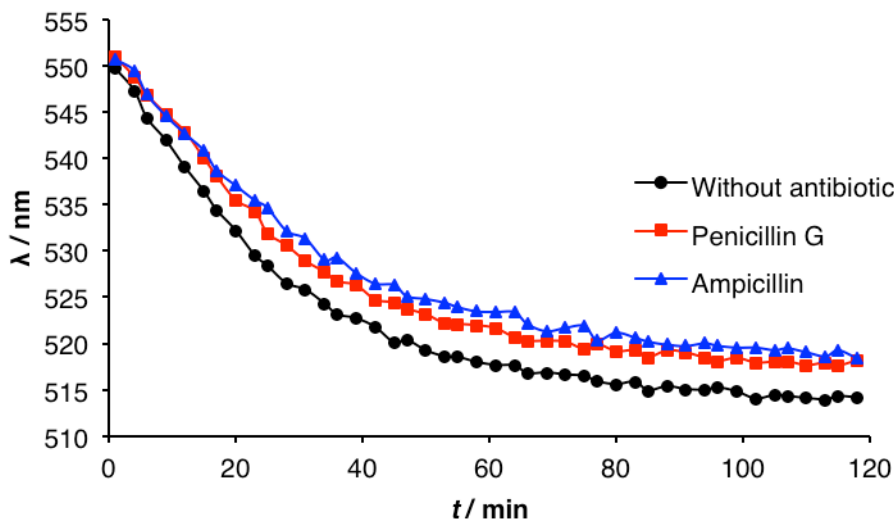
The *in vitro* drug screening function of Complex 4 with a series of beta-lactam antibiotics/inhibitors (100 μ M penicillin G, ampicillin, tazobactam, ceftazidime, methicillin, oxacillin and cephalothin) against the TEM-1 beta-lactamase (1.0 nM) was investigated by fluorescence measurements. Briefly, each of the drug candidates was incubated with TEM-1 for 30 min, followed by the addition of Complex 4 (10 μ M) to the sample solution. The fluorescence spectra of Complex 4 were then recorded as a function of time.

For penicillin G and ampicillin (which are not resistant to the hydrolytic activity of TEM-1) as the drug candidates, Complex 4 shows a significant decrease in emission wavelength from 550 nm to 517 nm and stronger fluorescence ($\lambda_{em} = 513$ nm) over the time course (Figure 4-2). For comparison, similar observations were also obtained with Complex 4 alone (without a drug candidate) (Figure 4-2). Similarly, Complex 4 also shows a decrease in emission wavelength and stronger fluorescence with ceftazidime as the drug candidate over the time course (Figure 4-3).

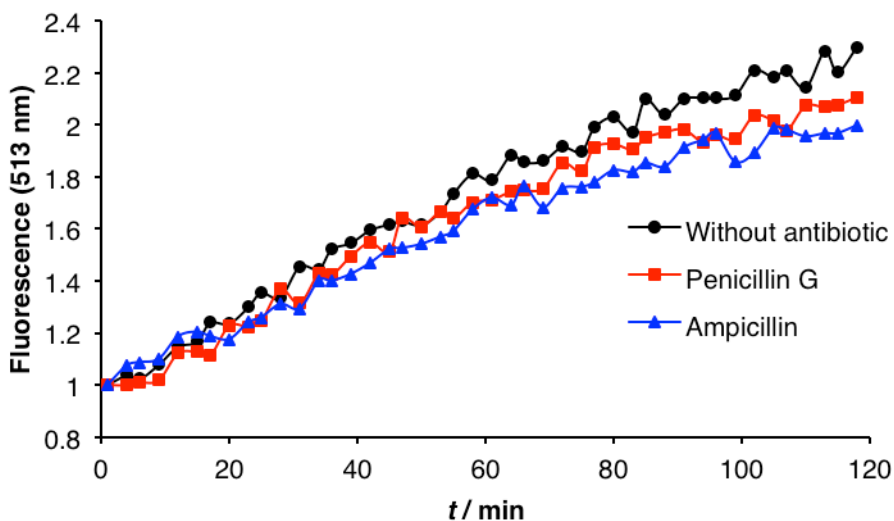
With tazobactam and methicillin as the drug candidates (which are resistant to the hydrolytic activity of TEM-1), Complex 4 shows no significant emission wavelength changes and fluorescence enhancements ($\lambda_{em} = 513$ nm) over the time course with respect to the case of Complex 4 alone (Figure 4-3).

In the presence of oxacillin and cephalothin, the emission wavelength of Complex 4 decreases from 550 nm to 542 and 530 nm (respectively) over the time course (Figure 4-4). Moreover, the fluorescence signals of Complex 4 increase only slightly over the time course in both cases (Figure 4-4).

To examine the accuracy of drug-screening function of Complex 4, we performed a similar fluorescence experiment on aspirin (a non-binder to TEM-1). As shown in Figure 4-4, Complex 4 (with aspirin) shows a similar decrease in emission wavelength compared to Complex 4 alone. Moreover, Complex 4 gives similar fluorescence enhancements ($\lambda_{em} = 513$ nm) in the absence and presence of aspirin (Figure 4-4).

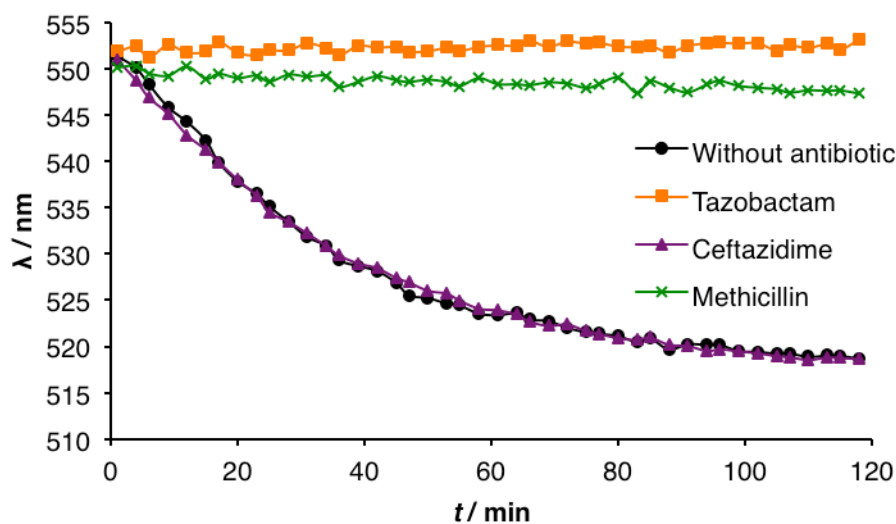


(a)

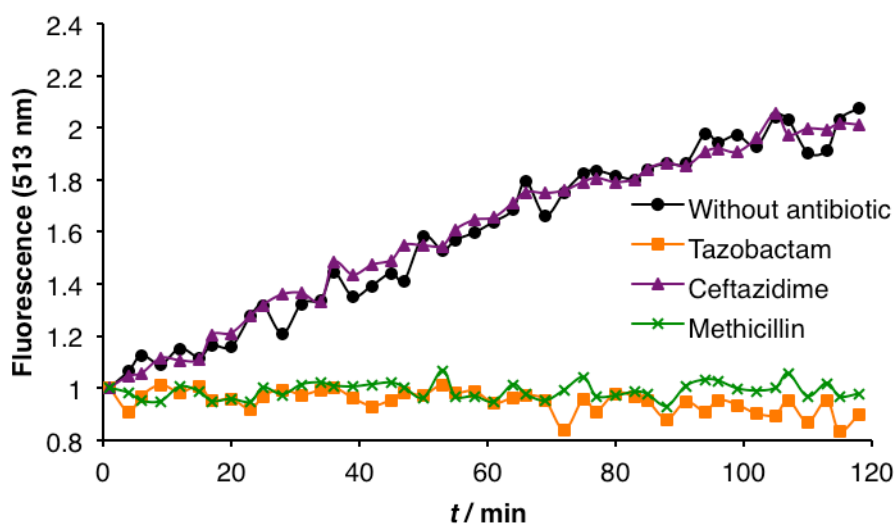


(b)

Figure 4-2 Time-course fluorescence measurements of Complex 4 in the presence of TEM-1 with and without penicillin G and ampicillin. **(a)** Plot of the emission wavelengths of Complex 4 at different time intervals **(b)** Plot of the fluorescence signals (513 nm) of Complex 4 at different time intervals. [TEM-1] = 1.0 nM; [Antibiotic] = 100 μ M; [Complex 4] = 10 μ M. Red line: penicillin G; blue line: ampicillin; black line: without antibiotic. TEM-1 was first mixed with each of the antibiotics for 30 min followed by the addition of Complex 4. Fluorescence measurements on Complex 4 were done in 50 mM sodium phosphate buffer (pH 7.0) with excitation at 350 nm.

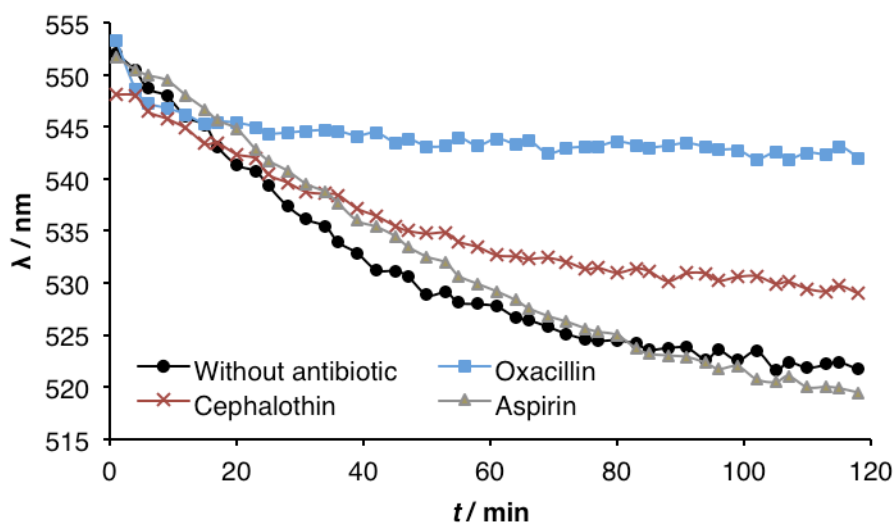


(a)

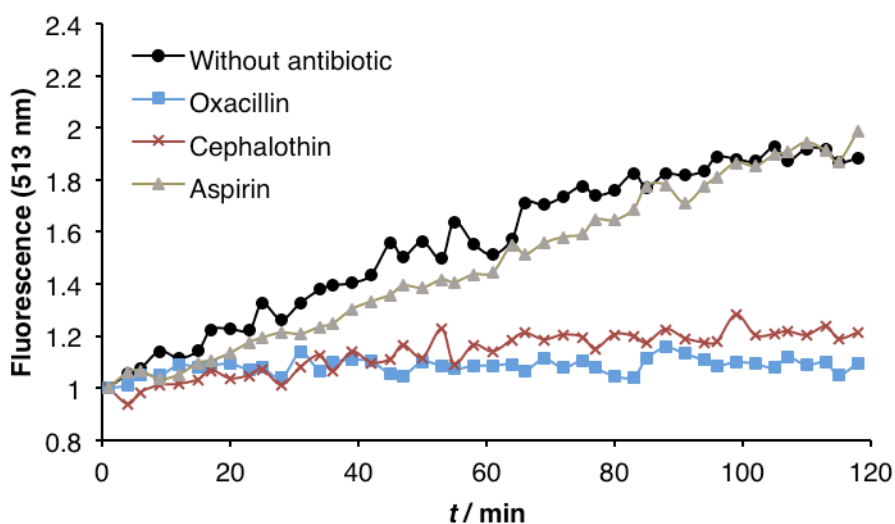


(b)

Figure 4-3 Time-course fluorescence measurements of Complex 4 in the presence of TEM-1 with and without tazobactam, ceftazidime and methicillin. **(a)** Plot of the emission wavelengths of Complex 4 at different time intervals. **(b)** Plot of the fluorescence signals (513 nm) of Complex 4 at different time intervals. [TEM-1] = 1.0 nM; [Antibiotic] = 100 μ M; [Complex 4] = 10 μ M. Black line: without antibiotic; orange line: tazobactam; purple line: ceftazidime; green line: methicillin. TEM-1 was first mixed with each of the antibiotics for 30 min followed by the addition of Complex 4. Fluorescence measurements on Complex 4 were done in 50 mM sodium phosphate buffer (pH 7.0) with excitation at 350 nm.



(a)



(b)

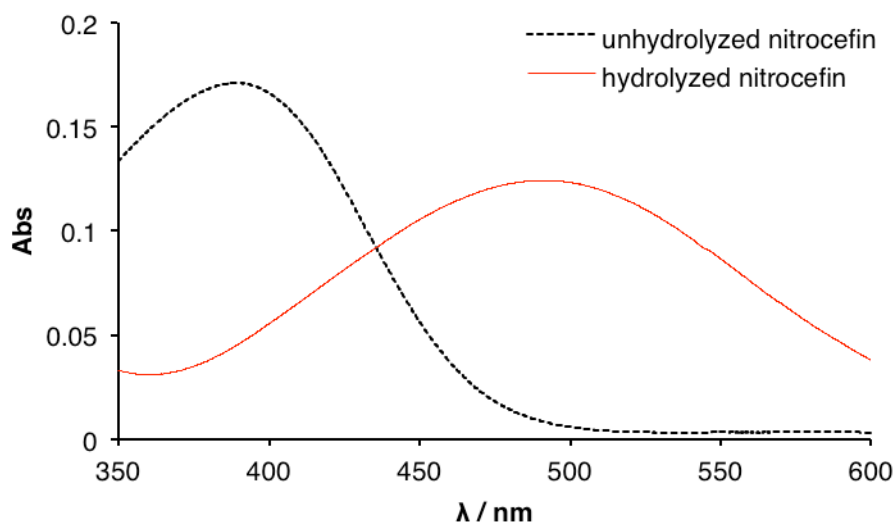
Figure 4-4 Time-course fluorescence measurements of Complex 4 in the presence of TEM-1 with and without oxacillin, cephalothin and aspirin. **(a)** Plot of the emission wavelengths of Complex 4 at different time intervals. **(b)** Plot of the fluorescence signals (513 nm) of Complex 4 at different time intervals. [TEM-1] = 1.0 nM; [Antibiotic/Drug] = 100 μ M; [Complex 4] = 10 μ M. Black line: without antibiotic/drug; blue line: oxacillin; brown line: cephalothin; grey line: aspirin. TEM-1 was first mixed with each of the antibiotics for 30 min followed by the addition of Complex 4. Fluorescence measurements on Complex 4 were done in 50 mM sodium phosphate buffer (pH 7.0) with excitation at 350 nm.

4.2.2 Nitrocefin assays

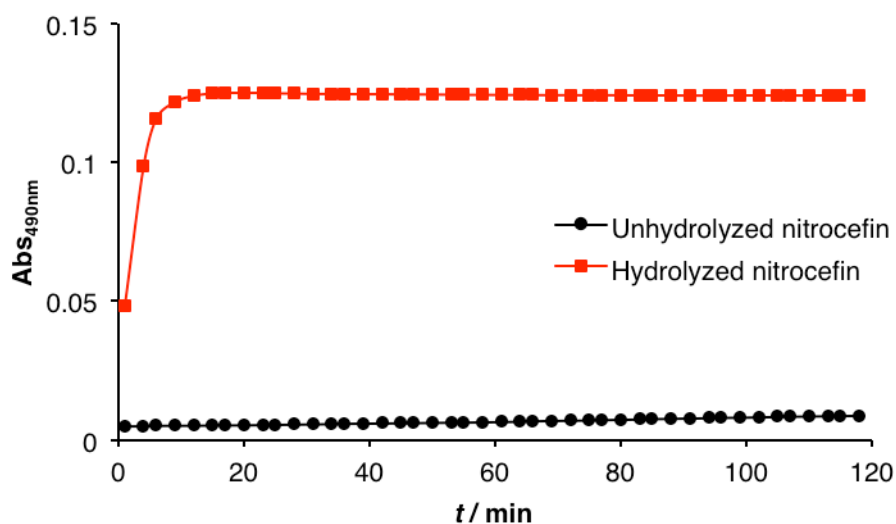
To verify the accuracy of the drug-screening results from Complex 4, we conducted nitrocefin assays on TEM-1 using tazobactam and penicillin G as the drug models (also tested in the drug screening studies by Complex 4) and then compared the experimental results from both studies. Nitrocefin has been routinely used as a colorimetric beta-lactam antibiotic to probe the inhibitory activities of antibiotics/inhibitors against beta-lactamases. The blocking effect of potent antibiotics/inhibitors on the active site of beta-lactamases leads to the suppression of formation of red acid product arising from the beta-lactam hydrolysis of nitrocefin (as a competitive binder).

Tazobactam is an effective inhibitor to TEM-1, whereas penicillin G is readily hydrolyzed by TEM-1. Before studying the potency of tazobactam and penicillin G against TEM-1 by nitrocefin, we first performed time-course absorbance measurements on nitrocefin with and without TEM-1. In the absence of TEM-1, nitrocefin shows an absorption peak at 390 nm, and there is no significant change in absorbance at 390 nm over the time course (Figure 4-5). We then conducted similar absorbance measurements on nitrocefin in the presence of TEM-1. In this case, an absorption peak at 490 nm appears (arising from the formation of red acid product after the beta-lactam hydrolysis of nitrocefin), and the absorbance at 490 nm increases rapidly in the first 10 min and then remains steady over the time course (Figure 4-5). When TEM-1 was first incubated with penicillin G for 30 min and then mixed with nitrocefin, an absorption peak at 490 nm appears, and the absorbance at 490 nm increases in the first 10 min and then becomes steady afterwards (Figure 4-6). A

similar inhibitory assay was also performed on tazobactam. In this case, the absorption peak of nitrocefin appears at 390 nm only (corresponding to the unhydrolyzed form), and the absorbance at 490 nm (corresponding to the hydrolyzed form) remains very weak over the time course (Figure 4-6). These experimental results are consistent with the facts that penicillin G is not resistant to the hydrolytic activity of TEM-1, whereas tazobactam can effectively inhibit the catalytic activity of TEM-1.

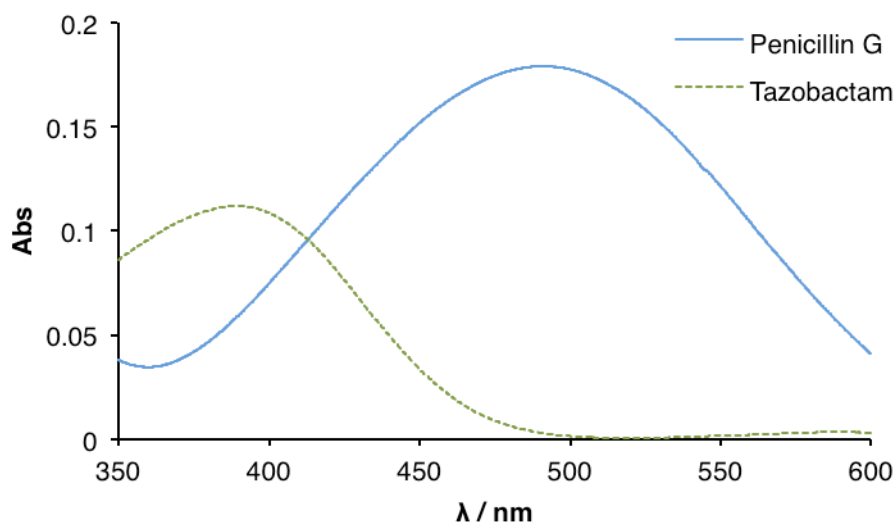


(a)

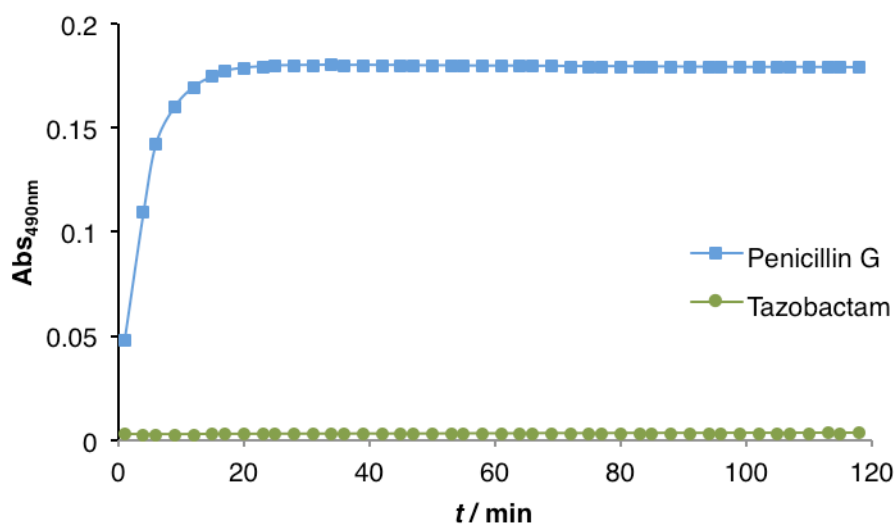


(b)

Figure 4-5 UV-Visible absorption measurements on nitrocefins with and without TEM-1. **(a)** UV-Visible absorption spectra of unhydrolyzed nitrocefins (black line) and hydrolyzed nitrocefins (red line). **(b)** Time-course absorbance (490 nm) measurements of nitrocefins in the presence of TEM-1 (red line) and absence of TEM-1 (black line). $[TEM-1] = 1.0$ nM; $[nitrocefins] = 10$ μ M. The assays were done in 50 mM sodium phosphate buffer (pH 7.0).



(a)



(b)

Figure 4-6 UV-Visible absorption measurements on nitrocefin with penicillin G and tazobactam in the presence of TEM-1. **(a)** UV-Visible absorption spectra of nitrocefin with TEM-1 and tazobactam (green line) and penicillin G (blue line). **(b)** Time-course absorbance (490 nm) measurements of nitrocefin in the presence of TEM-1 with penicillin G (blue line) and tazobactam (green line). [TEM-1] = 1.0 nM; [nitrocefin] = 10 μ M; [penicillin G/tazobactam] = 100 μ M. The assays were done in 50 mM sodium phosphate buffer (pH 7.0).

4.3 Discussion

Development of new-generation beta-lactam antibiotics and new inhibitors are of particular importance in combating antibiotic-resistant bacteria that can produce beta-lactamases. This critical work usually requires the selection of potential drug candidates/lead compounds capable of binding to the active site of beta-lactamases from drug/chemical libraries, and the inhibitory activities of the selected compounds must be tested against beta-lactamases *in vitro* in order to accurately assess their potency. Such research work will only be successful if a rapid, simple and sensitive drug screening tool is available.

Complex **4** can bind to the TEM-1 beta-lactamase with high specificity and directly probe its binding to the TEM-1's active site by giving stronger fluorescence and a significant blue shift in emission wavelength. Both photophysical changes serve as a reliable indicator to enable Complex **4** to reveal the ability of a drug compound to block the active site of the beta-lactamase target in *in vitro* drug screening; if the beta-lactamase target is effectively inhibited by the drug compound through active-site binding, Complex **4** (acting as a competitive binder) will be unable to occupy the active site to give the characteristic fluorescence enhancement and emission wavelength shift, and vice versa.

TEM-1 is an efficient enzyme for hydrolyzing penicillin antibiotics but not later-generation cephalosporin antibiotics and the conventional beta-lactamase inhibitors for class A enzymes (e.g. clavulanate and tazobactam).^{2,3} Table 4-1 shows the

hydrolysis rates of TEM-1 with various beta-lactam antibiotics and beta-lactamase inhibitor.

Table 4-1 Relative rates of beta-lactam hydrolysis for the beta-lactam antibiotics and beta-lactamase inhibitor ^a

	Rate of hydrolysis (%) ⁴						
	PEN-G	AMP	MET	OXA	CTZ ^{5,6}	CET	TZB ⁶
TEM-1	100	106	0	5	0	20	0 ^b

^a all hydrolytic rates (except for TZB) are relative to that of PEN-G; beta-lactam abbreviations are as follows: PEN-G = penicillin G, AMP = ampicillin, MET = methicillin, OXA = oxacillin, CTZ = ceftazidime, CET = cephalothin, TZB = tazobactam; ^b The hydrolytic rate of TZB is relative to that of AMP

As shown by the time-course fluorescence profiles for penicillin G and ampicillin, Complex **4** exhibits increasing fluorescence signals and decreasing emission wavelengths, indicating that these two antibiotics are unable to inhibit the hydrolytic activity of TEM-1 (Figure 4-2). A similar observation is also obtained from the data of the nitrocefin assay with TEM-1 and penicillin G, which reveal that TEM-1 can efficiently hydrolyze penicillin G (Figure 4-6). The fluorescence and spectrophotometric data are consistent with the facts that penicillin G and ampicillin are ineffective antibiotics against TEM-1 as they are readily hydrolyzed by TEM-1 (Table 4-1). Because of the extremely poor inhibitory activities of penicillin G and ampicillin, Complex **4** does not experience strong binding competitions and can therefore enter the active site of TEM-1 to give its characteristic fluorescence and emission wavelength changes.

For tazobactam and methicillin, Complex 4 does not show significant fluorescence enhancements and emission wavelength reductions compared to the case of Complex 4 alone (Figure 4-3). These results reveal that tazobactam and methicillin can effectively inhibit the hydrolytic activity of TEM-1 by blocking the active site, so that Complex 4 cannot occupy the active site. As a result, Complex 4 just stays in the aqueous environment and does not exhibit significant fluorescence and emission wavelength changes. The fluorescence results are, in fact, consistent with the fact that TEM-1 has extremely poor hydrolytic activity towards methicillin and tazobactam (an effective beta-lactamase inhibitor for class A beta-lactamases) [Table 4-1]. The strong inhibitory activity of tazobactam towards TEM-1 is also revealed by the result of the nitrocefin assay (Figure 4-6).

With oxacillin and cephalothin as the drug candidates, TEM-1 is only “partially inhibited” because of its slower hydrolytic rates towards these two antibiotics (Table 4-1). Oxacillin and cephalothin are not completely hydrolyzed by TEM-1 and therefore compete with Complex 4 for the active site of TEM-1. As a result, Complex 4 shows weaker fluorescence enhancements and emission wavelength reductions (Figure 4-4).

In the case of ceftazidime, this beta-lactam antibiotic has very poor binding interaction with TEM-1.⁷ Thus, Complex 4 experiences a very weak binding competition with ceftazidime and can therefore occupy the active site of TEM-1, giving its characteristic fluorescence enhancement and emission wavelength arising from active-site binding (Figure 4-3). Similar observations were also obtained from

the fluorescence measurements of Complex **4** with aspirin (a non-binder to TEM-1) (Figure 4-4).

Table 4-2 summarizes the results of the *in vitro* drug screening studies of Complex **4** with TEM-1. The fluorescence data for ineffective antibiotics (penicillin G and ampicillin), effective antibiotic/inhibitor (methicillin and tazobactam) and non-binder (aspirin) highlight the ability of Complex **4** to distinguish potent drugs from ineffective drugs and non-binders by exhibiting its characteristic and easy-to-analyze time-course fluorescence profiles.

Table 4-2 Fluorescence and emission wavelength changes of Complex **4** with TEM-1 and various beta-lactam antibiotics/beta-lactamase inhibitor

Fluorescence and emission wavelength changes of Complex 4 ^a							
	PEN-G	AMP	MET	OXA	CTZ	CET	TZB
TEM-1	+++	+++	-	+	+++	++	-

^a Beta-lactam abbreviations are as follows: PEN-G = penicillin G, AMP = ampicillin, MET = methicillin, OXA = oxacillin, CTZ = ceftazidime, CET = cephalothin, TZB = tazobactam. Symbols: +++ = very large change; ++ = large change; + = slight change; - = no change

4.4 Conclusions

We have successfully demonstrated the novel application of the fluorescent drug-based sensor (Complex 4) in *in vitro* drug screening using the TEM-1 beta-lactamase as the drug target. The drug-screening function of Complex 4 is based on its characteristic fluorescence responses in the binding competitions with drug candidates for beta-lactamases; different time-course fluorescence profiles are given by Complex 4 with potent drugs (no significant fluorescence and emission wavelength changes) and ineffective drugs/non-binders (concomitant fluorescence enhancements and emission wavelength reductions). Such distinctive fluorescence profiles are easy-to-analyze and allow rapid and convenient *in vitro* drug screening against beta-lactamases using Complex 4 as the drug sensor. This new exploration will greatly facilitate the drug discovery/development for other clinically significant beta-lactamases.

References

1. Liu, R.; Liew, R.; Zhou, J.; Xing, B. A simple and specific assay for real-time colorimetric visualization of beta-lactamase activity by using gold nanoparticles. *Angew Chem* **2007**, *46*, 8799-803.
2. Brown, N. G.; Shanker, S.; Prasad, B. V. V.; Palzkill, T. Structural and Biochemical Evidence That a TEM-1 beta-Lactamase N170G Active Site Mutant Acts via Substrate-assisted Catalysis. *J Biol Chem* **2009**, *284*, 33703-33712.
3. Cantu, C.; Huang, W.; Palzkill, T. Cephalosporin Substrate Specificity Determinants of TEM-1 β -Lactamase. *J Biol Chem* **1997**, *272*, 29144-29150.
4. Matthew, M.; Hedges, R. W.; Smith, J. T. Types of beta-Lactamase Determined by Plasmids in Gram-Negative Bacteria. *J Bacteriol* **1979**, *138*, 657-662.
5. Robin, F.; Delmas, J.; Archambaud, M.; Schweitzer, C.; Chanal, C.; Bonnet, R. CMT-Type beta-Lactamase TEM-125, an Emerging Problem for Extended-Spectrum beta-Lactamase Detection. *Antimicrob Agents Chemother* **2006**, *7*, 2403-2408.
6. Vakulenko, S.; Golemi, D. Mutant TEM beta-Lactamase Producing Resistance to Ceftazidime, Ampicillins, and beta-Lactamase Inhibitors. *Antimicrob Agents Chemother* **2002**, *46*, 646-653.
7. Labia, R.; Beguin-Billecoq, R.; Guionie, M. Behaviour of ceftazidime towards beta-lactamases. *J Antimicrob Chemother* **1981**, *8*, 141-146.

Chapter 5

General Conclusions and Further Studies

Bacterial antibiotic resistance has become a challenging global clinical problem. As a result of increasing human travels and logistic activities among various countries, superbugs carrying powerful beta-lactamases have been easily spread all over the world than before. A notorious example is NDM-1 which was first identified in India, but superbugs carrying the NDM-1 beta-lactamase have appeared in various countries. More worryingly, the beta-lactamase family is still rapidly expanding, leading to the increasing emergence of new beta-lactamases with broad antibiotic and activity profiles that compromise the clinical utility of many existing beta-lactam antibiotics. Clinical microbiologists have warned that we will soon enter the “post antibiotic” era in which only very few antibiotics are available for the clinical treatment of bacterial infections.

Beta-lactamase detection and new drugs development (e.g. new-generation beta-lactam antibiotics and new inhibitors) against clinically significant beta-lactamases are very important for resolving the clinical problem brought about by antibiotic-resistant bacteria. Both tasks play critical roles in the monitoring and control of spread of antibiotic-resistant bacteria, clinical diagnosis of bacterial infections, and antibacterial therapies. To address the two urgent needs, it is highly desirable to develop a rapid, specific and sensitive sensor capable of detecting beta-lactamases and performing *in vitro* drug screening. Our studies have shown that the “switch-on” fluorescent drug-based sensor (Complex 4), consisting of a cephalosporin antibiotic conjugated with an environment-sensitive fluorescent molecule (DTA), can specifically bind to the active site of the TEM-1 beta-lactamase, allowing the fluorescent DTA molecule to experience local environmental changes at the active site and subsequently give stronger fluorescence accompanied by a characteristic blue

shift in emission wavelength. Unlike nitrocefin, the AuNP method and other fluorogenic beta-lactam antibiotics (e.g. CCF2 and CCI) which detect beta-lactamase activity through the formation of colored/fluorescent products after beta-lactam hydrolysis, this biosensing strategy allows Complex 4 to directly probe the active site of beta-lactamases with high specificity and sensitivity; for example Complex 4 can detect TEM-1 down to sub-nanomolar levels. Furthermore, the characteristic fluorescence and emission wavelength changes arising from active-site binding enable Complex 4 to distinguish potent drugs from ineffective drugs and non-binders and to accurately identify drug candidates capable of binding to the active site of the beta-lactamase target in *in vitro* drug screening by exhibiting characteristic and easy-to-analyze time-course fluorescence profiles. With its versatile functions in both beta-lactamase detection and *in vitro* drug screening, Complex 4 will find its application in clinical diagnosis and drug discovery/development against clinically significant beta-lactamases.

Further studies will be focused on the X-ray crystallographic study of the binding interaction of Complex 4 with the TEM-1 beta-lactamase. This investigation will provide an important insight into the general fluorescent biosensing mechanism of Complex 4 with other serine-type beta-lactamases. The beta-lactamase-sensing and *in vitro* drug screening functions of Complex 4 with other clinically relevant beta-lactamases will be further studied. In particular, it would be interesting to investigate the binding interaction of Complex 4 with class B metallo-beta-lactamases of clinical concern [e.g. NDM-1, containing Zn(II) ion(s) in its active site] to see if the released DTA molecule (with a free -SH group) arising from beta-lactam hydrolysis can

coordinate with the Zn(II) ion and give characteristic fluorescence response and inhibitory activity.